

STOCHASTIC HYDROLOGIC ANALYSIS
OF SOIL-CROP-CLIMATE INTERACTIONS

by

ANGELOS L. PROTOPAPAS

Diploma in Civil Engineering
National Technical University of Athens, Greece
(1981)
M.Sc. in Operations Research and Information Science
University of Athens, Greece
(1983)
S.M. in Civil Engineering
Massachusetts Institute of Technology
(1986)

SUBMITTED IN PARTIAL FULFILLMENT
OF THE REQUIREMENTS OF THE
DEGREE OF

DOCTOR OF PHILOSOPHY

at the

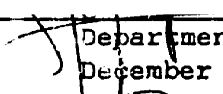
MASSACHUSETTS INSTITUTE OF TECHNOLOGY

February 1988


© Angelos L. Protopapas

The author hereby grants to M.I.T. permission to reproduce and to
distribute copies of this thesis document in whole or in part.

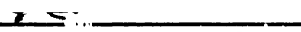
Signature of Author

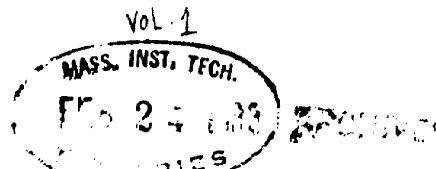

Department of Civil Engineering
December 30, 1987

Certified by


Rafael L. Bras
Thesis Supervisor

Accepted by


Ole S. Madsen
Chairman, Departmental Committee on Graduate Students



STOCHASTIC HYDROLOGIC ANALYSIS OF SOIL-CROP-CLIMATE INTERACTIONS

by

ANGELOS L. PROTOPAPAS

Submitted to the Department of Civil Engineering on
December 30, 1987, in partial fulfillment of the
requirements for the Degree of Doctor of Philosophy
in Hydrology and Water Resources

The objective of this study is to quantify the variability of crop and soil states due to uncertain climatic inputs and soil properties, using a mathematical representation of the physiological, biochemical, hydrological, and physical processes related to plant growth. To achieve this objective we model the soil-crop-climate interactions, we deal analytically with the problem of multidimensional infiltration in heterogeneous soils, and we propose new methods for uncertainty propagation in numerical models of flow and transport in the unsaturated zone.

A state-space deterministic model for the simulation of the seasonal growth of a crop under known climatic inputs, taking into account the moisture and salinity profiles in the soil, is developed. The three components of the model are : 1) a plant growth model, representing processes like CO₂ assimilation, transpiration, growth and maintenance of biomass, root distribution and water uptake over depth, 2) a moisture transport model, solving the unsaturated one-dimensional partial differential equation for flow, and 3) a solute transport model, solving the advection-dispersion partial differential equation for transport. The model has been used successfully for evaluating irrigation schemes and predicting the crop response under different conditions.

The issue whether the one-dimensional soil column model can reasonably and locally represent the processes over a field with spatially varying soil properties is investigated. New analytical solutions to the one- and two-dimensional unsteady linearized unsaturated flow equation are derived. The one-dimensional solutions are used to construct an approximate description of the multidimensional flow problem, which is compared to the exact solution. A criterion to test the validity of the one-dimensional approximation is proposed, in terms of parameters describing the soil type, the uniformity of the boundary conditions, and the soil heterogeneity in the horizontal and the vertical direction. Numerical solutions are also developed for general soil formations and the insight gained from the analytical solutions is tested against more complex situations. On the basis of the studied exponential and periodic variations, the conclusion is that for uniform irrigation over the entire field and for moderate scale of variation of the soil properties in space, the one-dimensional approximation is valid.

A linear model for the perturbations of the state and the inputs around the nominal (first-order mean) values is derived. The linear model is used for second-moment uncertainty propagation in the system due to fluctuations of the climatic forcing in time and the spatial variability of the soil properties. The effect of temporal variability of climatic variables is studied by assuming that the soil properties are known. The state perturbations are given by a linear time-varying system with the climatic time series as forcing term. Since the deviations of the climatic variables from their mean values are correlated at different time steps during a day, an explicit calculation is required for the non-vanishing cross terms in the covariance propagation step. The most important climatic variables affecting crop production are identified in a case study. Correlation of climatic inputs between days is found to increase the crop yield variance. The uncertainty of the climatic inputs does not affect significantly the soil state variables: soil matric potential and salinity.

The effect of spatial variability of soil properties is studied by assuming that the climatic inputs are known. Since the soil property parameters are time-invariant, the state perturbations are given as the product of a precomputable total sensitivity matrix and the soil parameter perturbations. A method for covariance propagation is used which is proven more efficient than recursive methods proposed in the past for studying propagation of uncertainty in groundwater flow systems. The predictions of the linearized transport model have been compared against Monte Carlo simulations for infiltration events with good results. The possibility of second-order prediction of the mean is also studied. The predictions of the composite soil-crop-climate linearized model have been compared successfully against results using a statistical averaging procedure, when the saturated hydraulic conductivity is a random variable lognormally distributed. Significant variance reduction is found in transforming uncertain soil properties to soil state variables and then to plant state variables. Using the one-dimensional approximation the covariance function of the plant and soil states over the horizontal is computed as a linear combination of the covariance functions of the soil property parameters.

This work quantifies the risk due to uncertain factors affecting crop and soil variables; it is a guide for more complex physiological models of crop production; it reveals unknown behavior of the stochastic differential equations for flow and transport in the unsaturated zone; it results in a better understanding of the generic properties of the multidimensional infiltration process; and it provides a framework for on-line forecasting of the crop state using weather data and for use of rational decision-making methods in farming activities.

Thesis Supervisor: Dr. Rafael L. Bras

Title: Professor of Civil Engineering

στη μνήμη του πατέρα μου

ACKNOWLEDGEMENTS

This study was sponsored by

- (a) The M.I.T. Technology Adaptation Program which is funded through a grant from the Agency for International Development, U. S. Department of State,
- (b) The National Science Foundation under NSF Grant No. 78-20245 ENG, and
- (c) The National Scholarship Foundation of Greece.

I wish to thank my thesis advisor, Professor R. L. Bras, for his directions and suggestions during the course of this work and his painstaking review of the final draft. More than once he demonstrated his openness to pursue unconventional research, insisting in solid reasoning and double-checking of results. His faith to my abilities has helped me to develop a sense of confidence important for the times to come.

My thesis reflects compromise and balance after the discussions and the arguments with the committee members. Professors M. Celia, H. Hemond and D. McLaughlin raised important issues, asked the right questions and contributed to explanations. Their influence is apparent at several points of my work. Thanks are very much extended to Professor D. Hillel for his continued support and his insightful comments. The influential teaching of Professors P. Eagleson and L. Gelhar stimulated my interest in the topics of my research.

I am thankful to Mrs. E. Healy and Mrs. C. Solomon for typing the document over the last year and actively participating the speed race of this past month.

People in Ralph M. Parsons Laboratory, in the Hellenic community of M.I.T.-Boston, and in the M.I.T. European Club provided a friendly social environment for work and study. I give special thanks to my good friends Effie, Telis, Spiros, Stavros, Evita, Denise, and, foremost, Melissa. Not to be dismissed are the Marlborough Street group, the Celtics and the Hydros, Aneroussa, the greek popular song, the Middle East Cafe, the Walker Memorial table...

Finally, I would like to acknowledge my parents. I thank my mother, who suffered two serious surgery operations during these years. Her inherent patience and her exhortations to first take care of myself inspired me during hard times. I dedicate my thesis to the memory of my father Loucas, who started his career as an elementary school teacher, teaching Greek in the villages of Macedonia. Being a progressive man, he demanded the best education for his children. I deeply regret that he did not live to see my doctoral graduation, for it would have given him great pleasure and self-fulfillment.

TABLE OF CONTENTS

	<u>Page</u>
Abstract.....	2
Acknowledgements.....	5
Table of Contents.....	6
List of Figures.....	10
List of Tables.....	13
CHAPTER 1: INTRODUCTION	
1.0 Introduction-Objectives.....	14
1.1 Literature Review.....	16
1.2 Thesis Outline.....	19
CHAPTER 2: STATE-SPACE SOIL-CROP-CLIMATE MODEL	
2.0 Soil-Plant-Atmosphere Interactions.....	23
2.1 Plant State Variables: The Plant Growth Model.....	27
2.1.1 Plant Water Status.....	29
2.1.2 Shoot and Root Weight.....	39
2.1.3 Reserve Weight.....	41
2.2 Soil State Variables: The Transport Models.....	43
2.2.1 Soil Matric Potential.....	44
2.2.2 Solute Concentration.....	48
2.3 Case Study Simulations.....	51
2.4 Summary-Comments.....	56

CHAPTER 3: MULTIDIMENSIONAL INFILTRATION IN HETEROGENEOUS SOILS

3.0	Introduction.....	58
3.1	General Formulation.....	59
3.2	The Three-Dimensional Water Transport Equation.....	61
3.3	Infiltration in Heterogeneous Soils: New Analytical Solutions.....	67
3.3.1	Unsteady One-Dimensional Unsaturated Flow.....	67
3.3.2	Unsteady Two-Dimensional Unsaturated Flow.....	69
3.3.3	Discussion of the Analytical Solutions.....	76
3.4	The Margin of Validity of the One-Dimensional Approximation.....	81
3.5	The General Case: Numerical Solutions.....	88
3.5.1	One-Dimensional Numerical Solution in the General Case.....	90
3.5.2	Two-Dimensional Numerical Solution in the General Case.....	93
3.5.3	Application for Periodic Soil Formations.....	97
3.6	Summary-Discussion.....	109

CHAPTER 4: LINEARIZATION OF THE SOIL-CROP-CLIMATE MODEL

4.0	Introduction.....	111
4.1	Techniques for Uncertainty Propagation.....	112
4.2	Details of the Linearization.....	119
4.2.1	Linearization of the Plant Growth Model.....	119
4.2.2	Linearization of the Water Transport Model.....	120
4.2.3	Linearization of the Solute Transport Model.....	125

4.3	Summary-Comments.....	132
CHAPTER 5: UNCERTAINTY OF CLIMATIC INPUTS IN TIME		
5.0	Introduction.....	134
5.1	Uncertainty of Climatic Inputs.....	134
5.2	Second-Moment Analysis for Temporal Variability of Climatic Variables.....	148
5.3	Models of Correlated Disturbances in Time.....	156
5.4	Case Study Results.....	164
5.5	Summary-Comments.....	171
CHAPTER 6: UNCERTAINTY OF SOIL PROPERTIES IN SPACE		
6.0	Introduction.....	174
6.1	Uncertainty of Soil Properties.....	175
6.2	Second-Moment Analysis for Spatial Variability of Soil Parameters.....	178
6.3	Uncertainty Propagation in Flow and Transport Models...	185
6.3.1	Stochastic One-Dimensional Unsaturated Flow and Transport.....	187
6.3.2	Second-Order Mean Prediction.....	199
6.4	Case Study Results.....	204
6.5	Summary-Comments.....	214
CHAPTER 7: CONCLUSIONS AND RECOMMENDATIONS FOR FUTURE RESEARCH		
7.0	Introduction	216

7.1	Findings and Conclusions.....	216
7.2	State-Space Measurement Model.....	222
7.2.1	Observability-State Estimation.....	224
7.2.2	System Identification-Parameter Estimation.....	226
7.2.3	Controllability-Linear Quadratic Control.....	227
7.3	More Recommendations for Future Research.....	228
	REFERENCES.....	231
APPENDIX A:	Solution of the Propagation Equation for Plant Water Potential in Case II.....	241
APPENDIX B:	Viewpoints in Modeling Unsaturated Flow.....	243
APPENDIX C:	Derivation of Analytical Solutions for Multidimensional Infiltration in Heterogeneous Soils.....	250
APPENDIX D:	Derivatives Required for Linearization of Plant Growth Model.....	271
APPENDIX E:	Inverse of a Tridiagonal Matrix.....	301
APPENDIX F:	Linearization of the Boundary Equations of the Transport Models.....	304
APPENDIX G:	Output Statistics of the Model of Correlated Disturbances.....	315
APPENDIX H:	Algebraic Operations for Sparse Matrices.....	318
APPENDIX I:	Statistics of Saturated Hydraulic Conductivity K_s ...	326
APPENDIX J:	Proof of Equivalence of Two Methods of Propagating Uncertainty in Flow and Transport Models.....	328
APPENDIX K:	Measurements of the State Variables.....	333

LIST OF FIGURES

<u>Figure Title</u>	<u>Page</u>
Schematic Representation of the Soil-Plant-Atmosphere Interactions	24
Time Evolution of State Variables (Case I: $c_o = 6000 \text{ mg/l}$, $r = 32 \text{ cm/day}$)	52
Time Evolution of State Variables (Case II: $c_o = 3000 \text{ mg/l}$, $r = 0.0$)	54
One-Dimensional Unsteady Infiltration Solutions with Constant Matric Potential at Saturation (left) and Constant Flux (right) Boundary Condition at the Surface.	70
Line Source at the Origin (Delta Function Flux) a. Homogeneous Soil ($S_x = 0.0$, $S_z = 0.0$)	73
Line Source at the Origin (Delta Function Flux) b. Heterogeneous in x Soil ($S_x = 1.0$, $S_z = 0.0$)	74
Line Source at the Origin (Delta Function Flux) c. Heterogeneous in z Soil ($S_x = 0.0$, $S_z = 1.0$)	75
Symmetric Strip Source (Constant Matric Potential at Saturation) a. Homogeneous Soil ($S_x = 0.0$, $S_z = 0.0$)	77
Symmetric Strip Source (Constant Matrix Potential at Saturation) b. Heterogeneous in x Soil ($S_x = 1.0$, $S_z = 0.0$)	78
Symmetric Strip Source (Constant Matrix Potential at Saturation) c. Heterogeneous in z Soil ($S_x = 0.0$, $S_z = 1.0$)	79
Effect of Soil Heterogeneity (S_x) and Source Length (L) Parameters on the One-Dimensional Approximation	83
Comparison of Two-Dimensional Analytical and Numerical Solution for a Homogeneous Soil ($T=0.1$)	98
Strip Source; One-Dimensional Approximation vs. Two-Dimensional Solution (Case A; $\omega_x = 0.0$, $\omega_z = 2\pi$; $T=0.1$)	101
Strip Source; One-Dimensional Approximation vs. Two-Dimensional Solution (Case A; $\omega_x = 2\pi$, $\omega_z = 2\pi$; $T=0.1$)	104
Strip Source; One-Dimensional Approximation vs. Two-Dimensional Solution (Case B; $\omega_x = 2\pi$, $\omega_z = 2\pi$, $S_x = 1.0$; $T=0.1$)	105

<u>Figure Title</u>	<u>Page</u>
Strip Source; One-Dimensional Approximation vs. Two-Dimensional Solution (Case C; $\omega_x = 2\pi$, $\omega_z = 0.0$; $T=0.1$)	106
Strip Source; One-Dimensional Approximation vs. Two-Dimensional Solution (Case C; $\omega_x = 2\pi$, $\omega_z = 2\pi$; $T=0.1$)	107
Strip Source; One-Dimensional Approximation vs. Two-Dimensional Solution (Case C; $\omega_x = 2\pi$, $\omega_z = 2\pi$; $T=0.5$)	108
Five Year Statistics of Daily Weather Data at Spokane, WA, from Richardson (1981)	136
Input Daily Weather Data for the Case Study (Flevoland, The Netherlands, 1972)	139
Output Climatic Sequences at the Simulation Time Step from the Weather Simulator	140
Means and Standard Deviations of the Climatic Sequences at the Desired Time Step Computed with Monte Carlo Simulations	143
Arrangements Resulting in Random Scalar or Vector Time Sequences with Separable Covariance Structure	157
Sample Paths of Input Process and Output Variance for Scalar Integrator Example	162
Relative Effect of Uncertainty of Particular Inputs to the Standard Deviation of Shoot (Upper Part) and Reserves (Lower Part) ($c_o = 0.0$, $r = 0.0$)	168
Mean \pm One-Standard-Deviation of State Variables for the Cases when the Sequences of Absorbed Visible Radiation are Correlated or Uncorrelated Between Days ($c_o = 0.0$, $r = 0.0$)	169
Soil Hydraulic Properties Used in the Examples	189
Log-normal Distributions for Saturated Hydraulic Conductivity used in the Examples	190
Mean, Standard Deviation and Coefficient of Variation Profiles for Infiltration Example, Using Monte Carlo Simulations ($\sigma_{K_s}^2 = (100 \text{ cm/day})^2$)	192

<u>Figure Title</u>	<u>Page</u>
Mean, Standard Deviation and Coefficient of Variation Profiles for Infiltration Example, Using Monte Carlo Simulations ($\sigma_{K_s}^2 = (300 \text{ cm/day})^2$)	193
Mean, Standard Deviation and Coefficient of Variation Profiles for Infiltration Example, Using First-Order Linearization Method ($\sigma_{K_s}^2 = (100 \text{ cm/day})^2$)	194
Mean, Standard Deviation and Coefficient of Variation Profiles for Infiltration Example, Using First-Order Linearization Method ($\sigma_{K_s}^2 = (300 \text{ cm/day})^2$)	195
Mean, Standard Deviation and Coefficient of Variation Profiles for Infiltration Example, Using Second-Order Linearization Method for the Mean ψ ($\sigma_{K_s}^2 = (100 \text{ cm/day})^2$)	203
Mean \pm One-Standard-Deviation Profiles of Matric Potential (Upper Part) and Solute Concentration (Lower Part), Using the Linearization Method (K_s Perfectly Correlated Over Depth), (triangular initial profile of c_o , no irrigation)	206
Mean \pm One-Standard-Deviation Profiles of Matric Potential (Upper Part) and Solute Concentration (Lower Part), Using the Statistical Averaging Method, (K_s Perfectly Correlated Over Depth) (triangular initial profile of c_o , no irrigation)	208
Time Evolution of Mean \pm One-Standard-Deviation for Plant Water Potential and Crop Weights (c_o as in Figure 6.8, $r = 0.0$)	209
Mean \pm One-Standard Deviation Profiles of Matric Potential (Upper Part) and Solute Concentration (Lower Part), Using the Linearization Method (K_s Perfectly Correlated Over Depth) ($c_o = 3000 \text{ mg/l}$, $r = 6 \text{ cm/day}$)	211
Mean \pm One-Standard Deviation Profiles of Matric Potential (Upper Part) and Solute Concentration (Lower Part), Using the Linearization Method (K_s Exponentially Correlated Over Depth, $\chi_c = 25 \text{ cm}$)	212
Comparison of Required CPU for Computing ABA^T with Sparse Matrix and Direct Algorithms	320

LIST OF TABLES

		<u>Page</u>
Table 5.1	Correlation Coefficient of Daily Climatic Variables from Richardson (1981)	137
Table 6.1	Second Moment Statistics from Different Soils	177

CHAPTER 1

INTRODUCTION

1.0 INTRODUCTION - OBJECTIVES

The demand for agricultural products is expected to increase continuously as a result of growing populations and higher incomes. Modern agriculture, a specialized and mechanized industry which transforms solar energy into useful organic products, is foreseen to increase its output by the expansion of arable land and, mainly, by the intensified use and better management of the production factors. Developing tactics for efficient use of resources in agriculture requires a better understanding of the interactions of the underlying physical processes. From the hydrologist's point of view, we are interested in agricultural use of water for irrigation. The main factors that influence farming decisions on scheduling irrigation are the characteristics of climate, soil, crop, quality and availability of water, irrigation technology and societal considerations. The complex interactions of the above factors become even more complicated as they are affected by uncertainties of varied degree and source.

The objective of this study is to quantify the variability of crop and soil variables due to uncertain climate inputs and soil parameters, not from an empirical-statistical point of view, but based on a mathematical representation of the physiological, biochemical, hydrological and physical processes that result in plant growth. Such information is necessary for optimal irrigation scheduling and for other farming activities. We are pursuing an analysis that focuses on the hydrological aspects of crop productivity and,

therefore, other important factors as nutrient supply are assumed to be non-limiting.

In achieving the above objectives, we address and contribute to several other issues of hydrologic interest:

- We develop an integrated, comprehensive, and representative model of the dynamics of the soil-crop-climate system. It is physically based and analytically tractable. Also, its principles are simple, well understood and experimentally verifiable.
- We deal with the dynamics of water transport in heterogeneous soils, a topic of active theoretical and field research. We investigate under which conditions a set of one-dimensional local models can represent the flow conditions in a spatially variable natural soil, an approximation that simplifies the modeling effort.
- We approach the problem of uncertainty propagation in flow and transport models for the unsaturated zone, assuming that the soil properties vary randomly in space. These phenomena are very much of transient nature and we suggest new methods for reliable prediction of the mean and the variance of the output variables.
- We creatively use state-space linearization methods for second-moment propagation in systems driven by correlated inputs or by constant-but-random inputs. We are also innovative in a number of other computational details and procedures.

1.1 LITERATURE REVIEW

Theoretical modeling of the climate, soil and vegetation interactions in a stochastic-analytical framework has been advanced by Eagleson (1978a-g). In his monumental study he computes the mean and variance of the components of the annual water balance as functions of soil and climatic variables, hypothesizing equilibrium vegetation densities. In the crop and soil science literature we find a number of physically based models for dynamically simulating the seasonal growth of a crop as related to moisture and salinity conditions in the soil (Childs, et al., 1977; Zur and Jones, 1981; Huck and Hillel, 1983; Ritchie and Otter, 1985). These models share a common objective but vary significantly in the degree of detail. All are presented in the form of simulation computer programs and, therefore, are not suitable for analytical work.

Studies which review temporal variability of crop yield take the form of statistical analyses of long records of annual yield for a specific crop and site. Many researchers have proposed agricultural production functions, which are regression models trying to correlate the realized yield to the production factors used. Of interest to hydrologists are production functions that use the total actual evapotranspiration or the total water applied as a surrogate measure of crop yield (Stewart, et al., 1977; Cordova and Bras, 1981).

Spatial variability studies of crop yield historically are related to early results on random fields. Whittle (1956), analyzing crop yield data as a realization of a stationary stochastic process, discovered that the

correlation function must fall off relatively slowly at large distances. He found that power-type correlation functions fitted his data better than exponential-type functions. He also postulated that common features in models that provide this type of covariance function are nonlinearity and time and space dependence. In a later paper Whittle (1962) visualized a mechanism that can produce this form: the diffusion of water, nutrients and salts through the three-dimensional soil medium. Diffusion has mixing effect but cultivation and weather continuously introduce new variation. Eventually a balance is reached between these two effects and this should be evident in the spatial correlation of the crop yield output. Writing a randomly driven diffusion equation, Whittle was able to obtain the hypothesized power law.

Recently attention has been paid to the relation between field soil properties variability and crop spatial variability. The statistical analysis of Bresler, et al. (1981) finds the auto- and cross-correlations of soil properties (namely, water content before and after irrigation and saturated hydraulic conductivity) and yield components (namely, fresh pod yield, fresh hay yield and total dry yield). Yield components have negative correlation with saturated hydraulic conductivity. The coefficient of variation of yield is smaller than that of the soil properties. About 60% of the yield variance is assigned to additional random factors (genetic factors, irrigation uniformity, salinity, etc.). Similar statistical analysis on field data is reported by Russo (1984b), including salinity measurements.

Warrick and Gardner (1983) use a relation between yield Y and water applied W which is linear for $W > W_e$ and gives maximum yield for $W > W_m$.

The authors follow a derived distribution approach and conclude that the more uncertain the threshold value for optimal yield W_m (related indirectly to the variable soil properties), the less mean yield is obtained. They do not consider soil salinity, irrigation water salinity, spatial structure of the soil properties or any dependence on climate.

Russo (1983) favors a geostatistical modeling approach. From point measurements on a 5 Ha field the semivariograms of the saturated hydraulic conductivity, K_s , and of the capillarity index, α , are found and kriging is employed to estimate their values over the entire field. Then, using locally a linearized steady state solution for infiltration from a shallow circular pond, the midway pressure head, h_c , between two trickle irrigation emitters is found and mapped. The spatial structure of $\log \alpha$ is much smoother than of $\log K_s$. The spatial structure of h_c is highly correlated to that of $\log \alpha$. A quadratic dependence of crop yield on \bar{h}_c is assumed and a map of relative yield with respect to the yield corresponding to the mean h_c is created. Yield is found to be less variable than h_c and with an integral scale close to the arithmetic mean of the integral scales of K_s and α . Field experiments (Russo, 1984a) verify the predictions of his model.

Following up on this approach Russo (1986) attempts a more realistic representation of soil-crop-climate interactions by using simplified water and solute dynamics and a yield-transpiration model. Using generated realizations of the soil properties and the crop response model, he studies the effect of uncertainty and spatial variability of inputs (retention curve, initial moisture, initial salinity) on the outputs (soil salinity, moisture, crop yield) by means of conditional simulations.

There is no study in the literature investigating the effect of random climatic inputs and spatially varying soil properties on plant and soil states and using a detailed, analytical, physically based representation of the soil-crop-climate interactions. This is precisely the principal objective of our study.

1.2 THESIS OUTLINE

In Chapter 2 we develop a deterministic state-space model for the simulation of the seasonal growth of a crop under known climatic inputs and taking into account the moisture and salinity profiles in the soil. The three components of the model are: 1) a plant growth model, representing processes like CO₂ assimilation, transpiration, growth, and maintenance of biomass, root distribution and water uptake over depth, 2) a moisture transport model, solving the unsaturated one-dimensional partial differential equation for flow, and 3) a solute transport model, solving the advection-dispersion partial differential equation for transport.

In Chapter 3 we investigate the idea of approximating the soil water dynamics over a field with spatially varying hydraulic properties by means of a set of decoupled noninteracting local soil column models. Analytical solutions to the one- and two-dimensional unsteady unsaturated flow equation are derived for a special (exponential) variation of the saturated hydraulic conductivity in space. The one-dimensional solutions are used to construct an approximate description of the multidimensional flow problem, which is compared to the exact solution. A criterion for the validity of the

one-dimensional approximation is derived, in terms of parameters describing the soil type, the uniformity of the boundary conditions, and the soil heterogeneity in the horizontal and the vertical direction. Numerical solutions are also developed for general soil formations and the insight gained from the analytical solutions is tested against more complex situations. The conclusion is that for uniform irrigation over the entire field and for the expected moderate scale of variation of the soil properties in space, the one-dimensional approximation is valid over the time scale of irrigation events of interest.

In light of the above results, we employ the one-dimensional soil-crop-climate model as an analytical tool for uncertainty propagation studies. In Chapter 4 we identify two sources of uncertainty in the system, namely, the fluctuation of the climatic forcing in time and the spatial variability of the soil properties. Within a second-moment analysis, we want to predict, at any time, the mean and the variance of the state variables of interest. Monte Carlo and derived distribution methods for propagating uncertainty are found to be inapplicable for this type of problem. The questions of interest can only be addressed with linearization methods. The algebraically intensive step of deriving a linear model for the perturbations of the state and the inputs around the nominal (first-order mean) values is accomplished in this chapter.

In Chapter 5 we study the effect of temporal variability of climatic variables, assuming that the soil properties are known. The state perturbations are given by a linear time-varying system with the climatic time series

as forcing term. Since the deviations of the climatic variables from their mean value are correlated at different time steps during a day the standard covariance propagation methods are not sufficient in this case. An explicit calculation for the non-vanishing cross terms is carried out. In a case study the most important climatic variables affecting crop production are identified quantitatively.

In Chapter 6 we study the effect of spatial variability of soil properties, assuming that the climatic inputs are known. Since the soil property parameters are time-invariant, it turns out that the state perturbations are given as the product of a precomputable 'total sensitivity' matrix, which summarizes the unforced system dynamics and the specific way that the soil parameters affect the solution, and the soil parameter perturbations. Based on this fact, a new method for covariance propagation is used, which is proved to be mathematically equivalent and computationally more efficient than recursive methods proposed in the past for studying propagation of uncertainty in groundwater flow systems. The predictions of the linearized transport model have been compared against Monte Carlo simulations for an infiltration event. The possibility of second-order prediction of the mean using second-moment information is also studied. The predictions of the composite linearized model have been compared successfully against results using a statistical averaging procedure.

In Chapter 7 we address the issue of observing the system. First we review a variety of methods for real-time observations of the state variables by using in-situ or remote sensing techniques. The derivation of linearized

models for the dynamics and the observations facilitates the use of a rich variety of estimation, identification, and control methodologies which we discuss briefly. In the same chapter we recapitulate our findings and we suggest directions of future research.

CHAPTER 2

STATE-SPACE SOIL-CROP-CLIMATE MODEL

2.0 SOIL-PLANT ATMOSPHERE INTERACTIONS

The objective of this chapter is to model the seasonal growth of a crop under known climatic forcing as a result of the underlying physical, biological, physiological and hydrological processes. We are particularly interested in the effect of soil moisture and salinity concentration on the crop production. The original development of our simulation model can be found in Protopapas and Bras (1986), and a review table of other integrated soil-crop-climate models is given in Protopapas and Bras (1987). The difference between the previous studies and the presentation herein is that we want to cast the simulation model in a state-space form so that it can be used as an analytical tool for uncertainty studies.

Consider a crop growing on a relatively large field (in the order of a few hectares). A schematic representation of the soil-plant-atmosphere interactions of this system is shown in Figure 2.1. The dynamics of this system are summarized as follows: The climatic inputs act on the canopy of the crop resulting in photosynthesis and transpiration, and on the soil surface resulting in a water and temperature flux from or into the soil. The photosynthesis process replenishes the plant reserves. The assimilated products that are stored in a reserve pool as starch are utilized for growth and maintenance of structural biomass in the shoot and in the root. Climate also imposes a transpiration demand, which is satisfied by water uptake via the root system at a rate which depends on the moisture and salinity profiles in the soil. In order to equate demand and uptake, the plant adjusts its

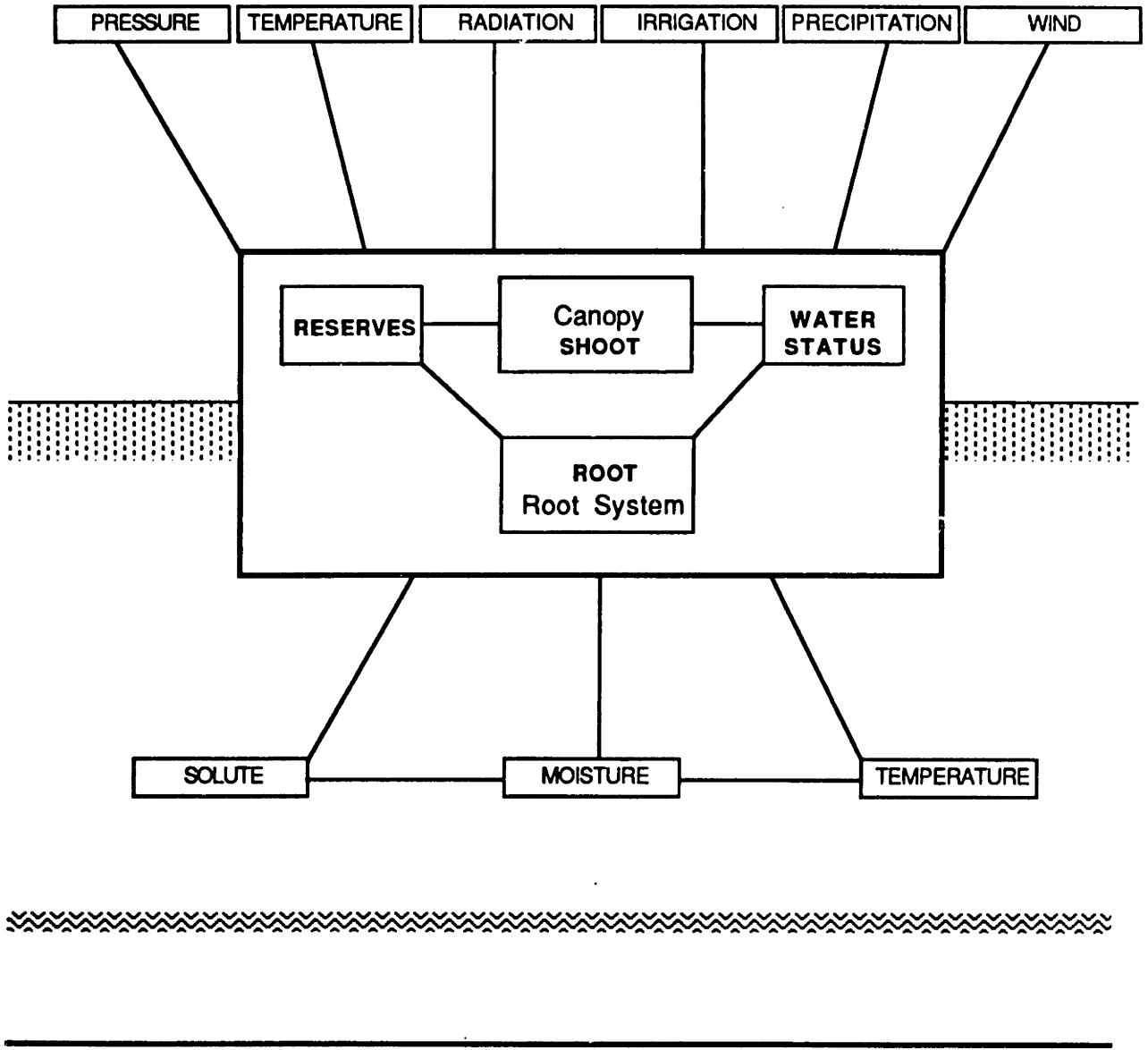


Figure 2.1 Schematic Representation of the Soil-Plant-Atmosphere Interactions

water content, which determines the partitioning of produced biomass in shoot and root. In the soil column, transport of water, solutes and heat takes place.

In the following paragraphs we summarize the conceptual framework for the mathematical description of the above processes as developed in Protopapas and Bras (1986).

If assimilation controls the transpiration process or, alternatively, if solar radiation is the factor limiting growth, the transpiration rate is computed by the Penman-Monteith equation and is a function of climatic variables, namely, air temperature, dew point temperature, wind speed and solar radiation. In the opposite case, that is, if the water status of the plant is the limiting factor, transpiration is a function of climatic variables and of the relative water content of the plant.

The photosynthesis is modeled as a CO_2 diffusion process, restricted however by the hyperbolic light response curve, which gives the photosynthesis rate as a function of available photosynthetically active radiation. Since water vapor and CO_2 follow the same path through the stomata pores, the photosynthesis and the transpiration are closely related. This fact is used to compute the leaf resistance.

Absorption of water occurs along gradients of decreasing soil water potential from the soil to the root system. The existence of solutes in the soil creates osmotic pressures, which result in more negative potentials in the soil and thus in a decrease of the uptake rate. By adjusting its water potential, the plant is able to equate the water loss through transpiration and the water uptake by the root system.

The available reserves, the water status of the plant, and the temperature determine the growth rate of root and shoot. Growth and maintenance are the two processes utilizing the products of photosynthesis to create and sustain useful organic matter. The amount of reserves is updated by writing a mass balance for a conceptual pool of reserves. Inflow is the photosynthesis rate and outflow is the use of reserves for growth and maintenance.

The soil moisture profile is computed numerically by solving the one-dimensional equation for water transport in an unsaturated-saturated cropped soil column. A known climatically imposed flux is used as boundary condition at the soil surface and a known flux or a known matric potential is used at the bottom of the soil profile. The sink term in this equation is the uptake rate at each soil depth. To compute this term, a model for the development of the root system is used in which the produced root biomass is distributed over depth so that the uptake rate is maximized and simple biological constraints are satisfied.

The solute concentration profile is computed by solving the one-dimensional equation for solute transport in a soil column, including the effects of advection, dispersion, adsorption, and chemical activity. A known solute flux or solute concentration is used as boundary condition at the soil surface and at the bottom of the soil column. The required water fluxes are found from the water transport model.

The three components of the integrated model are, therefore, the plant growth model, the water transport model, and the solute transport model. In the following sections we derive a state-space form of this model, that is, a set of nonlinear equations for the propagation of the state variables.

This form differs drastically from any other soil-crop-climate model and is desirable because it facilitates analytical work as well as simulation studies.

2.1 PLANT STATE VARIABLES: THE PLANT GROWTH MODEL

The biological model of plant growth is based on the principles presented in de Wit, et al. (1978) and in Penning de Vries and van Laar (1982). Their studies also report extensive controlled experiments to validate the conceptual description of the underlying individual processes and to identify the required parameters. Similar concepts and formulation are used in other models (Childs et al., 1977; Zur and Jones, 1981; Huck and Hillel, 1983; Ritchie and Otter, 1985). Variables which need to be discussed are: the weight of reserves, the water status of the plant, the morphology and weight of the shoot, and the morphology and weight of the root.

Let us introduce a vector of state variables, the use of which will become clear in the following sections, by writing:

$$x(\kappa) = [\psi_p \text{ RES } W_S \vdots RT_{y1} \dots RT_{yN} \vdots RT_{o1} \dots RT_{oN} \vdots \psi_1 \dots \psi_N \vdots c_1 \dots c_N]^T$$

where $x(\kappa)$ = vector of state variables at time κ

ψ_p = plant water potential (in bars)

RES = weight of reserves (in Kg/HA)

W_S = weight of shoot (in Kg/HA)

RT_{yj} = weight of young roots at node j (in Kg/HA)

RT_{oj} = weight of old roots at node j (in Kg/HA)

ψ_j = matric water potential at node j (in cm)

c_j = solute concentration at node j (in mg/l)

The state vector has dimension $(3+4N,1)$, where N is the number of discretization nodes over depth, and contains all the necessary information that is required in order to describe the system at any time in the future given known inputs. We assume perfect knowledge of the initial state. For methodological purposes, we further partition the state into plant and soil state variables

$$x(\kappa) = [x_p(\kappa) \quad \vdots \quad x_s(\kappa)]^T$$

where

$x_p(\kappa)$ = vector of the first $3+2N$ plant related state variables, and

$x_s(\kappa)$ = vector of the rest $2N$ soil related state variables.

Let us also define a vector of climatic inputs as

$$\xi(\kappa) = [R_n \quad R_v \quad T_a \quad T_d \quad T_s \quad u \quad r \quad R_s]^T$$

where

$\xi(\kappa)$ = vector of input climatic variables at time κ with dimension $(8,1)$

R_n = net absorbed solar radiation (in $J/m^2 \text{ s}$)

R_v = net absorbed visible radiation (in $J/m^2 \text{ s}$)

T_a = air temperature (in $^{\circ}C$)

T_d = dew point temperature (in $^{\circ}C$)

T_s = soil temperature (in $^{\circ}C$)

u = wind speed (in m/s)

r = irrigation or precipitation rate (in cm/day)

R_s = radiation flux reaching the soil surface (in $J/m^2 \text{ s}$).

The sequences of climatic variables at the simulation time step are obtained as the output of a weather simulator which uses daily measurements as input (Chapter 5). The state-space formulation gives the plant state at time $\kappa+1$ explicitly as a nonlinear function of the state and the input climatic variables at time κ or

$$x_p(\kappa+1) = f_p(x_p(\kappa), \xi(\kappa), x_s(\kappa)).$$

2.1.1 Plant Water Status

The water status of the crop is characterized by the plant water potential ψ_p (in bars). This variable regulates the stomatal behavior when the plant suffers a water stress. In such cases the transpiration decreases because of increased leaf resistance to water vapor diffusion.

The net absorbed radiation by the canopy, R_n , imposes a transpiration rate, which can be found by the Penman-Monteith equation

$$LE(\kappa) = \frac{\Delta(\kappa)R_n(\kappa) + (e_s(\kappa) - e_a(\kappa)) \frac{\rho C_p}{r_b(\kappa)} LAI(\kappa)}{\Delta(\kappa) + \gamma \left(1 + \frac{r_l(\kappa)}{r_b(\kappa)}\right)} \quad (2.1)$$

where

$R_n(\kappa)$ = net absorbed radiation in the canopy in J/m^2 -soil s

$LAI(\kappa)$ = leaf area index in m^2 -leaf/ m^2 -soil

$e_s(\kappa)$ = saturated vapor pressure at the current air temperature,
obtained in mbars from

$$e_s(\kappa) = 6.11 \exp\left(\frac{17.4T_a(\kappa)}{239+T_a(\kappa)}\right) \quad (2.2)$$

$e_a(\kappa)$ = actual vapor pressure at the current air temperature,
given in mbars from the above expression where $T_d(\kappa)$ is
used instead of $T_a(\kappa)$

$\Delta(\kappa) = \frac{de_s(\kappa)}{dT_a(\kappa)}$ slope of the curve of saturated vapor pressure vs.
temperature at the current air temperature, obtained in
mbars/°C from

$$\Delta(\kappa) = \frac{4158.6}{(T_a(\kappa)+239)^2} 6.11 \exp\left(\frac{17.4T_a(\kappa)}{239+T_a(\kappa)}\right) \quad (2.3)$$

L = latent heat of vaporization of water = 2390 J/gr

$E(\kappa)$ = mass flux of evaporated water or transpiration rate in
gr/m²-soil s

γ = psychrometric constant = 0.67 mbars/°C

ρC_p = volumetric heat capacity of the air = 1200 J/m³°C

$r_b(\kappa)$ = boundary layer resistance to water vapor diffusion, computed
in s/m from

$$r_b(\kappa) = a \sqrt{\frac{w}{u(\kappa)}}$$

where u = wind speed above the canopy in m/s

w = characteristic width of the leaves in the direction of
wind in m

a = empirical constant = 185 in $s^{1/2}/m$

$r_l(\kappa)$ = leaf resistance to water vapor diffusion in s/m which must be
computed by simultaneous consideration of the photosynthesis and
the transpiration process since carbon dioxide and water vapor
follow the same pathways into the intercellular space.

At the same time the absorbed visible radiation by the canopy, $R_v(\kappa)$,
which is Photosynthetically Active, (PAR), determines the net CO_2
assimilation rate $F_n(\kappa)$ according to the light response curve. This
hyperbolic function approaches a maximum at high light intensities and is
given by

$$F_n(\kappa) = \left\{ (F_m(\kappa) - F_d) \left[1 - \exp\left(\frac{-\epsilon R_v(\kappa)}{F_m(\kappa) LAI(\kappa)}\right) \right] + F_d \right\} \frac{LAI(\kappa)}{3600} \quad (2.4)$$

where

$R_v(\kappa)$ = absorbed visible radiation flux (PAR) in J/m^2 -soil s

$F_n(\kappa)$ = net CO_2 assimilation rate in $Kg CO_2/HA$ -soil s (expressed
per second)

F_d = net assimilation rate in the dark (dark respiration and thus
negative in sign) in $Kg CO_2/HA$ -leaf h (expressed per hour)

ϵ = efficiency at light compensation point in Kg CO₂/J or
 more practically in $\frac{\text{Kg CO}_2}{\text{HA-leaf h}} \frac{\text{m}^2\text{-leaf s}}{\text{J}}$

$F_m(\kappa)$ = maximum rate of net CO₂ assimilation at high light
 intensities in Kg CO₂/HA-leaf h; it is obtained from

$$F_m(\kappa) = F_m^* f_r(\kappa)$$

F_m^* = potential net CO₂ assimilation rate in Kg CO₂/HA-leaf h;

$f_r(\kappa)$ = reduction factor due to the feedback effect of the reserve
 level on the assimilation rate, i.e., if a large amount of
 reserves is available the potential rate is reduced; this
 factor is given by

$$f_r(\kappa) = \begin{cases} 1.0 & \text{RL}(\kappa) < 0.20 \\ 5.0 - 20.0 \text{RL}(\kappa) & 0.20 < \text{RL}(\kappa) < 0.25 \\ 0.0 & 0.25 < \text{RL}(\kappa) \end{cases}$$

$\text{RL}(\kappa)$ = the reserve level equal to the ratio of reserve weight over
 total existing biomass

$$\text{RL}(\kappa) = \frac{\text{RES}(\kappa)}{\text{RES}(\kappa) + W_S(\kappa) + \sum_j (\text{RT}_{yj}(\kappa) + R_{oj}(\kappa))}$$

Typical values of the parameters F_m^* , ϵ , F_d for the two main categories
 of plants are given below (Penning de Vries and van Laar, 1982). C₃ plants
 are small grains (wheat, barley, oats, rye, rice), temperate grasses (brome,
 alfalfa), sugarbeet, potato, etc.; C₄ plants are tropical grasses (maize,
 sorghum, millet, sugar cane), halophytes, etc.

	$F_m^* \left(\frac{\text{Kg CO}_2}{\text{HA h}} \right)$	$\epsilon \left(\frac{\text{Kg CO}_2}{\text{HA h}} \frac{\text{m}^2}{\text{J}} \right)$	$F_d \left(\frac{\text{Kg CO}_2}{\text{HA h}} \right)$
C ₃	15 to 50	0.39	-1.50 to -5.00
C ₄	30 to 90	0.50	-3.00 to -9.00

Photosynthesis also can be seen as a diffusion process, since CO₂ enters the leaf driven by its concentration gradient between the photosynthesizing sites and the ambient air. For many plants, such as maize and bean, experiments indicate that the flux of CO₂ follows a linear law (Goudriaan and van Laar, 1978)

$$F_n(\kappa) = \left\{ 68.4 \frac{\Delta c}{\hat{\Sigma} r_1(\kappa)} \right\} \frac{\text{LAI}(\kappa)}{3600} = \left\{ 68.4 \frac{c_e - c_i}{\hat{r}_b(\kappa) + \hat{r}_l(\kappa)} \right\} \frac{\text{LAI}(\kappa)}{3600} \quad (2.5)$$

where Δc = CO₂ concentration gradient in vppm (volume parts per million), i.e., cm³ CO₂/m³.

c_e = external CO₂ concentration in vppm = 330 vppm in our study

c_i = internal CO₂ concentration in vppm, given as

for C₃ plants: $c_i = \min(c_i^*, 0.7 c_e)$ with $c_i^* = 210$ vppm

for C₄ plants: $c_i = \min(c_i^*, 0.6 c_e)$ with $c_i^* = 120$ vppm

$\hat{\Sigma} r_1(\kappa)$ = total resistance of the leaf to CO₂ diffusion in s/m

= $\hat{r}_b(\kappa) + \hat{r}_l(\kappa)$. The relation between the resistances to CO₂ and water vapor diffusion is

$$\hat{r}_b(\kappa) = 1.32 r_b(\kappa) \quad \text{and} \quad \hat{r}_l(\kappa) = 1.66 r_l(\kappa) \quad (2.6)$$

The constant 68.4 is necessary for dimensional consistency.

Given the amount of absorbed visible radiation, the net CO₂ assimilation rate $F_n(\kappa)$ is computed from Equation (2.4) and then $r_l(\kappa)$ is found from Equation (2.5) as

$$r_l(\kappa) = \frac{68.4 \frac{c_e - c_i}{F_n(\kappa)} \frac{LAI(\kappa)}{3600} - 1.32r_b(\kappa)}{1.66} \quad (2.7)$$

At the same time the water status of the plant determines a different value of $r_l(\kappa)$, which is a function of the plant water potential (de Wit et al., 1978, p. 70)

$$r_l(\kappa) = \begin{cases} \frac{1}{\alpha_1 \psi_p(\kappa) + \alpha_2} & - 4.055 \text{ bars} \leq \psi_p \leq 0 \\ 10000 \text{ s/m} & \psi_p \leq - 4.055 \text{ bars} \end{cases} \quad (2.8)$$

where $\alpha_1 = 3.504 \cdot 10^{-3} \text{ m/s bar}$ and $\alpha_2 = 14.29 \cdot 10^{-3} \text{ m/s}$ are empirical parameters.

Clearly the actual leaf resistance for transpiration is the maximum of the values resulting from Equations (2.7) and (2.8). If the latter is greater, then water stress conditions limit CO₂ assimilation and $F_n(\kappa)$ must be computed in an inverse way as

$$F_n(\kappa) = \left\{ 68.4 \frac{c_e - c_i}{1.66 r_l(\kappa) + 1.32r_b(\kappa)} \right\} \frac{LAI(\kappa)}{3600} \quad (2.9)$$

If the former is greater the biochemical rates of photosynthesis reactions determine $r_l(\kappa)$ and, thus, the rate of transpiration via Equation (2.1). Two cases therefore need to be considered. We will refer to these cases

using the following terms:

CASE I: Photosynthesis controls Transpiration (Equation (2.7))

CASE II: Transpiration controls Photosynthesis (Equation (2.8))

The transpiration rate $E(\kappa)$ is the amount of water that the canopy demands as forced by the atmospheric conditions, the intensity of photosynthesis, and the water status of the plant. By adjusting the water potential, the plant is able to equate the water loss by transpiration $E(\kappa)$ and the water uptake by the root system $U(\kappa)$, which is the sum of the water uptake rates over the soil compartments in the root zone or

$$U(\kappa) = \sum_j U_j(\kappa) = \sum_j [\psi_{sj}(\kappa) - \psi_p(\kappa+1)] \frac{RT_{yj}(\kappa) + p RT_{oj}(\kappa)}{K_R} f_T(\kappa) f_{\psi_{sj}}(\kappa) \quad (2.10)$$

where $U_j(\kappa)$ = water uptake rate at the j soil compartment in $\text{gr}/\text{m}^2 \text{ s}$,

$$\psi_{sj}(\kappa) = 0.9804 \cdot 10^{-3} (\psi_j(\kappa) - 0.581 c_j(\kappa)) \quad (2.11)$$

= the effective water potential in the soil in bars; it accounts for the osmotic potential due to solute concentration in the soil, which affects the water uptake by the roots

$\psi_p(\kappa+1)$ = the water potential in the roots, characterizing the water status of the plant in bars (1 bar = 1020 cm)

p = the fraction of old roots active in water uptake = 0.30

K_R = effective conductive ability of the root system

$$\text{per unit weight of roots} = 2500 \frac{\text{Kg of roots}}{\text{HA}} \frac{\text{bar m}^2 \text{s}}{\text{gr of H}_2\text{O}}$$

$f_T(\kappa)$ = effect of soil temperature on root conductance given by

$$f_T(\kappa) = \begin{cases} 0.0 & T_s(\kappa) < 5^\circ\text{C} \\ 0.0338 - 0.0125 T_s + 0.0018 T_s^2 - 1.94 \cdot 10^{-5} T_s^3 & 5^\circ \leq T_s(\kappa) \leq 36^\circ\text{C} \\ 1.0 & 36^\circ < T_s(\kappa) \end{cases} \quad (2.12)$$

(the root conductance is monotonically decreased as soil temperature drops below 36°C (de Wit et al., 1978, p. 30))

$f_{\psi_{sj}}(\kappa)$ = effect of soil potential on root conductance given by

$$f_{\psi_{sj}}(\kappa) = \begin{cases} -0.02 \psi_{sj} & -50 < \psi_{sj}(\kappa) \leq 0 \\ 1.0 & -300 < \psi_{sj}(\kappa) \leq -50 \text{ cm} \\ 68.0272 \cdot 10^{-6} \psi_{sj} + 1.0204 & -15000 < \psi_{sj}(\kappa) \leq -300 \text{ cm} \end{cases} \quad (2.13)$$

(the root conductance decreases in very dry or in very wet soil conditions (Feddes et al., 1978)).

Let us now express the dynamics of the plant water potential $\psi_p(\kappa)$ using the above concepts. At time κ we know the state $x_p(\kappa)$ and the inputs $\xi(\kappa)$. The uptake rate $U(\kappa)$ is given from Equation (2.10) and the transpiration rate from Equation (2.1), in which the leaf resistance $r_l(\kappa)$ is the maximum of the values computed from Equations (2.7) and (2.8).

In the first case (Case I), the leaf resistance is a function of climatic inputs (wind speed through r_b and absorbed visible radiation through F_n) and of state variables other than plant water potential (crop weights through F_n). Thus, equating $E(\kappa)$ and $U(\kappa)$ yields a linear equation for $\psi_p(\kappa+1)$ with solution

$$\psi_p(\kappa+1) = - \frac{E(\kappa) - \sum_j \psi_{sj}(\kappa) \frac{RT_{yj}(\kappa) + p RT_{oj}(\kappa)}{K_R} f_T(\kappa) f_{\psi_{sj}}(\kappa)}{\sum_j \frac{RT_{yj}(\kappa) + p RT_{oj}(\kappa)}{K_R} f_T(\kappa) f_{\psi_{sj}}(\kappa)} \quad (2.14)$$

This equation propagates the plant water potential provided that the time step is sufficiently small. The computation for Case I (Photosynthesis controls Transpiration) is summarized as follows:

Compute $F_n(\kappa)$ from (2.4); $r_l(\kappa)$ from (2.7); $E(\kappa)$ from (2.1);
 $\psi_p(\kappa+1)$ from (2.14);

Check if indeed $r_l(\kappa) > \frac{1}{\alpha_1 \psi_p(\kappa+1) + \alpha_2}$.

If this is not true, the leaf resistance must be computed from Equation (2.8) being a function of the adjusted plant water potential (Case II). In this case, equating as before $E(\kappa)$ and $U(\kappa)$, we find

$$\sum_j [\psi_{s_j}(\kappa) - \psi_p(\kappa+1)] \frac{RT_{y_j}(\kappa) + p RT_{o_j}(\kappa)}{K_R} f_T(\kappa) f_{\psi_{s_j}}(\kappa) = \frac{1}{L} \frac{\Delta(\kappa) R_n(\kappa) + (e_s(\kappa) - e_a(\kappa)) \frac{\rho C_p}{r_b(\kappa)} LAI(\kappa)}{\Delta(\kappa) + \gamma \left[1 + \frac{1}{r_b(\kappa) (\alpha_1 \psi_p(\kappa+1) + \alpha_2)} \right]} \quad (2.15)$$

The above is a quadratic equation on $\psi_p(\kappa+1)$, solved in Appendix A. The computation proceeds as follows:

Compute $\psi_p(\kappa+1)$ as the acceptable solution of (2.15);

$r_l(\kappa)$ from (2.8);

Check for consistency if indeed the value of leaf resistance from

(2.8) is larger than the value from (2.7);

Compute $E(\kappa)$ from (2.1) and $F_n(\kappa)$ from (2.9).

Thus, considering the interdependence of the photosynthesis and the transpiration process and writing a balance equation for the flow of water from the soil to the atmosphere, we are able to deduce a propagation equation for the plant water potential.

At this point let us discuss the computation of the canopy temperature, which affects the growth and maintenance of the shoot biomass (Section 2.1.2). From the energy balance of the canopy, we have

$$R_n(\kappa) = LE(\kappa) + H(\kappa) LAI(\kappa)$$

where $H(\kappa)$ is the sensible heat loss in the canopy in $J/m^2\text{-leaf s}$.

Then the temperature of the canopy is found from

$$T_c(\kappa) = T_a(\kappa) + H(\kappa) \frac{r_b(\kappa)}{\rho C_p} = T_a(\kappa) + (R_n(\kappa) - LE(\kappa)) \frac{1}{LAI(\kappa)} \frac{r_b(\kappa)}{\rho C_p} \quad (2.16)$$

with the transpiration rate $E(\kappa)$ computed using the proper value of leaf resistance in each of the defined cases I or II.

During nighttime period there is no transpiration. We assume that the plant water potential remains constant

$$\psi_p(\kappa+1) = \psi_p(\kappa)$$

The canopy does not photosynthesize, instead it respire at a rate

$$F_n(\kappa) = - \frac{F_d}{3600} LAI(\kappa)$$

and the canopy temperature is given by

$$T_c(\kappa) = T_a(\kappa) + \frac{R_n(\kappa)}{LAI(\kappa)} \frac{r_b(\kappa)}{\rho C_p}$$

2.1.2 Shoot and Root Weight

The growth rate of shoot is computed from

$$G_S(\kappa) = \text{RES}(\kappa) r_c g_T(T_c(\kappa)) g_p(\psi_p(\kappa+1)) \quad (2.17)$$

where

r_c = relative consumption rate of reserves; for plants that do not accumulate starch, it is set equal to 1 Kg-biomass/Kg-starch day, so that reserves are consumed almost entirely within a day.

g_T = effect of temperature growth of shoot using the canopy temperature $T_c(\kappa)$ (Equation (2.16)), given by

$$g_T(T_c) = \begin{cases} 0.0 & 0 < T_c(\kappa) \leq 10^\circ\text{C} \\ 66.66 \cdot 10^{-3} T_c + 0.6667 & 10 < T_c(\kappa) \leq 25^\circ\text{C} \\ 1.0 & 25 < T_c(\kappa) \leq 35^\circ\text{C} \\ -0.200 T_c + 8.0 & 35 < T_c(\kappa) \leq 40^\circ\text{C} \end{cases} \quad (2.18)$$

(growth is optimal in the temperature window 25 to 35°C)

g_p = effect of water status on growth of shoot given by

$$g_p(\psi_p) = 0.9965 + 0.21909 \psi_p + 1.9125 \cdot 10^{-2} \psi_p^2 + 575.7806 \cdot 10^{-6} \psi_p^3$$

which accounts for the fact that due to the functional balance between root and shoot, growth of root is favored at more negative plant water potentials while shoot growth is favored at less negative potentials.

The shoot weight is found from

$$W_S(\kappa+1) = W_S(\kappa) + G_S(\kappa)\Delta t = W_S(\kappa) + \text{RES}(\kappa) r_c g_T(T_c(\kappa)) g_p(\psi_p(\kappa+1))\Delta t \quad (2.19)$$

where Δt = time step of the simulation (in s).

Similarly, the growth rate of young roots is

$$G_R(\kappa) = \text{RES}(\kappa) r_c g_T(T_S(\kappa)) [1 - g_p(\psi_p(\kappa+1))] \quad (2.20)$$

where the soil temperature $T_S(\kappa)$ is used in the growth function g_T .

For the expression of the root weight, we must consider that the produced root biomass is distributed over depth at a fraction $p_j(\kappa)$ for each soil compartment, and also that roots suberize and die at time constants $\tau_S = 5$ days and $\tau_r = 1$ year, respectively (both expressed in s). Then

$$RT_{yj}(\kappa+1) = RT_{yj}(\kappa) + \left[p_j(\kappa) G_R(\kappa) - \frac{RT_{yj}(\kappa)}{\tau_S} f_T(T_S(\kappa)) \right] \Delta t$$

$$RT_{oj}(\kappa+1) = RT_{oj}(\kappa) + \left[\frac{RT_{yj}(\kappa)}{\tau_S} f_T(T_S(\kappa)) - \frac{RT_{oj}(\kappa)}{\tau_r} \right] \Delta t$$

where $f_T(T_S(\kappa))$ is the effect of soil temperature on root suberization given by Equation (2.12). Protopapas and Bras (1987) compute the fractions $p_j(\kappa)$ so that the water uptake rate by the root system is maximized and, at the same time, certain biological constraints are satisfied. Clearly, any other model for the development of the root system can be used.

Rearranging terms and using Equation (2.19), we get

$$RT_{yj}(\kappa+1) = \left[1 - \frac{\Delta t}{\tau_S} f_T(T_S(\kappa)) \right] RT_{yj}(\kappa) + p_j(\kappa) \text{RES}(\kappa) r_c g_T(T_S(\kappa)) [1 - g_p(\psi_p(\kappa+1))] \quad (2.21)$$

$$RT_{oj}(\kappa+1) = \left(1 - \frac{\Delta t}{\tau_r} \right) RT_{oj}(\kappa) + \frac{\Delta t}{\tau_S} f_T(T_S(\kappa)) RT_{yj}(\kappa) \quad (2.22)$$

Equations (2.19), (2.21), and (2.22) propagate the weight of shoot and of young and old roots at each node respectively. For each of the two transpiration cases discussed previously the functional dependence of $T_c(\kappa)$ on state and inputs is different. During the night the equations are the same with use of the proper expression for the canopy temperature.

2.1.3 Reserve Weight

The products of photosynthesis are used for the growth and maintenance of the shoot and the root. The starch requirement for growth of shoot and root is

$$S_S(\kappa) = G_S(\kappa) c_G = RES(\kappa) r_c g_T(T_c(\kappa)) g_p(\psi_p(\kappa+1)) c_G \quad (2.23)$$

$$S_R(\kappa) = G_R(\kappa) c_G = RES(\kappa) r_c g_T(T_s(\kappa)) [1 - g_p(\psi_p(\kappa+1))] c_G \quad (2.24)$$

where c_G = conversion factor of starch to useful organic matter, where the different components of biomass (proteins, fats, lignin etc.) have been properly weighted (data from de Wit, et al., 1978)

$$= 1.41 \text{ kg-starch/kg-biomass}$$

The starch requirement for maintenance of shoot and root is

$$M_S(\kappa) = W_S(\kappa) c_M m(T_c(\kappa)) \quad (2.25)$$

$$M_R(\kappa) = \sum_j (R_{yj}(\kappa) + R_{oj}(\kappa)) c_M m(T_s(\kappa)) \quad (2.26)$$

where c_M = starch requirement for maintenance for a unit weight of biomass
 $= 0.0066 \text{ kg-starch/kg-biomass day.}$

$m(T)$ = effect of temperature on maintenance given by

$$m(T) = Q_{10}^{0.1T-2.5}$$

where Q_{10} = the augmentation of activity by increasing the temperature 10 degrees from 25° to 35°C, taken as 2

T = related temperature in °C, i.e., canopy temperature for the shoot and soil temperature for the root.

Having defined the starch requirements for growth and maintenance, the rate of use of reserves in Kg/HA s is

$$\left[\begin{array}{c} \text{rate of use of} \\ \text{reserves} \end{array} \right] = \left[\begin{array}{c} \text{starch requirement} \\ \text{for growth} \end{array} \right] + \left[\begin{array}{c} \text{starch requirement} \\ \text{for maintenance} \end{array} \right]$$

We then derive the state propagation equation to time $\kappa+1$ for the reserves by writing a mass balance equation for the starch in the plant in the form

$$RES(\kappa+1) = RES(\kappa) + \left\{ \left[\begin{array}{c} \text{rate of CO}_2 \text{ assimilation} \\ \text{equivalent in starch} \end{array} \right] - \left[\begin{array}{c} \text{rate of use} \\ \text{of reserves} \end{array} \right] \right\} \Delta t$$

$$RES(\kappa+1) = RES(\kappa) + \left[\frac{F_n(\kappa)}{1.629} - (S_S(\kappa) + S_R(\kappa) + M_S(\kappa) + M_R(\kappa)) \right] \Delta t$$

or

$$RES(\kappa+1) = RES(\kappa) \left[1 - r_c c_G \Delta t g_T(T_c(\kappa)) g_p(\psi_p(\kappa+1)) \right.$$

$$\left. - r_c c_G \Delta t g_T(T_s(\kappa)) [1 - g_p(\psi_p(\kappa+1))] \right] + \frac{F_n(\kappa)}{1.629} \Delta t$$

$$- c_M \Delta t \left[W_S(\kappa) m(T_c(\kappa)) + \sum_j (RT_{yj}(\kappa) + RT_{oj}(\kappa)) m(T_s(\kappa)) \right] \quad (2.27)$$

Again the proper expressions for $F_n(\kappa)$ and $T_c(\kappa)$ must be used for each case (Case I and II).

Equations (2.14) or (2.15), (2.18), (2.21), (2.22), and (2.27) are the propagation equations for each plant state variable. As promised in the introductory section 2.1, these equations can be written in short form as

$$x_p(\kappa+1) = f_p(x_p(\kappa), \xi(\kappa), x_s(\kappa)) \quad (2.28)$$

where $x_p(\kappa)$ = vector with the plant state variables at time κ

$\xi(\kappa)$ = vector with the climatic inputs, and

$x_s(\kappa)$ = vector with the soil state variables, as defined before.

2.2 SOIL STATE VARIABLES: THE TRANSPORT MODELS

The computation of the time-varying moisture and salinity profiles over depth requires the numerical solution of the relevant moisture and solute transport partial differential equations. In the following sections, we summarize the matrix forms, which approximate the solutions of the governing equations at discrete nodes. The full discretization procedure is presented in Protopapas and Bras (1986). These matrix forms lead directly to a non-linear state-space formulation of the transport models in terms of the soil state variables, namely the soil matric potential and the solute concentration at each nodal point, denoted collectively as a vector $x_s(\kappa)$. Again the matrices depend on the vectors of plant and soil state variables at the previous time step κ , on the climatic inputs $\xi(\kappa)$ and on a vector of time-invariant soil parameters, denoted as ζ , which are used to parameterize the soil hydraulic properties, namely the soil hydraulic conductivity and the soil moisture retention curve. The general form of the system of nonlinear equations, which propagate the soil state variables is

$$A(x_s(\kappa), \zeta) x_s(\kappa+1) = B(x_s(\kappa), \zeta, \xi(\kappa), x_p(\kappa))$$

2.2.1 Soil Matrix Potential

Assuming a) a heterogeneous and nondeforming soil, and b) one-dimensional (vertical), transient, one-phase, incompressible and isothermal flow, the combination of conservation of mass and Darcy's equation for an unsaturated soil leads to the following governing expression,

$$\frac{\partial \psi}{\partial t} = \frac{1}{C(\psi)} \frac{\partial}{\partial z} [K(\psi) \left(\frac{\partial \psi}{\partial z} + 1 \right)] - \frac{S(\psi)}{C(\psi)} \quad (2.29)$$

where $C(\psi) = \frac{d\theta}{d\psi}$ = differential soil moisture capacity (in cm^{-1})

ψ = soil matrix potential, other components such as osmotic and pneumatic potentials being ignored in the flow problem (in cm)

θ = volumetric soil moisture content, water volume per bulk volume (in cm^3/cm^3)

t = time (in days)

z = vertical coordinate with origin at the soil surface (in cm) (positive upwards)

S = volume of water uptaken by the root system per unit bulk volume of soil and unit time (in cm^3/cm^3 day; i.e., day^{-1})

$K(\psi)$ = hydraulic conductivity as a function of matrix potential ψ (in cm/day).

The above is a non-linear partial differential equation with analytical solution only under certain assumptions (Chapter 3). The numerical solution of this equation requires the soil properties $K(\psi)$ and $C(\psi)$, the sink function $S(\psi)$ and a set of boundary and initial conditions.

Typical soil hydraulic properties can be described by using a small number of soil parameters (Section 6.1). The sink term $S(\psi)$ is simply the water uptake rate (Equation (2.10)) per unit of depth in consistent units, i.e., per day. As initial conditions, either the pressure head $\psi(z)$ or the soil moisture $\theta(z)$ must be specified.

The discretization of the above partial differential equation using an implicit finite difference scheme as developed in Protopapas and Bras (1986) leads to a linear system of equations for the unknowns $\psi_{j(\kappa+1)}$ in the form (the notation ψ_j^κ and $\psi_{j(\kappa)}$ is equivalent)

$$\begin{bmatrix} \frac{\Delta z^2}{\Delta t} C(\psi_1^\kappa) + A_1 & & & & & & & & & & \\ & -D_2 & & & & & & & & & \\ & & \frac{\Delta z^2}{\Delta t} C(\psi_2^\kappa) + A_2 + D_2 & & & & & & & & \\ & & & \ddots & & & & & & & \\ & & & & -D_j & & \frac{\Delta z^2}{\Delta t} C(\psi_j^\kappa) + A_j + D_j & & & & \\ & & & & & \ddots & & & & & \\ & & & & & & & -D_{N-1} & & & \\ & & & & & & & & \frac{\Delta z^2}{\Delta t} C(\psi_{N-1}^\kappa) + A_{N-1} + D_{N-1} & & \\ & & & & & & & & & -D_N & \\ & & & & & & & & & & \frac{\Delta z^2}{\Delta t} C(\psi_N^\kappa) + D_N \end{bmatrix} \begin{bmatrix} \psi_1^{\kappa+1} \\ \psi_2^{\kappa+1} \\ \vdots \\ \psi_j^{\kappa+1} \\ \vdots \\ \psi_{N-1}^{\kappa+1} \\ \psi_N^{\kappa+1} \end{bmatrix}$$

$$= \begin{bmatrix} \frac{\Delta z^2}{\Delta t} \psi_1^\kappa - \Delta z q_t^\kappa - \Delta z A_1 - \Delta z^2 S(\psi_1^\kappa) \\ \frac{\Delta z^2}{\Delta t} \psi_2^\kappa + \Delta z D_2 - \Delta z A_2 - \Delta z^2 S(\psi_2^\kappa) \\ \vdots \\ \frac{\Delta z^2}{\Delta t} \psi_j^\kappa + \Delta z D_j - \Delta z A_j - \Delta z^2 S(\psi_j^\kappa) \\ \vdots \\ \frac{\Delta z^2}{\Delta t} \psi_{N-1}^\kappa + \Delta z D_{N-1} - \Delta z A_{N-1} - \Delta z^2 S(\psi_{N-1}^\kappa) \\ \frac{\Delta z^2}{\Delta t} \psi_N^\kappa + \Delta z D_N + \Delta z q_b^\kappa - \Delta z^2 S(\psi_N^\kappa) \end{bmatrix} \quad (2.30)$$

In the above equations we use

N = number of unsaturated nodes of discretization

Δz = step size between nodes in cm

Δt = time step of simulation expressed in days

ψ_j^k = soil matric potential at node j at time κ in cm

$C(\psi_j^k)$ = differential soil moisture capacity at node j at time κ

$D_j^k = K(\psi_{j-1/2}^k)$ = hydraulic conductivity between nodes j and $j-1$ in cm/day which is taken to be the geometric mean, i.e.,

$$K(\psi_{j-1/2}^k) = \sqrt{K(\psi_j^k) K(\psi_{j-1}^k)}$$

$$A_j = K(\psi_{j+1/2}^k) = \sqrt{K(\psi_j^k) K(\psi_{j+1}^k)}$$

$S(\psi_j^k)$ = sink term at node j at time κ , i.e., volume of water uptaken by the root system per unit bulk volume of soil and unit time in day⁻¹ which is

$$S(\psi_j^k) = 8.64 \frac{U_j(\kappa)}{\Delta z} = \frac{8.64}{\Delta z} [\psi_{sj}(\kappa) - \psi_p(\kappa+1)] \frac{RT_{yj}(\kappa) + p RT_{oj}(\kappa)}{K_R} f_T(\kappa) f_{\psi_{sj}}(\kappa)$$

q_t^k = flux at the soil surface which is defined by the climatic and the soil conditions. The climatic forcing imposes a potential flux given as

$$q^*(0, \kappa) = e(\kappa) - r(\kappa)$$

where $e(\kappa)$ = evaporation flux (cm/day) given from

$$Le(\kappa) = 8.64 \frac{\Delta(\kappa)R_s(\kappa) + (e_s(\kappa) - e_a(\kappa)) \frac{\rho C_p}{r_b(\kappa)}}{\Delta(\kappa) + \gamma}$$

In the above, $R_s(\kappa)$ = net radiation reaching the soil surface in $J/m^2 s$

$r_b(\kappa)$ = boundary layer resistance given in s/m by an empirical relationship as

$$r_b(\kappa) = \frac{1147}{u(\kappa)}$$

$r(\kappa)$ = effective precipitation or irrigation flux (cm/day).

The feasible flux, which is the flux that can be handled by soil, depends on the moisture conditions in the soil and is found from

$$q(0, \kappa) = -K(\psi_{1/2}^K) \left[\frac{\psi_t^K - \psi_1^K}{\Delta z/2} + 1 \right]$$

where ψ_t^K = soil matric potential at the soil surface (cm).

During infiltration ($q^*(0, \kappa) \leq 0$, $q(0, \kappa) \leq 0$)

$$\psi_t^K = 0.0 \quad \text{and} \quad q_t^K = \max[q(0, \kappa), q^*(0, \kappa)]$$

During evaporation ($q^*(0, \kappa) > 0$, $q(0, \kappa) > 0$)

$$\psi_t^K = \psi_{\min} \quad \text{and} \quad q_t^K = \min[q(0, \kappa), q^*(0, \kappa)]$$

where ψ_{\min} = minimum soil potential corresponding to dry air conditions.

In any other case $q_t^K = 0.0$.

q_b^k = flux at the bottom of the soil column, which for the case of free drainage is equal to the saturated hydraulic conductivity of the bottom compartment K_s^b .

In short form the system of equations (2.30) can be written

$$A_f(\psi(\kappa), \zeta) \psi(\kappa+1) = e(\psi(\kappa), \zeta, x_p(\kappa), \xi(\kappa)) \quad (2.31)$$

where A_f = tridiagonal matrix (subscript f stands for flow)

$\psi(\kappa)$ = vector with the matric potentials at the nodes

ζ = vector with the soil parameters at the nodes which the parametric soil hydraulic properties $K(\psi_j^k)$ and $C(\psi_j^k)$, and

$x_p(\kappa)$ = vector with the plant state variables at time κ , as defined.

2.2.2 Solute Concentration

The equation of conservation of mass of a non-reactive solute under the assumptions of one-dimensional (vertical) unsaturated, transient flow is

$$\frac{\partial}{\partial t} (\theta c r_d) + \frac{\partial}{\partial z} (qc) = \frac{\partial}{\partial z} [D_s^*(\theta, u) \frac{\partial c}{\partial z}] \quad (2.32)$$

where θ = volumetric soil moisture content, solution volume per void volume

c = solute concentration, mass of solute per solution volume (in mg/l)

z = vertical coordinate (cm) with origin at the soil surface

(positive upwards)

r_d = retardation factor found from $r_d = 1 + \frac{\rho_b K_d}{\theta}$,

K_d = distribution coefficient (in l/mg),

ρ_b = bulk density of the nondeforming soil (in mg/l),

q = Darcy flux (cm/day)

u = actual velocity in the pores = $\frac{q}{\theta}$ (cm/day);

$D_s^*(\theta, u) = D_d^* \theta + \alpha_L |q|$ = coefficient of hydrodynamic dispersion (cm²/d)

D_d^* = molecular diffusivity (cm²/day), and

α_L = dispersivity of the soil medium (cm).

Numerical solution of this equation requires knowledge of the fluxes q and the soil moisture profile θ , which are obtained from the flow model; the dispersion coefficient $D_s^*(\theta, u)$; the soil properties K_d and ρ_b ; and a set of boundary and initial conditions.

As initial condition the concentration profile $c(z)$ is specified. The boundary condition at the soil surface and at the bottom either can be known solute concentration or known solute flux.

The discretization of the above partial differential equation using a Crank-Nicolson finite difference scheme as developed in Protopapas and Bras (1986) leads to a linear system of equations in the form

$$\begin{bmatrix} \cdot 1 & & & & & & & & & -1 \\ & \cdot & & & & & & & & \cdot \\ & & \cdot & & & & & & & \cdot \\ & & & \cdot & & & & & & \cdot \\ -Q_j^- - D_j^- & & \frac{\theta_j^{k+1}}{\Delta t} & & -Q_j^- + D_j^- + Q_j^+ + D_j^+ & & & & & Q_j^+ - D_j^+ \\ & & & \cdot & & & & & & \cdot \\ & & & & \cdot & & & & & \cdot \\ & & & & & \cdot & & & & \cdot \\ & & & & & & D_N^+ & & & \\ & & & & & & & \frac{q_b^k}{2\Delta z} - D_N^+ & & \\ & & & & & & & & & c_1^{k+1} \\ & & & & & & & & & \vdots \\ & & & & & & & & & c_j^{k+1} \\ & & & & & & & & & \vdots \\ & & & & & & & & & c_N^{k+1} \end{bmatrix} = \begin{bmatrix} c_1^{k+1} \\ \vdots \\ c_j^{k+1} \\ \vdots \\ c_N^{k+1} \end{bmatrix}$$

$$\begin{bmatrix} -1 & & & & & & & & & 1 \\ & \cdot & & & & & & & & \cdot \\ & & \cdot & & & & & & & \cdot \\ & & & \cdot & & & & & & \cdot \\ Q_j^- + D_j^- & & \frac{\theta_j^k}{\Delta t} & & -Q_j^- - D_j^- - Q_j^+ - D_j^+ & & & & & -Q_j^+ + D_j^+ \\ & & & \cdot & & & & & & \cdot \\ & & & & \cdot & & & & & \cdot \\ & & & & & \cdot & & & & \cdot \\ & & & & & & -D_N^+ & & & \\ & & & & & & & \frac{q_b^k}{2\Delta z} & & \\ & & & & & & & & & c_1^k \\ & & & & & & & & & \vdots \\ & & & & & & & & & c_j^k \\ & & & & & & & & & \vdots \\ & & & & & & & & & c_N^k \end{bmatrix} \begin{bmatrix} c_1^k \\ \vdots \\ c_j^k \\ \vdots \\ c_N^k \end{bmatrix} \quad (2.33)$$

In the above equations

$$Q_j^- = \frac{q_{j-1/2}^{\kappa+1/2}}{4\Delta z} = f(\psi(\kappa), \zeta) \quad ; \quad Q_j^+ = \frac{q_{j+1/2}^{\kappa+1/2}}{4\Delta z}$$

$$D_j^- = \frac{(D_s^*)_{j-1/2}^{\kappa+1/2}}{2\Delta z^2} = f(\psi(\kappa), \zeta; \alpha_L, D_d^*) \quad ; \quad D_j^+ = \frac{(D_s^*)_{j+1/2}^{\kappa+1/2}}{2\Delta z^2}$$

where we approximate $(\cdot)_j^{\kappa+1/2} \approx (\cdot)_j^\kappa$ for the linearization (Section 4.2.3).

The fluxes between the nodes are given as

$$q_{j+1/2}^\kappa = -K(\psi_{j+1/2}^\kappa) \left[\frac{\psi_j^\kappa - \psi_{j+1}^\kappa}{\Delta z} + 1 \right]$$

The above matrix form differs from the detailed development in Protopapas and Bras (1986) in that we use $r_d = 1$ and we exclude the additional term that approximates the second-order time derivatives in the Taylor series expansion in order to account for numerical dispersion. The boundary condition at the top is constant solute concentration during infiltration and zero solute flux otherwise. The boundary condition at the bottom is known solute flux as determined by the bottom moisture flux and the existing solutes.

In short form the system of equations (2.33) can be written as

$$A_s(\psi(\kappa), \zeta) c(\kappa+1) = B_s(\psi(\kappa), \zeta) c(\kappa) \quad (2.34)$$

where A_s = tridiagonal matrix (subscript s stands for solute transport)

$c(\kappa+1)$ = vector of the solute concentrations at the nodes

and the other vectors are as defined previously.

2.3 CASE STUDY SIMULATIONS

We have used the composite model developed in the previous sections with field data for a maize crop in Flevoland (Netherlands, latitude 52°) in 1972 (de Wit, et al., 1978). The plant density was 10 plants/m² and the crop was harvested to measure crop yield (total shoot weight) and leaf area index at regular time intervals of 7-14 days.

The weather conditions during the simulations are plotted and discussed in Section 5.1. A Panoche clay loam soil is assumed with soil properties as reported in Warrick, et al. (1971) (Figure 6.1, exponential form). The initial condition for soil moisture is a uniform value of 0.30 down to 50 cm depth and then a linear increase to a value of 0.37 at 125 cm. The inter-nodal spacing was 5 cm and the time step was 900 sec. The simulation starts on June 25 (day 175) and ends on September 10 (day 253). In Figures 2.2 and 2.3 we present the time trajectories of the state variables for a case of optimal growth (Photosynthesis controls Transpiration - Case I; initial salinity $c_0 = 6000$ mg/l; irrigation rate $r = 32$ cm/d for 7 hours every 7 days, that is 9.3 cm of water applied 10 times in the growing season), and for the opposite case (Transpiration controls Photosynthesis - Case II; $c_0 = 6000$ mg/l; no irrigation). The development of the root system in these results is modeled so that the uptake rate is maximized.

In the first case (Figure 2.2) the plant water potential is maintained close to zero for most of the time. Starting at a very negative value due to the high initial salinity, immediately after the first irrigation, the potential takes its optimal values. In the period between two irrigations, it is again reduced. This variable shows a clear diurnal pattern with

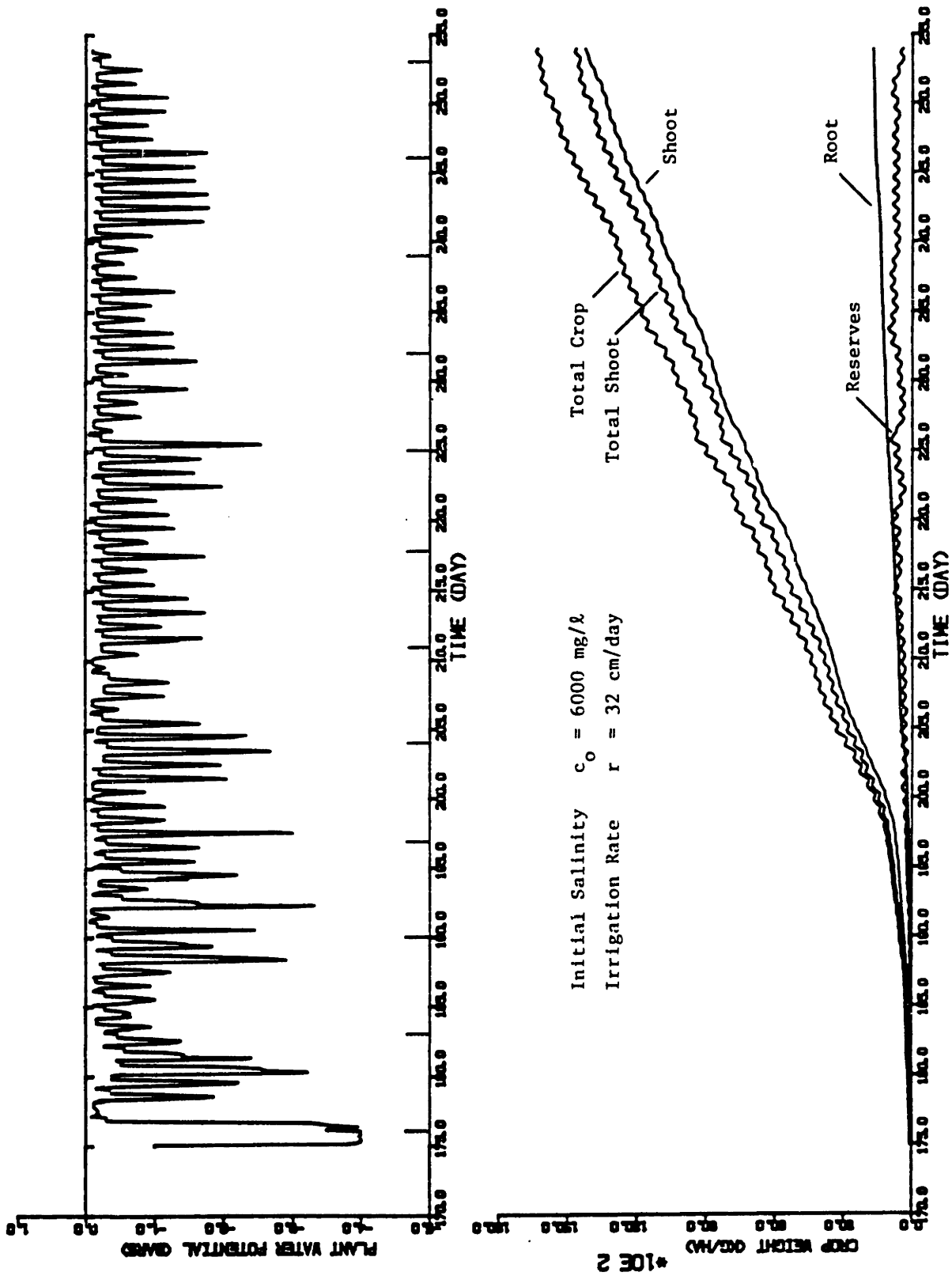


Figure 2.2 Time Evolution of State Variables (Case I: $c_0 = 6000 \text{ mg/l}$, $r = 32 \text{ cm/day}$) (Continued)

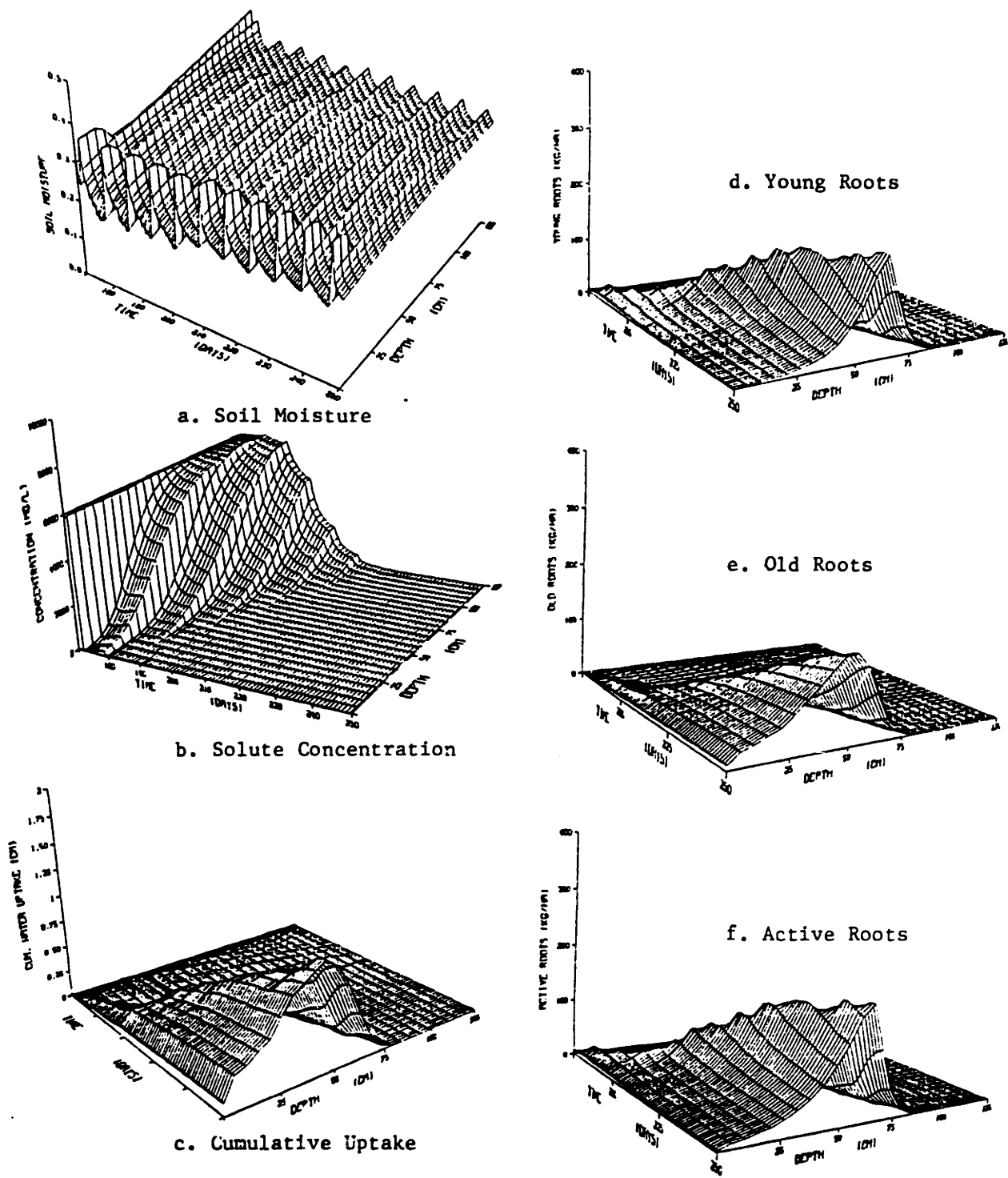


Figure 2.2 Time Evolution of State Variables
 (Case I: $c_0 = 6000 \text{ mg/l}$, $r = 32 \text{ cm/day}$)

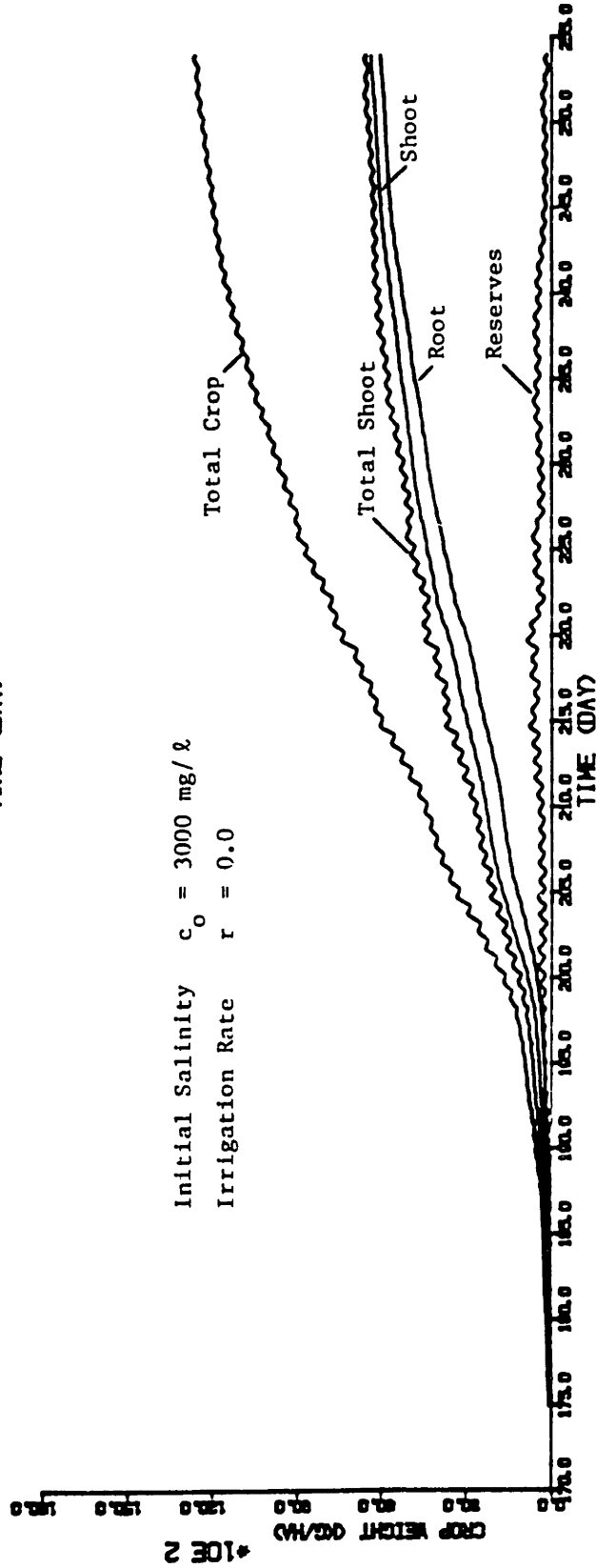
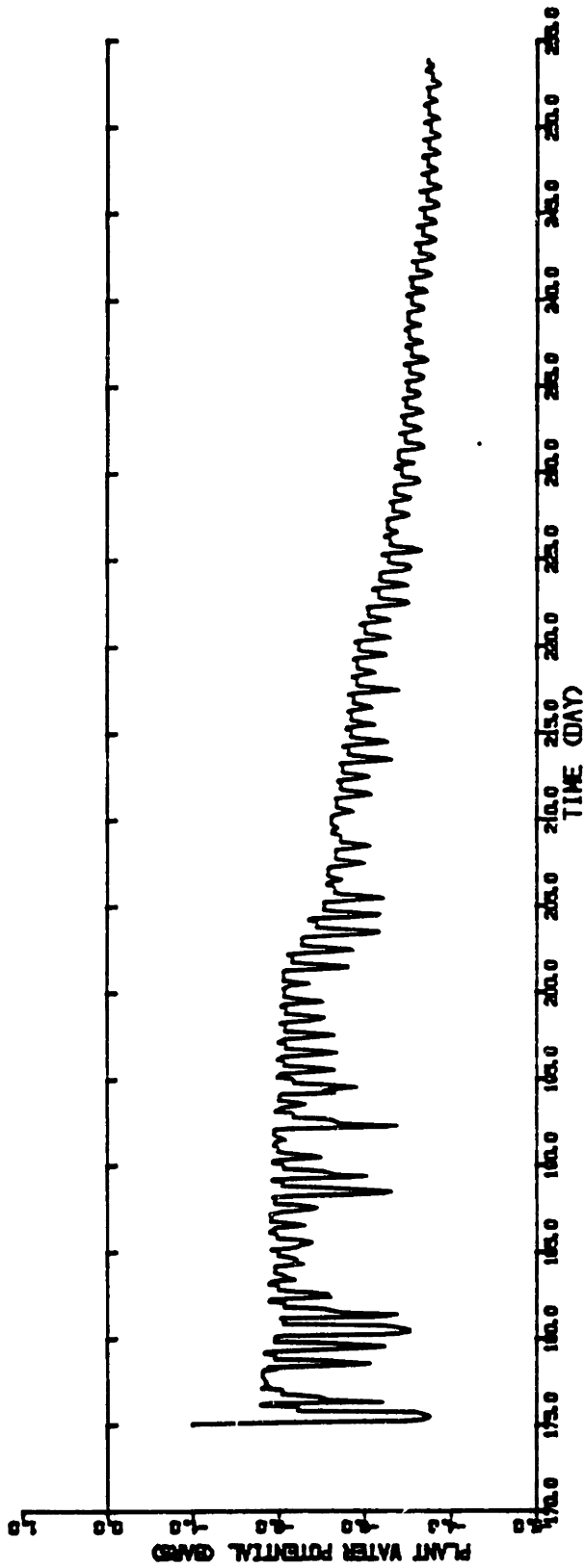
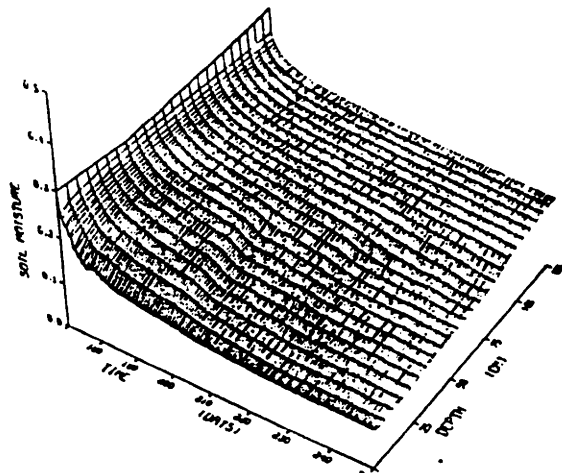
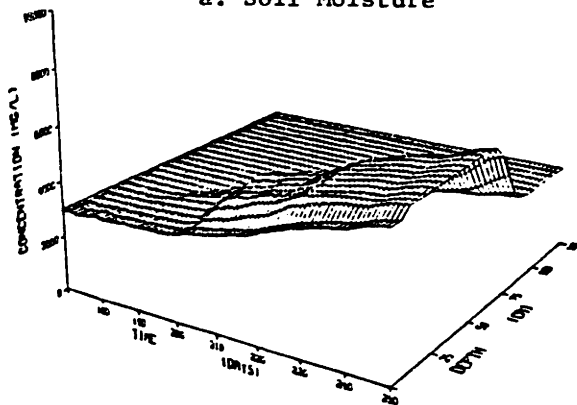


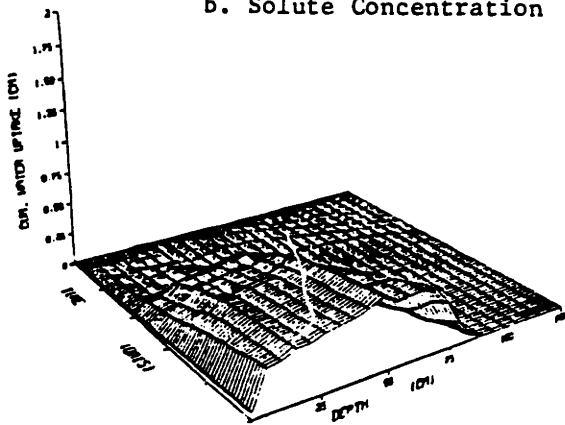
Figure 2.3 Time Evolution of State Variables (Case II: $c_0 = 3000 \text{ mg/l}$, $r = 0.0$) (Continued)



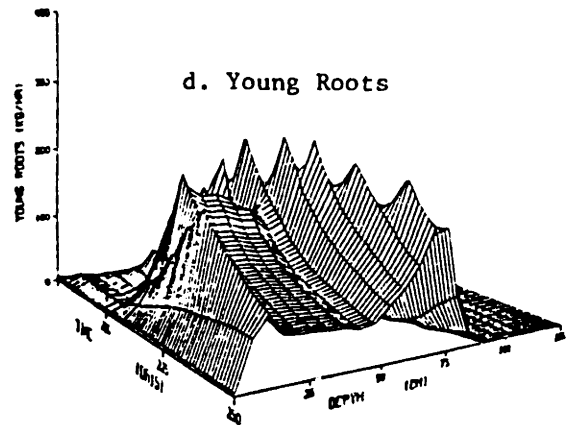
a. Soil Moisture



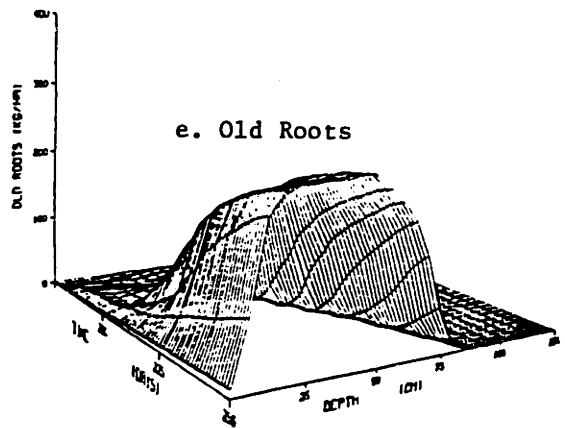
b. Solute Concentration



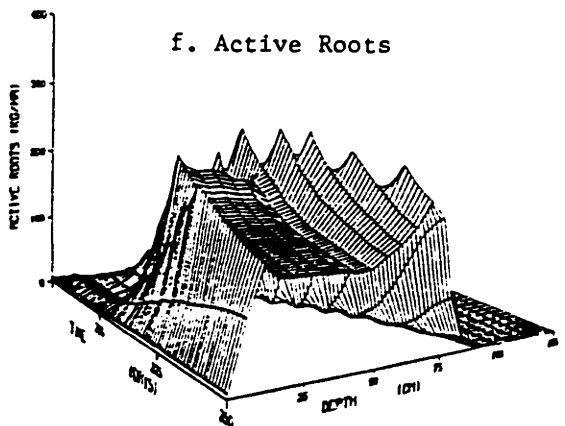
c. Cumulative Uptake



d. Young Roots



e. Old Roots



f. Active Roots

Figure 2.3 Time Evolution of State Variables
(Case II: $c_0 = 3000 \text{ mg/l}$, $r = 0.0$)

minimum value around noon time. The same pattern is also observed for the weight of reserves, since the absorbed visible radiation has its maximum at noon. Since the crop does not suffer a water stress most of the photosynthetically produced biomass is allocated to shoot growth. After an initial period of slow growth, the shoot weight increases almost linearly with time. The soil moisture (equivalent to the soil matric potential) shows the wetting of the soil profile immediately after each irrigation and the subsequent draining of the soil column to the field capacity level (about 0.20). The initial high concentration of salts gradually disappears after seven irrigations, as the solutes are leached below the soil profile. The root zone reaches the depth of 75 cm. The root system is asymmetric with more active part at about 60 cm.

In the second case (Figure 2.3) the plant water potential at night drops continuously to more negative values and the crop is under water stress throughout the growing season. The limited products of photosynthesis are equally distributed to root and shoot and the nonlinear response of the crop weights in time is apparent. The soil moisture profile dries continuously, while solutes are accumulated in the root zone due to water extraction by the root system. The roots develop deeper and more uniformly than in the previous case to a depth of 90 cm. Additional discussion and applications can be found in Protopapas and Bras (1985).

2.4 SUMMARY - COMMENTS

In this chapter we developed a dynamic conceptual model of the soil-crop-climate interactions in state-space form. In Section 2.1 we provided

the conceptual framework for crop simulation. In Section 2.2 we presented in detail the three components of the model, namely: 1) the plant growth model, representing processes such as CO₂ assimilation, transpiration, growth and maintenance of biomass, root distribution and water uptake over depth; 2) the moisture transport model, solving the unsaturated one-dimensional partial differential equation for flow; and 3) the solute transport model, solving the advection-dispersion equation for transport. In Section 2.3 we demonstrated the application of the composite model in two different cases.

The integrated soil-crop-climate model in the state-space form is a useful analytical tool for studying the links and interconnections of the physical processes above and below the soil surface. We intend to build on this idea in Chapters 5 and 6. Although there is need for additional overall testing of such models in the field along the lines of the work of Hoogenboom et al., (1987), the concepts used in this chapter for both the plant growth and the transport processes have been the object of numerous validation studies in controlled environments and, therefore, are well documented. The integrated approach helps one to see the whole picture and to understand the relative importance of soil and climatic factors. The sensitivity of the model predictions to the biological parameters also requires further study.

The model is also useful for evaluating irrigation practices. For example, we have used the model presented here to predict the crop production function, i.e., the crop response in time for different initial conditions and different irrigation policies. In our study we find that after a point the marginal contribution of additional irrigation to crop yield is minimal (Protopapas and Bras, 1986).

CHAPTER 3

MULTIDIMENSIONAL INFILTRATION IN HETEROGENEOUS SOILS

3.0 INTRODUCTION

In situations, such as irrigated farming or runoff generation, in which a relatively uniform application of water over a field has to be modeled, a one-dimensional approximation of the flow is commonly employed. If the soil medium is homogeneous this conceptualization is fully valid. In reality, however, field hydraulic properties vary in space (Nielsen et al., 1973; and many others). Nevertheless, the one-dimensional approximation has been commonly used without much investigation of its accuracy. If the approximation is justified for the moisture transport problem, we can argue that the one-dimensional soil-crop-climate model of the previous Chapter 2 is a good description of the processes at local areas over the field.

In this chapter we attempt to check the error introduced by modeling a heterogeneous soil as a set of noninteracting soil columns. In Section 3.1 we give the general formulation of the approach used in assessing the significance of lateral fluxes in multidimensional infiltration. In Section 3.2 we develop the three-dimensional water transport equation within a deterministic-analytical framework, but with soil properties varying in space. We defer to Appendix B a review and discussion of various other methodologies that have been used to study the same problem. In Section 3.3, we summarize analytical solutions for one- and two-dimensional problems for a special form of the variation of saturated hydraulic conductivity in space, giving the details of the derivation in Appendix C. The results indicate that for a time period, which depends on the the uniformity of the imposed

infiltrating source and the scale of the fluctuations of the saturated hydraulic conductivity, the one-dimensional approximation is accurate. In Section 3.4 numerical studies are carried out for more complicated soil formations and are used to test the ideas gained from the analytical solutions. The material in this chapter is quite independent from the other chapters and the reader should be alert to the sometimes identical and confusing notation used for otherwise unrelated variables.

3.1 GENERAL FORMULATION

When studying multidimensional infiltration in heterogeneous soils, we are concerned about the significance of the lateral fluxes. The reasons for lateral flow can be identified as:

- soil heterogeneity and anisotropy;
- topographic nonuniformity on the surface; and
- lateral moisture gradients due to localized boundary conditions.

In studying runoff generation mechanisms and its sensitivity to soil hydraulic parameters several researchers have proposed different models. Milly and Eagleson (1982) give a hierarchy of increasingly simplified such models, which deal with the two- and three-dimensional flow problem. Apparently direct solution of the three-dimensional boundary value problem with spatially varying soil properties and including the dynamics of overland flow is the most general approach. Unfortunately at this stage numerical solutions of this problem are not available. Assuming uniformity in one lateral direction the two-dimensional cross-sectional model can be used as a substitute (Zaslavsky and Sinai, 1981). Further assuming that lateral flows are negligible, the two-dimensional problem reduces to a number of one-

dimensional vertical problems in neighboring non-interacting soil columns. Using such a model, Hillel and Hornberger (1979) study the sensitivity of runoff to clay/loam fraction and relative location on a hillslope. A further simplifying step is to use a simple lumped infiltration model instead of the partial differential equation, but still using a model for the overland flow in the horizontal direction, as in the previous cases. Freeze (1980) relaxes also this last constraint. He studied storm surface runoff from a hillslope, assuming that precipitation that cannot infiltrate where it falls is simply drained. He uses stochastic fields for storm parameters, soil properties, topography, and initial conditions.

Many authors have employed the one-dimensional approximation of the soil system (Milly and Eagleson, 1982; Russo and Bresler, 1981; Dagan and Bresler, 1983) but its justification in the literature is very limited. It is not known whether it is equally good for all types of soil or whether it is invalid due to soil heterogeneity or nonuniform boundary conditions at the soil surface. We address these questions in the present chapter.

Our approach is to consider the soil medium as a set of decoupled soil columns with different soil properties and derive solutions to the flow problem for each one of them in a dimensionless form. Then for any realization of soil properties in space the one-dimensional solution can be used to obtain an approximation for the multidimensional flow problem. Finally, we also solve the multidimensional flow equation and compare the approximation to the exact solution. We limit our study only to variations of saturated hydraulic conductivity in space.

The problem of water transport in an unsaturated porous medium has been studied by analytical or numerical techniques in a deterministic or

a stochastic framework. In this chapter we adopt the deterministic-analytical viewpoint to check our hypothesis. The analytical method requires restrictive assumptions, the hydraulic conductivity must be an exponential function of the pressure head and a linear function of the soil moisture. With these assumptions the multidimensional flow equation can be linearized and solved (Raats, 1971; Philip, 1972; Warrick and Lomen, 1976; Batu, 1982). The numerical method can solve problems with complex soil formations and different boundary conditions (Perrens and Watson, 1977; U. S. Nuclear Regulatory Commission, 1983; many others).

3.2 THE THREE-DIMENSIONAL WATER TRANSPORT EQUATION

Consider the problem of water transport in an unsaturated porous medium with spatially varying hydraulic properties. Under the assumptions of:

- a. heterogeneous, nondeforming and isotropic soil, and
- b. transient, one-phase, incompressible and isothermal flow,

the conservation of mass equation in a soil column is:

$$\frac{\partial \theta}{\partial t} + \nabla \cdot \underline{q} = 0 \quad (3.1)$$

where θ = volumetric soil moisture content, water volume per bulk volume
(cm^3/cm^3);

t = time (days);

q = soil moisture flux (cm/day),

Darcy's equation gives

$$\underline{q} = -K(\underline{r}, \psi) \nabla \psi = -K(\underline{r}, \psi) \nabla \psi + K(\underline{r}, \psi) \nabla z \quad (3.2)$$

where $K(\underline{r}, \psi)$ = hydraulic conductivity (cm/day),

ψ = hydraulic head (cm), which is assumed to be the sum of the matric potential ψ and the gravitational potential z , other components like osmotic and pneumatic potential being negligible (the vertical coordinate z has been assumed positive downwards), and

$$\underline{r} = \text{vector of spatial coordinates} = [x \ y \ z]^T = [r_x \ r_y \ r_z]^T.$$

Substituting Equation (3.2) in Equation (3.1) we find

$$\frac{\partial \theta}{\partial t} = \frac{\partial}{\partial x} \left(K(\underline{r}, \psi) \frac{\partial \psi}{\partial x} \right) + \frac{\partial}{\partial y} \left(K(\underline{r}, \psi) \frac{\partial \psi}{\partial y} \right) + \frac{\partial}{\partial z} \left(K(\underline{r}, \psi) \left(\frac{\partial \psi}{\partial z} - 1 \right) \right) \quad (3.3)$$

and using $C(\underline{r}, \psi) = \frac{\partial \theta}{\partial \psi}$ where $C(\psi)$ is the differential moisture capacity

(cm^{-1}), we obtain the governing flow equation

$$C(\underline{r}, \psi) \frac{\partial \psi}{\partial t} = \frac{\partial}{\partial x} \left(K(\underline{r}, \psi) \frac{\partial \psi}{\partial x} \right) + \frac{\partial}{\partial y} \left(K(\underline{r}, \psi) \frac{\partial \psi}{\partial y} \right) + \frac{\partial}{\partial z} \left(K(\underline{r}, \psi) \left(\frac{\partial \psi}{\partial z} - 1 \right) \right) \quad (3.4)$$

with initial condition $\psi(\underline{r}, 0) = \psi(\underline{r})$ known.

For the infiltration problem the boundary condition at the soil surface is defined as follows:

- the climatic forcing or irrigation practice imposes a potential flux

$$v^*(\underline{r}, t) \Big|_{z=0}.$$

- the feasible flux, i.e., the flux that can be handled by the soil, the ability of which to transmit water depends on the soil moisture conditions, is

$$v(\underline{r}, t) \Big|_{z=0} = -K(\underline{r}, \psi) \left(\frac{\partial \psi}{\partial z} - 1 \right) \Big|_{z=0}$$

During infiltration the fluxes are positive and the actual flux is

$$v_t(\underline{r}, t) \Big|_{z=0} = \min [v^*(\underline{r}, t) \Big|_{z=0}, v(\underline{r}, t) \Big|_{z=0}]$$

In this case the surface is saturated, implying that $\psi(\underline{r}, t) \Big|_{z=0} = 0.0$ in the region of the infiltrating source and $\psi(\underline{r}, t) \Big|_{z=0} = -\infty$ outside this region.

The boundary conditions far away from the sources are

$$\psi(\underline{r}, t) \rightarrow -\infty \quad \text{and} \quad \frac{\partial \psi}{\partial r_i} \rightarrow 0 \quad \text{as} \quad x^2 + y^2 + z^2 \rightarrow \infty.$$

The deterministic-analytical study of Equation (3.4) is based on the fact that the transformation $\Theta = \int_{-\infty}^{\psi} K(\underline{r}, \psi) d\psi$ linearizes the flow equation for heterogeneous isotropic media provided that an exponential dependence of the hydraulic conductivity on the pressure head holds, $K(\underline{r}, \psi) = K_s(\underline{r})e^{\alpha\psi}$, where $K_s(\underline{r})$ = saturated hydraulic conductivity (cm/day), and

α = capillarity index (cm^{-1}), $\alpha > 0$. Then,

$$\Theta(\underline{r}, \psi) = \int_{-\infty}^{\psi} K_s(\underline{r})e^{\alpha\psi} d\psi = K_s(\underline{r}) \int_{-\infty}^{\psi} e^{\alpha\psi} d\psi = \frac{K_s(\underline{r})e^{\alpha\psi}}{\alpha} = \frac{K(\underline{r}, \psi)}{\alpha}$$

By direct differentiation of above result we get

$$\frac{\partial \theta}{\partial r_i} = \frac{\partial k_s(\underline{r})}{\partial r_i} \frac{e^{\alpha \psi}}{\alpha} + K(\underline{r}, \psi) \frac{\partial \psi}{\partial r_i}$$

The gradient of θ is then expressed as

$$\nabla \theta(\underline{r}, \psi) = K(\underline{r}, \psi) \nabla \psi + \frac{1}{K_s(\underline{r})} \nabla K_s(\underline{r}) \theta(\underline{r}, \psi) = K(\underline{r}, \psi) \nabla \psi + \nabla \ln K_s(\underline{r}) \theta(\underline{r}, \psi) \quad (3.5)$$

Using Equation (3.5) in Equation (3.2), and then substituting in (3.1) yields

$$\begin{aligned} \frac{\partial \theta}{\partial t} &= \nabla \cdot [\nabla \theta(\underline{r}, \psi) - \nabla \ln K_s(\underline{r}) \theta(\underline{r}, \psi)] - \frac{\partial K(\underline{r}, \psi)}{\partial z} \\ \frac{\partial \theta}{\partial t} &= \nabla^2 \theta(\underline{r}, \psi) - \frac{\partial \ln K_s}{\partial x} \frac{\partial \theta(\underline{r}, \psi)}{\partial x} - \frac{\partial \ln K_s}{\partial y} \frac{\partial \theta(\underline{r}, \psi)}{\partial y} \\ &\quad - \left(\frac{\partial \ln K_s}{\partial z} + \alpha \right) \frac{\partial \theta(\underline{r}, \psi)}{\partial z} - \nabla^2 \ln K_s(\underline{r}) \theta(\underline{r}, \psi) \end{aligned}$$

If we adopt a deterministic exponential variation of the saturated hydraulic conductivity in space in the form $K_s(\underline{r}) = K_o \exp[-\lambda_x |x| - \lambda_y |y| - \lambda_z |z|]$, where $\lambda_x, \lambda_y, \lambda_z > 0$ can be interpreted as length constants showing how fast the conductivity decreases in each physical direction away from a region of high conductivity at the origin, we can verify that $\frac{\partial \ln K_s}{\partial r_i} = -\lambda_i, (x, y, z > 0)$

and $\frac{\partial^2 \nabla \ln K_s}{\partial r_i^2} = 0$, resulting in

$$\frac{\partial \theta}{\partial t} = \nabla^2 \theta(\underline{r}, \psi) + \lambda_x \frac{\partial \theta}{\partial x} + \lambda_y \frac{\partial \theta}{\partial y} + (\lambda_z - \alpha) \frac{\partial \theta}{\partial z}$$

Clearly the steady state problem has already been linearized. For the unsteady problem we write (dropping for a moment the dependence of the involved variables on the spatial coordinates \underline{x})

$$\frac{\partial \theta}{\partial t} = \frac{\partial \theta}{\partial K} \frac{\partial K}{\partial t} = \frac{\partial \theta}{\partial K} \alpha \frac{\partial \theta}{\partial t} = \alpha \frac{\partial \theta}{\partial K} \frac{\partial \theta}{\partial t}$$

If we introduce $\frac{\partial K}{\partial \theta} = \mu$, where $\mu > 0$, implying that the hydraulic conductivity increases linearly with soil moisture, we get

$$K = \mu \theta = K_s(\underline{x}) e^{\alpha \theta} \quad \text{or} \quad \theta = \frac{1}{\mu} K_s(\underline{x}) e^{\alpha \theta} = \theta_s(\underline{x}) e^{\alpha \theta}$$

This assumption means that the dependence of both K and θ on the matric potential is identical and the spatial variation of porosity is similar (with a proportionality factor $1/\mu$) to that of saturated hydraulic conductivity.

The validity of the above assumption is discussed in Ben-Asher et al., (1978). Then

$$\frac{\partial \theta}{\partial t} = \frac{\mu}{\alpha} \nabla^2 \theta + \frac{\lambda_x \mu}{\alpha} \frac{\partial \theta}{\partial x} + \frac{\lambda_y \mu}{\alpha} \frac{\partial \theta}{\partial y} + \frac{(\lambda_z - \alpha) \mu}{\alpha} \frac{\partial \theta}{\partial z} \quad (3.6)$$

while the most general form of the above equation is

$$\alpha \frac{\partial \theta}{\partial K} \frac{\partial \theta}{\partial t} = \nabla^2 \theta - \frac{\partial \ln K_s}{\partial x} \frac{\partial \theta}{\partial x} - \frac{\partial \ln K_s}{\partial y} \frac{\partial \theta}{\partial y} - \left(\frac{\partial \ln K_s}{\partial z} + \alpha \right) \frac{\partial \theta}{\partial z} - \nabla^2 \ln K_s \theta \quad (3.7)$$

Notice that since $\theta = \frac{K(\underline{x}, \psi)}{\alpha} = \frac{\mu \theta}{\alpha}$, the variables θ, θ are related through a soil dependent proportionality factor.

The fluxes are computed as:

$$v = -K(\underline{r}, \psi) \left(\frac{\partial \psi}{\partial z} - 1 \right) = - \left(\frac{\partial \theta}{\partial z} + \lambda_z \frac{K(\underline{r}, \psi)}{\alpha} \right) + K(\underline{r}, \psi) = - \frac{\partial \theta}{\partial z} + (\alpha - \lambda_z) \theta$$

$$u = -K(\underline{r}, \psi) \frac{\partial \psi}{\partial x} = - \left(\frac{\partial \theta}{\partial x} + \lambda_x \frac{K(\underline{r}, \psi)}{\alpha} \right) = - \frac{\partial \theta}{\partial x} - \lambda_x \theta$$

$$\omega = -K(\underline{r}, \psi) \frac{\partial \psi}{\partial y} = - \left(\frac{\partial \theta}{\partial y} + \lambda_y \frac{K(\underline{r}, \psi)}{\alpha} \right) = - \frac{\partial \theta}{\partial y} - \lambda_y \theta$$

where v = vertical moisture flux (cm/day), and

u, ω = horizontal moisture fluxes (cm/day).

This method to linearize the heat equation with conductivities dependent on the unknown variable dates back to the studies of Kirchoff. Equation (3.6) is applicable in the problems of steady state infiltration from point and line sources in a homogeneous soil (Raats, 1971) or in a heterogeneous soil in the vertical direction (Philip, 1972; Philip and Forester, 1975). Other related studies deal with unsteady infiltration from strip sources in homogeneous soils (Warrick and Lomen, 1976; Batu, 1982). We should emphasize that only Philip(1972) deals with the one-dimensional infiltration in a vertically heterogeneous soil. Equations (3.6) and (3.7) have not been derived in the literature.

In the next section new one- and two-dimensional analytical solutions are presented for infiltration in heterogeneous soils, using the linearized Equation (3.6). Technically Equation (3.6) is an advection-dispersion equation, which has been studied in different context. Solutions are reported in Cleary and Ungs (1978) (one-, two- and three-dimensional) and in van Genuchten and Alves (1982) (one-dimensional).

In Appendix B we present the deterministic-numerical and the

stochastic-analytical and numerical approaches used by other investigators to study the issue of multidimensional unsaturated flow in porous media. There we summarize their findings about the extent of lateral versus vertical flow during infiltration events.

3.3 INFILTRATION IN HETEROGENEOUS SOILS: NEW ANALYTICAL SOLUTIONS

3.3.1 Unsteady One-Dimensional Unsaturated Flow

If the soil is heterogeneous in the vertical direction, the governing one-dimensional version of Equation (3.6) is

$$\frac{\partial \theta}{\partial t} = \frac{\mu}{\alpha} \frac{\partial^2 \theta}{\partial z^2} + \frac{(\lambda_z - \alpha)\mu}{\alpha} \frac{\partial \theta}{\partial z} \quad (3.8)$$

with initial condition

$$\theta(z, 0) = 0 \quad (3.9)$$

and boundary conditions

$$\theta(z, t) \rightarrow 0 \quad \text{as } z \rightarrow \infty \quad (3.10)$$

$$v = - \frac{\partial \theta}{\partial z} + (\alpha - \lambda_z) \theta \Big|_{z=0} = v_0 \quad (\text{known flux}) \quad (3.11a)$$

$$\theta(0, t) = \frac{K_0}{\alpha} \quad (\text{known } \psi(0, t) = 0) \quad (3.11b)$$

In these equations the parameters α and λ_z are positive. The z axis is positive downwards.

Introducing the dimensionless variables

$$Z = \frac{\alpha z}{2}, \quad X = \frac{\alpha x}{2}, \quad T = \frac{\alpha \mu t}{4}, \quad S_z = \frac{\lambda z}{\alpha}$$

we derive in Appendix C the following solutions:

A. Known Flux Boundary Condition

The final result in terms of the dimensionless variable Φ_f is

$$\begin{aligned} \Phi_f(Z, T) = \frac{\Theta \alpha}{2v_o} = \int_0^{\sqrt{T}} & \left[\frac{2}{\sqrt{\pi}} \exp\left\{Z(1-S_z) - (1-S_z)^2 \xi^2 - \frac{Z^2}{4\xi^2}\right\} \right. \\ & \left. - 2\xi(1-S_z) \exp\{2Z(1-S_z)\} \operatorname{erfc}\left\{\frac{Z}{2\xi} + (1-S_z)\xi\right\} \right] d\xi \end{aligned} \quad (3.12)$$

$$\Phi_f(Z, T) = \frac{\Theta \alpha}{2v_o} = \int_0^{\sqrt{T}} h_f(Z, \xi) d\xi$$

where $h_f(Z, \xi)$ is the function inside the large brackets in Equation (3.12).

B. Known Matrix Potential at Saturation at the Surface

In terms of the dimensionless variable Φ_p , we get the result

$$\Phi_p(Z, T) = \frac{\Theta \alpha}{K_o} = \int_0^{\sqrt{T}} \left[\frac{1}{\sqrt{\pi}} \frac{Z}{\xi^2} \exp\left\{(1-S_z)Z - (1-S_z)^2 \xi^2 - \frac{Z^2}{4\xi^2}\right\} \right] d\xi$$

$$\Phi_p(Z, T) = \frac{\Theta \alpha}{K_c} = \int_0^{\sqrt{T}} h_p(Z, \xi) d\xi \quad (3.13)$$

The behavior of the one-dimensional solutions in Equations (3.12) and (3.13) is shown in Figure 3.1 for $S_z = 0, 0.5$ and 1.0 and for different times.

3.3.2 Unsteady Two-Dimensional Unsaturated Flow

If the soil is heterogeneous in both the vertical and the horizontal direction with different length constants, Equation (3.6) takes the form:

$$\frac{\partial \theta}{\partial t} = \frac{\mu}{\alpha} \nabla^2 \theta + \frac{\lambda_x \mu}{\alpha} \frac{\partial \theta}{\partial x} + \frac{(\lambda_z - \alpha) \mu}{\alpha} \frac{\partial \theta}{\partial z} \quad (3.14)$$

with initial condition

$$\theta(x, z, 0) = 0 \quad (3.15)$$

and boundary conditions

$$\theta(x, z, t) \rightarrow 0 \quad \text{as } x^2 + z^2 \rightarrow \infty \quad (3.16)$$

$$u(x) = - \frac{\partial \theta}{\partial z} + (\alpha - \lambda_z) \theta \Big|_{z=0} = v_0(x) \quad (3.17a)$$

or

$$\theta(x, 0, t) = \begin{cases} \frac{K_s(x)}{\alpha} & \text{for } x \text{ in } \ell \\ 0 & \text{otherwise} \end{cases} \quad (3.17b)$$

where ℓ is the length of the infiltrating source. In these equations, the parameters $\alpha, \lambda_x, \lambda_z$ are positive. Also $z > 0$ and $-\infty < x < \infty$.

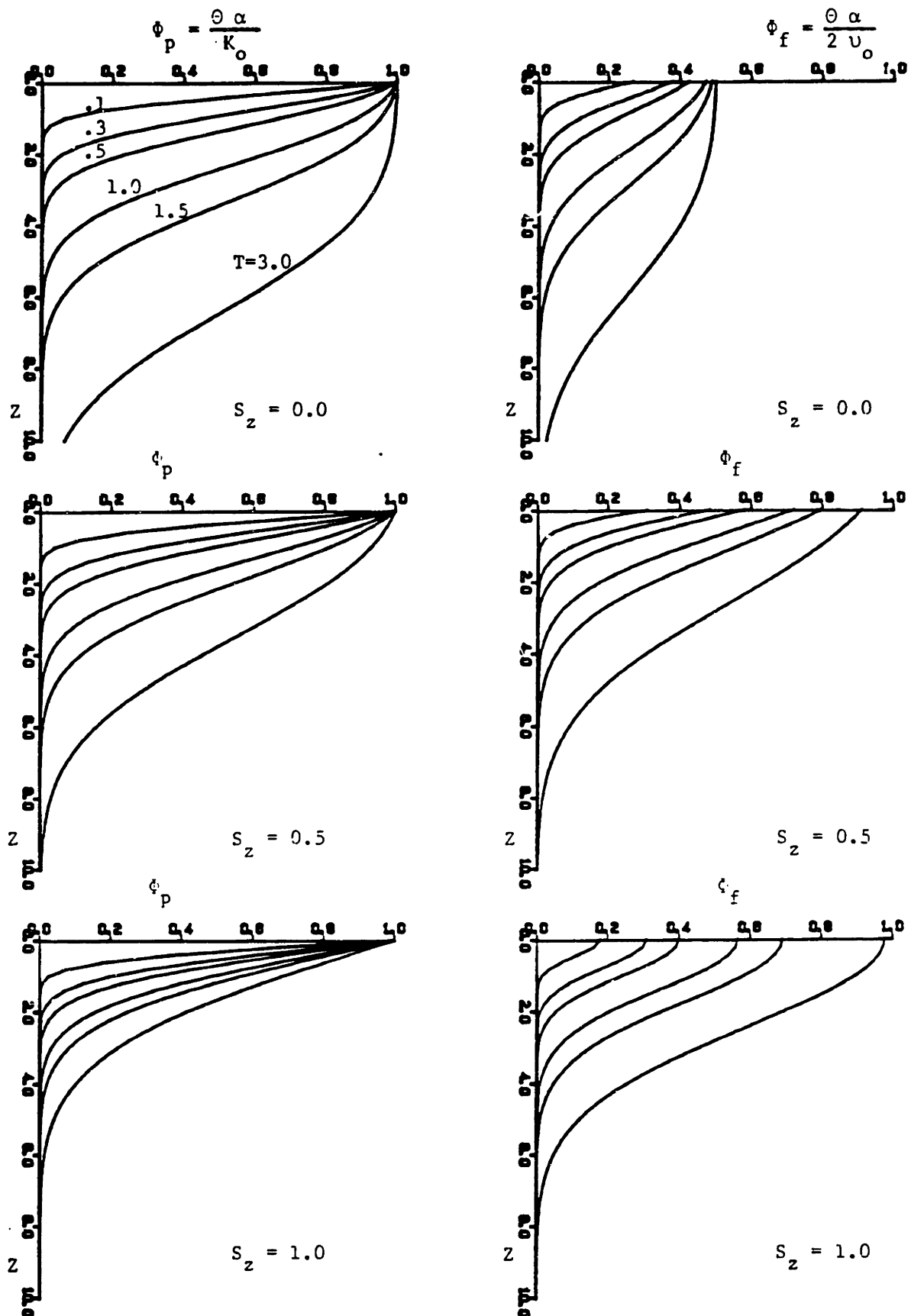


Figure 3.1 One-Dimensional Unsteady Infiltration Solutions with Constant Matric Potential at Saturation (left) and Constant Flux (right) Boundary Condition at the Surface.

The application of the known flux boundary condition deserves special attention. For heterogeneous soils in the x direction, the use of an arbitrary but known flux $\psi^*(x,0,t)$ is not appropriate. For example, in regions of low hydraulic conductivity the imposed flux may not be physically realizable and the solution can not represent the actual flow. In such cases the matric potential boundary condition should be used with $\psi(x,0,t) = 0.0$ (at saturation underneath the sources). In Appendix C we derive the solution to the known flux boundary condition problem for a localized flux at the origin, which is a valid case, and for a known constant flux of finite length which is correct only for a homogeneous soil in the horizontal ($S_x = 0$). The cases for known matric potential at saturation are also derived.

A. Known Flux Boundary Condition

i. Delta function flux at $x = 0$

Using the dimensionless variables defined previously and $S_x = \frac{\lambda_x}{\alpha}$ the solution for $x > 0$ (since θ is even in X, the solution is symmetric) is

$$\Phi_f(X,Z,T) = \frac{\theta\alpha}{2u_o} = \frac{1}{\sqrt{\pi}} \int_0^{\sqrt{T}} h_f(Z,\xi) \frac{1}{\xi} \exp\left\{-S_x^2 \xi^2 - \frac{x^2}{4\xi^2}\right\} \exp\{-S_x X\} d\xi \quad (3.18)$$

where $h_f(Z,\xi)$ is the same function as in Equation (3.12).

The behavior of this solution is shown in Figure 3.2 for the cases of a homogeneous soil, a heterogeneous in x soil with $S_x = 1.0$, $S_z = 0.0$ and a heterogeneous in z soil with $S_x = 0.0$, $S_z = 1.0$. In this and in the following figures the background gray tones become darker as the saturated hydraulic conductivity K_s decreases. Only the lower part (corresponding to later time) illustrates the shading.

ii. Uniform Flux of Finite Length

The solution takes the form, using the dimensionless source length $L = \frac{\alpha l}{2}$

$$\begin{aligned} \Phi_f(X, Z, T) &= \frac{\Theta\alpha}{2v_0} = \frac{1}{2} \int_0^{\sqrt{T}} h_f(Z, \xi) \exp\{-XS_x\} \\ &[\exp\{-XS_x\} [\operatorname{erf}\{S_x\xi - \frac{X}{2\xi}\} - \operatorname{erf}\{S_x\xi - \frac{L+X}{2\xi}\}] + \exp\{XS_x\} [\operatorname{erf}\{S_x\xi + \frac{X}{2\xi}\} \\ &- \operatorname{erf}\{S_x\xi - \frac{L-X}{2\xi}\}]] d\xi = \frac{1}{2} \int_0^{\sqrt{T}} h_f(Z, \xi) [\exp\{-2XS_x\} [\operatorname{erf}\{S_x\xi - \frac{X}{2\xi}\} \\ &- \operatorname{erf}\{S_x\xi - \frac{L-X}{2\xi}\}] + [\operatorname{erf}\{S_x\xi + \frac{X}{2\xi}\} - \operatorname{erf}\{S_x\xi - \frac{L-X}{2\xi}\}]] d\xi \quad (3.19) \end{aligned}$$

B. Known matrix potential at saturation

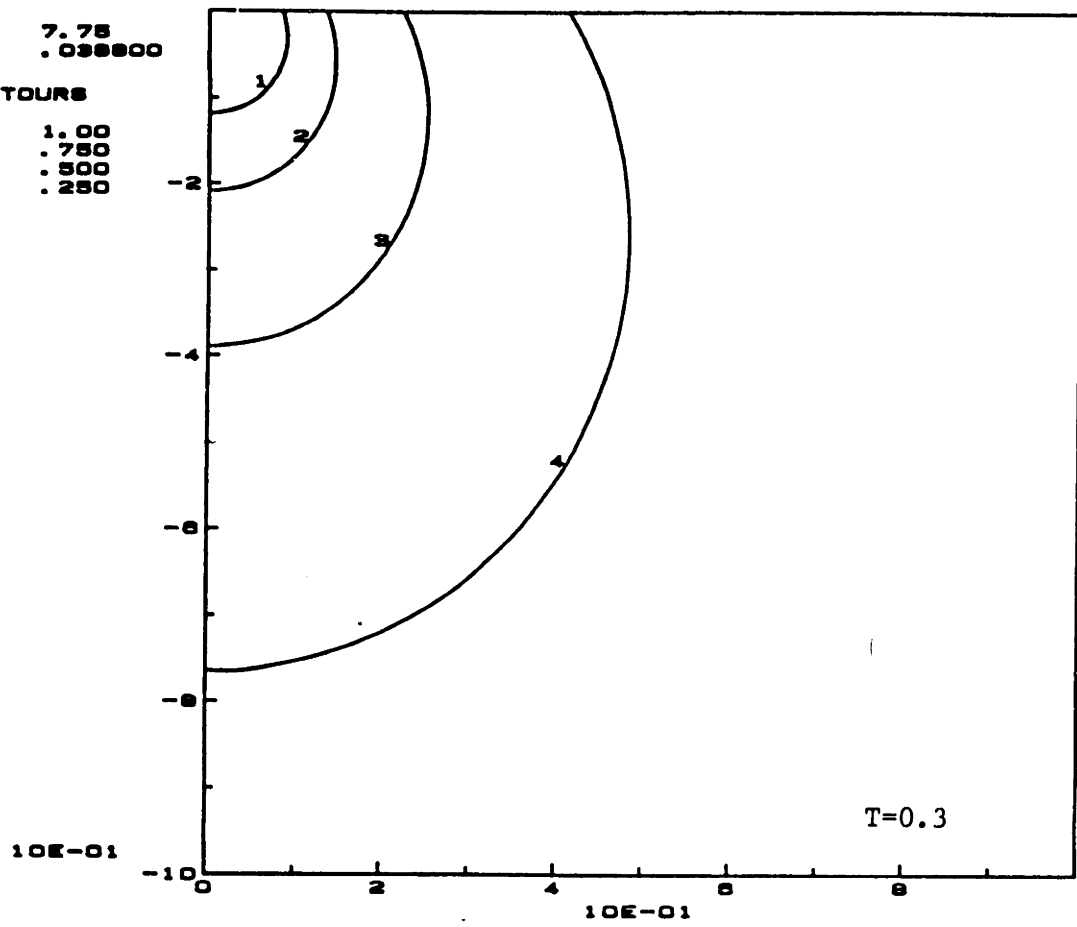
i. Infiltrating point source at the origin

$$\Phi_f(X, Z, T) = \frac{\Theta\alpha}{K_0} = \frac{2}{\sqrt{\pi}} \int_0^{\sqrt{T}} h_p(Z, \xi) \frac{1}{\xi} \exp\{-S_x^2\xi^2 - \frac{X^2}{4\xi^2}\} \exp\{-S_x X\} d\xi \quad (3.20)$$

MAX 7.75
MIN .038800

CONTOURS

1 1.00
2 .750
3 .500
4 .250



MAX 7.82000
MIN .082800

CONTOURS

1 1.00
2 .750
3 .500
4 .250

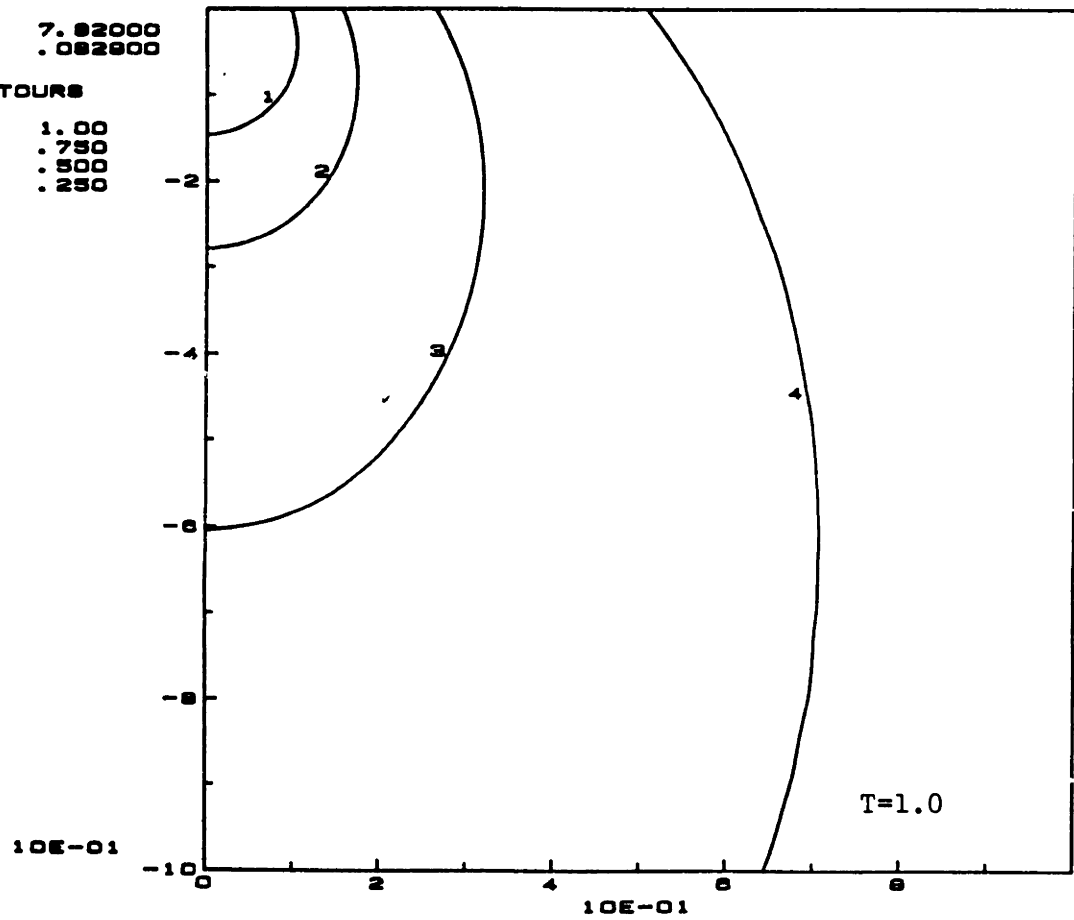
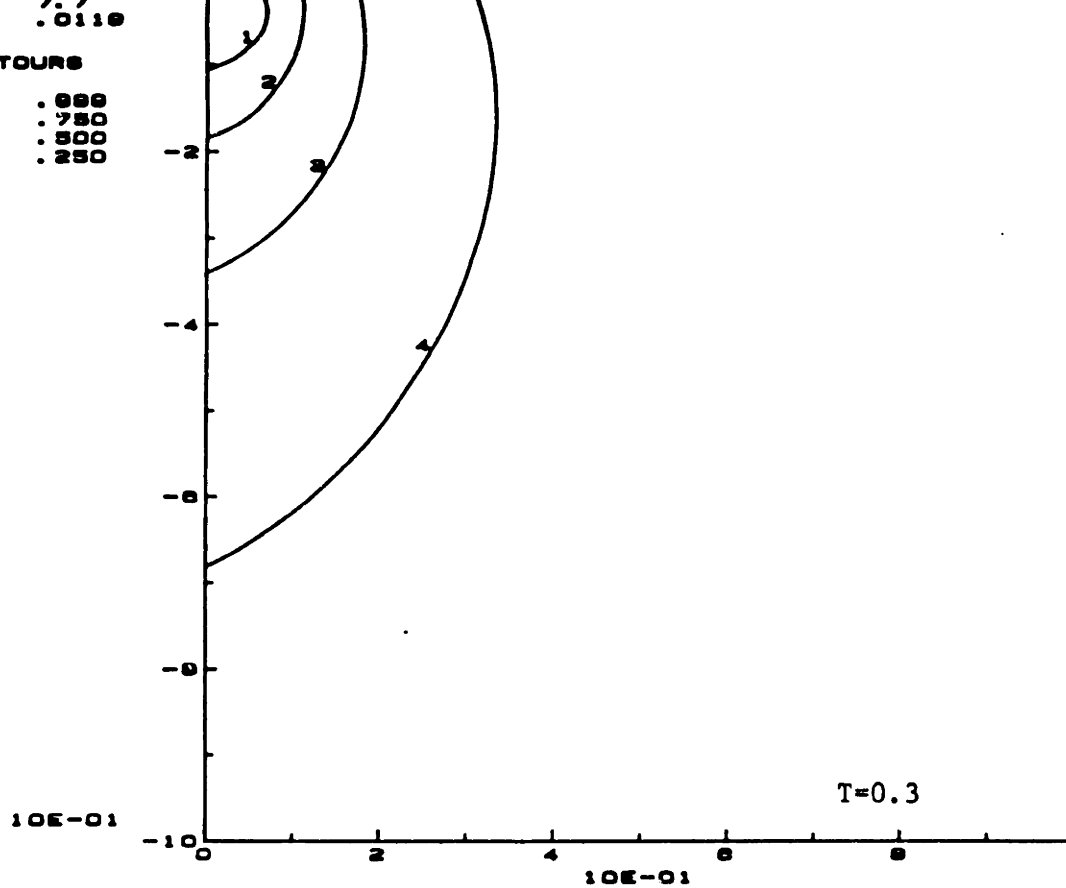


Figure 3.2a Line Source at the Origin (Delta Function Flux)
a. Homogeneous Soil ($S_x=0.0$, $S_z=0.0$)

MAX 7.75
MIN .0218

CONTOURS

1 .688
2 .750
3 .800
4 .850



MAX 7.75
MIN .0218

CONTOURS

1 1.00
2 .750
3 .500
4 .250

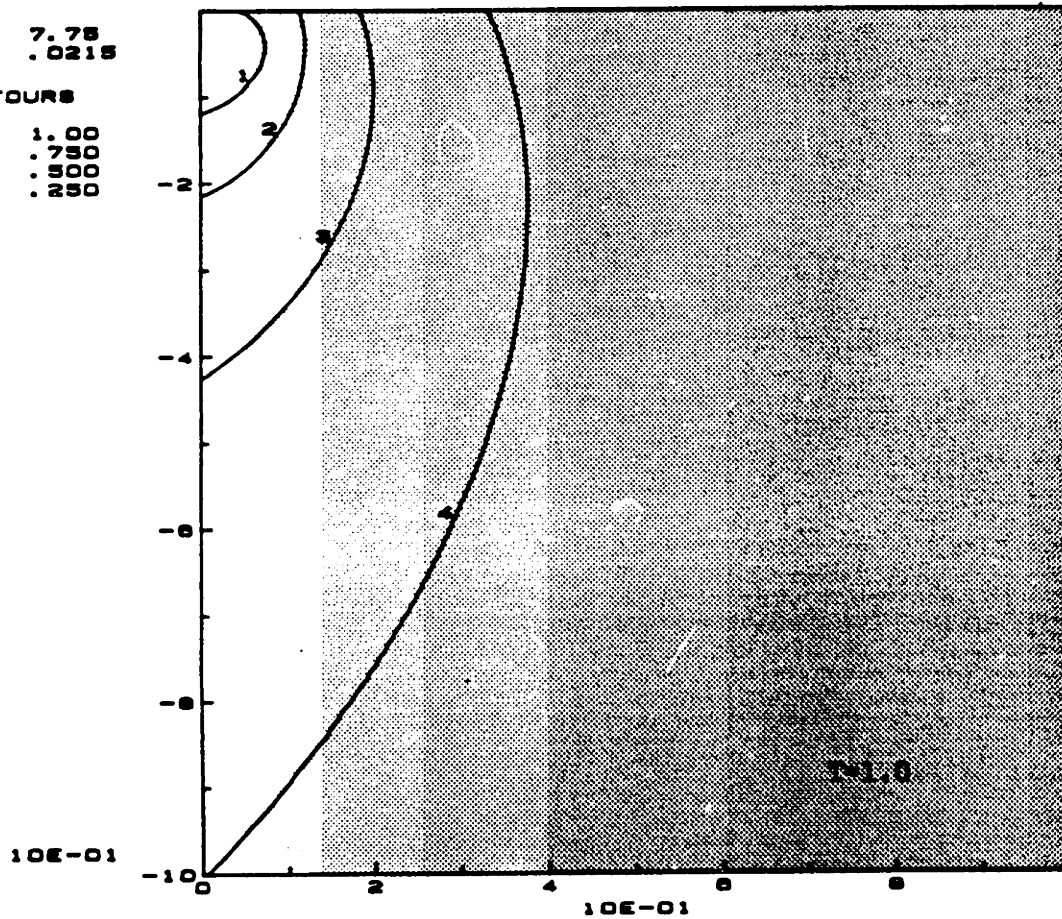
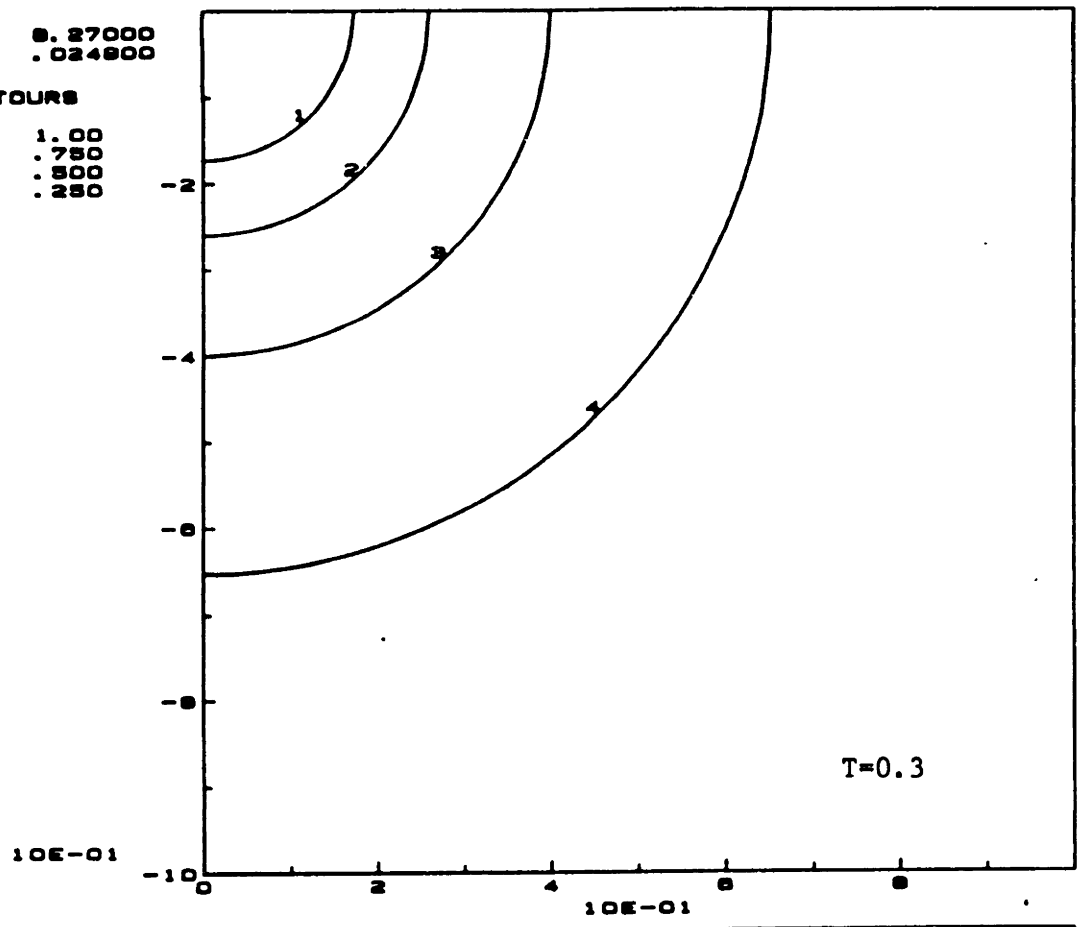


Figure 3.2b Line Source at the Origin (Delta Function Flux)
b. Heterogeneous in x Soil ($S_x=1.0$, $S_z=0.0$)

MAX 0.27000
MIN .024000

CONTOURS

1 1.00
2 .750
3 .500
4 .250



MAX 0.64000
MIN .170000

CONTOURS

1 1.00
2 .750
3 .500
4 .250

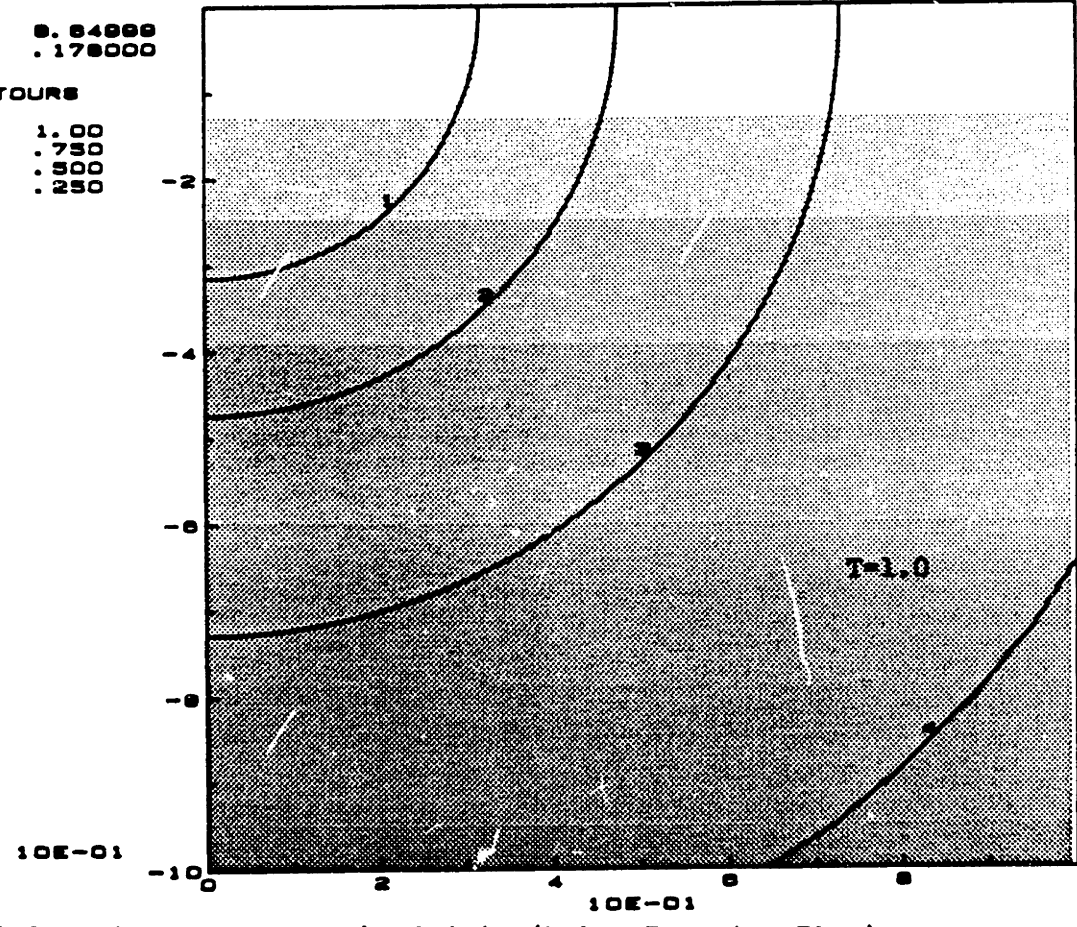


Figure 3.2c Line Source at the Origin (Delta Function Flux)
c. Heterogeneous in z Soil ($S_x=0.0$, $S_z=1.0$)

ii. Infiltrating source of finite length

$$\begin{aligned}
 \Phi_p(X, Z, T) &= \frac{\Theta\alpha}{K_o} = \frac{1}{2} \int_0^{\sqrt{T}} h_p(Z, \xi) \exp\{-S_x X\} \left[\exp\{-XS_x\} \left[-\operatorname{erf}\left\{S_x \xi - \frac{X}{2\xi}\right\} \right. \right. \\
 &+ \left. \left. \operatorname{erf}\left\{S_x \xi + \frac{L-X}{2\xi}\right\} \right] + \exp\{XS_x\} \left[-\operatorname{erf}\left\{S_x \xi + \frac{X}{2\xi}\right\} + \operatorname{erf}\left\{S_x \xi + \frac{L+X}{2\xi}\right\} \right] \right] d\xi \\
 &= \frac{1}{2} \int_0^{\sqrt{T}} h_p(Z, \xi) \left[\exp\{-2XS_x\} \left[-\operatorname{erf}\left\{S_x \xi - \frac{X}{2\xi}\right\} + \operatorname{erf}\left\{S_x \xi + \frac{L-X}{2\xi}\right\} \right] \right. \\
 &+ \left. \left[-\operatorname{erf}\left\{S_x \xi + \frac{X}{2\xi}\right\} + \operatorname{erf}\left\{S_x \xi + \frac{L+X}{2\xi}\right\} \right] \right] d\xi \quad (3.21)
 \end{aligned}$$

This solution for a single strip source of length 0.5, centered at the origin, is shown in Figure 3.3 for the cases $S_x = S_z = 0.0$; $S_x = 0.0$, $S_z = 1.0$ and $S_x = 1.0$, $S_z = 0.0$.

3.3.3 Discussion of the Analytical Solutions

In the collection of analytical solutions to the one-dimensional advection-dispersion equation by van Genuchten and Alves(1982) the solutions given by Equations (3.12) and (3.13) are reported in closed form as follows:

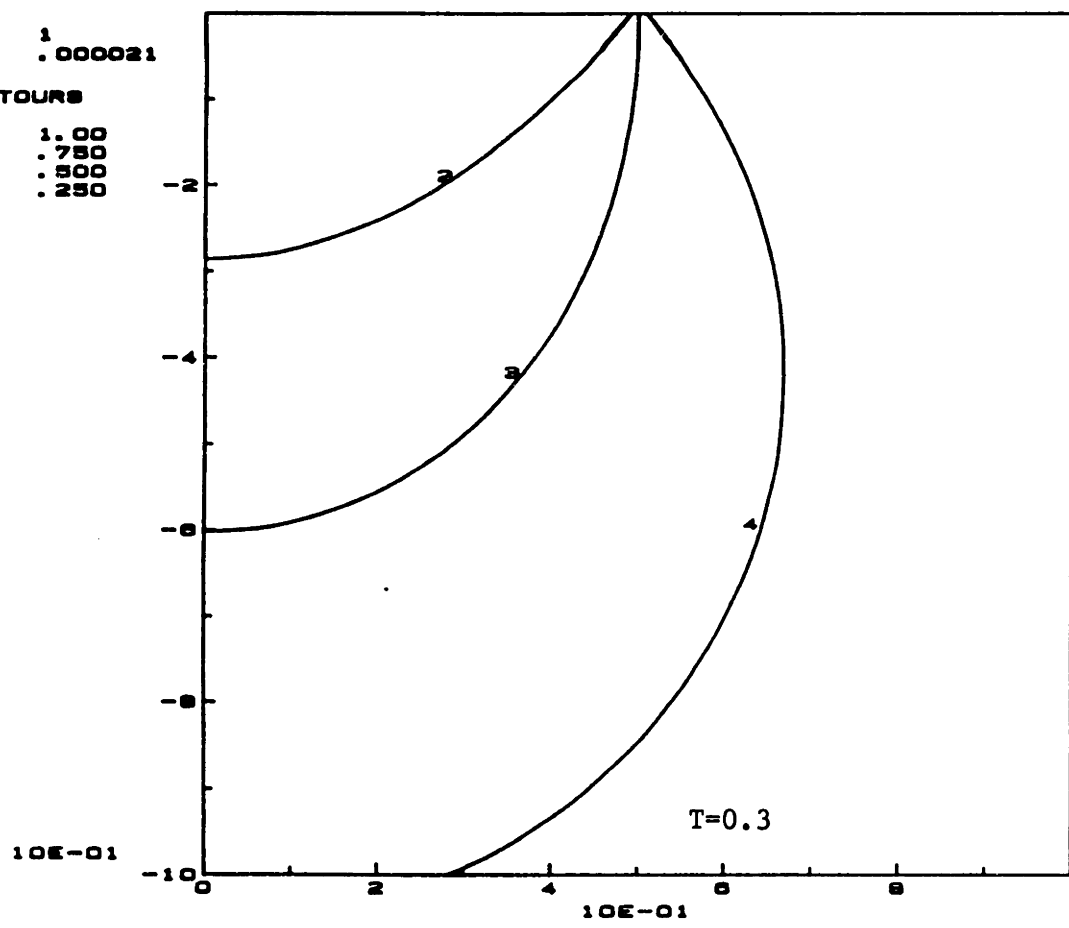
Known Flux Boundary Condition

$$\begin{aligned}
 \Phi_f(Z, T) &= \frac{\Theta\alpha}{2v_o} = \frac{1}{4(1-S_z)} \operatorname{erfc} \left\{ \frac{Z}{2\sqrt{T}} - (1-S_z) \sqrt{T} \right\} + \frac{\sqrt{T}}{\sqrt{\pi}} \exp\left\{-\left(\frac{Z}{2\sqrt{T}} - (1-S_z) \sqrt{T}\right)^2\right\} - \\
 &\frac{1}{4(1-S_z)} \left[1 + 2(1-S_z)Z + 4(1-S_z)^2 T \right] \exp\{2(1-S_z)Z\} \operatorname{erfc}\left\{ \frac{Z}{2\sqrt{T}} + (1-S_z) \sqrt{T} \right\}
 \end{aligned}$$

MAX 1
MIN .000021

CONTOURS

1 1.00
2 .750
3 .500
4 .250



MAX 1
MIN .000020

CONTOURS

1 1.00
2 .750
3 .500
4 .250

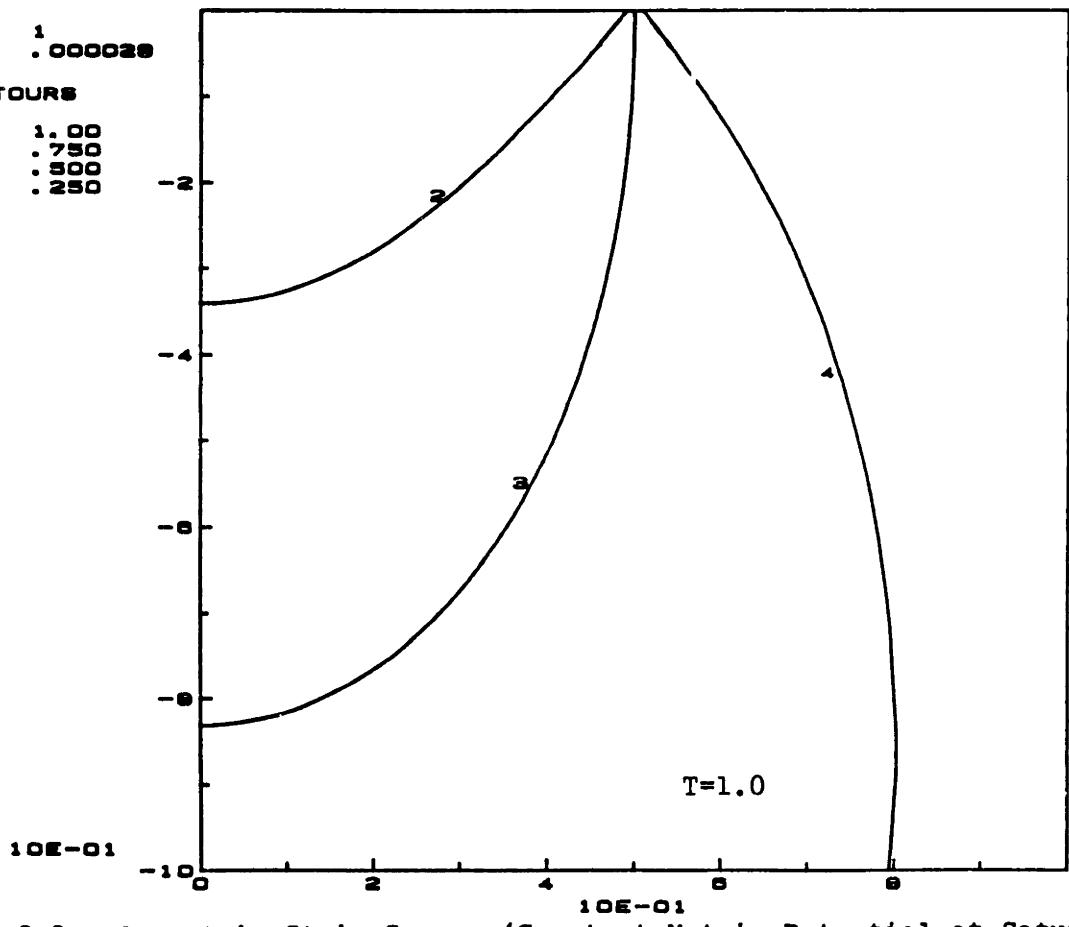
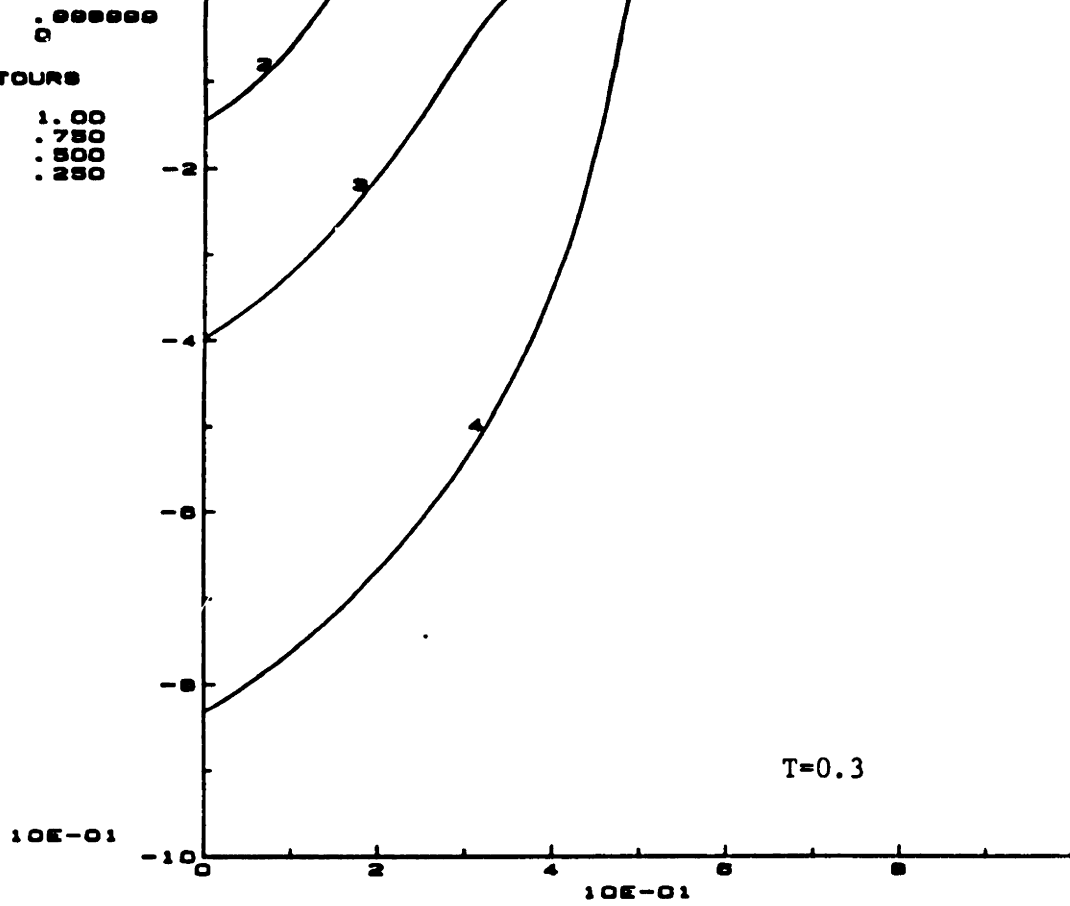


Figure 3.3a Symmetric Strip Source (Constant Matric Potential at Saturation)
a. Homogeneous Soil ($S_x=0.0$, $S_z=0.0$)

MAX .999999
MIN 0

CONTOURS

1 1.00
2 .750
3 .500
4 .250



MAX .999999
MIN 0

CONTOURS

1 1.00
2 .750
3 .500
4 .250

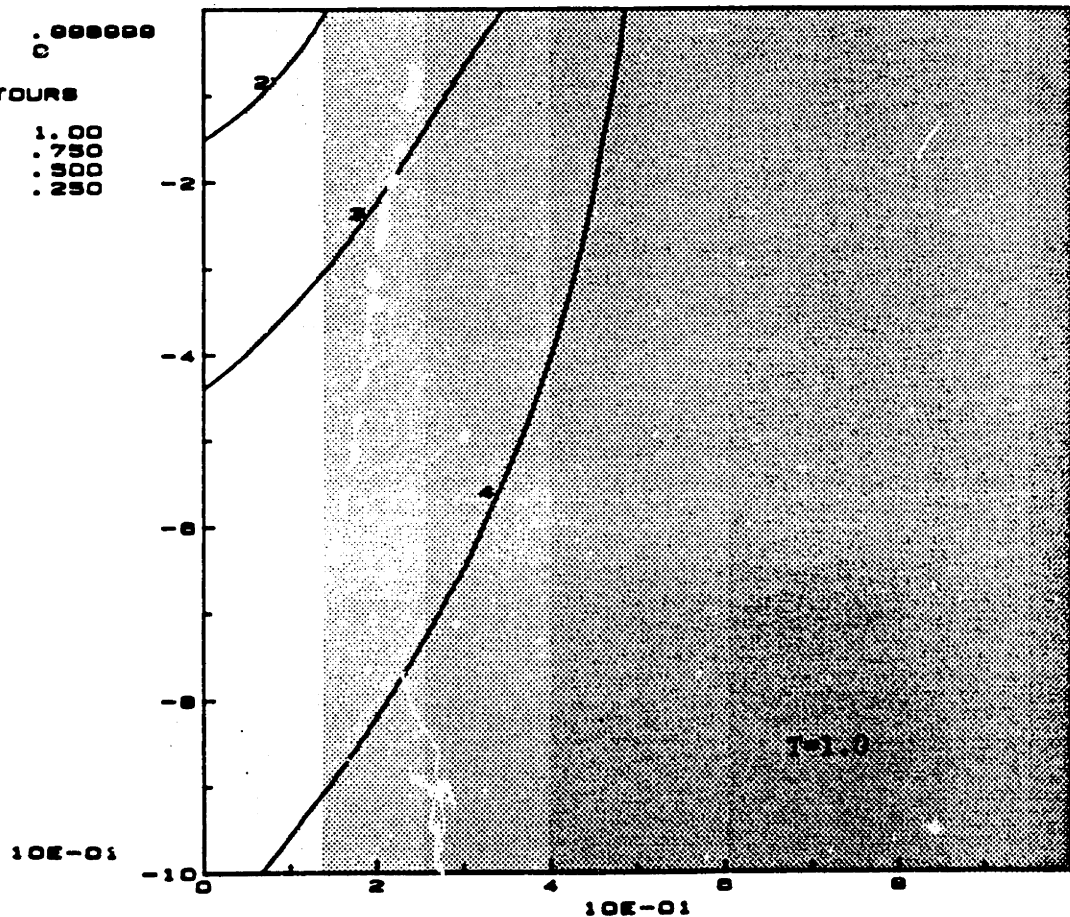
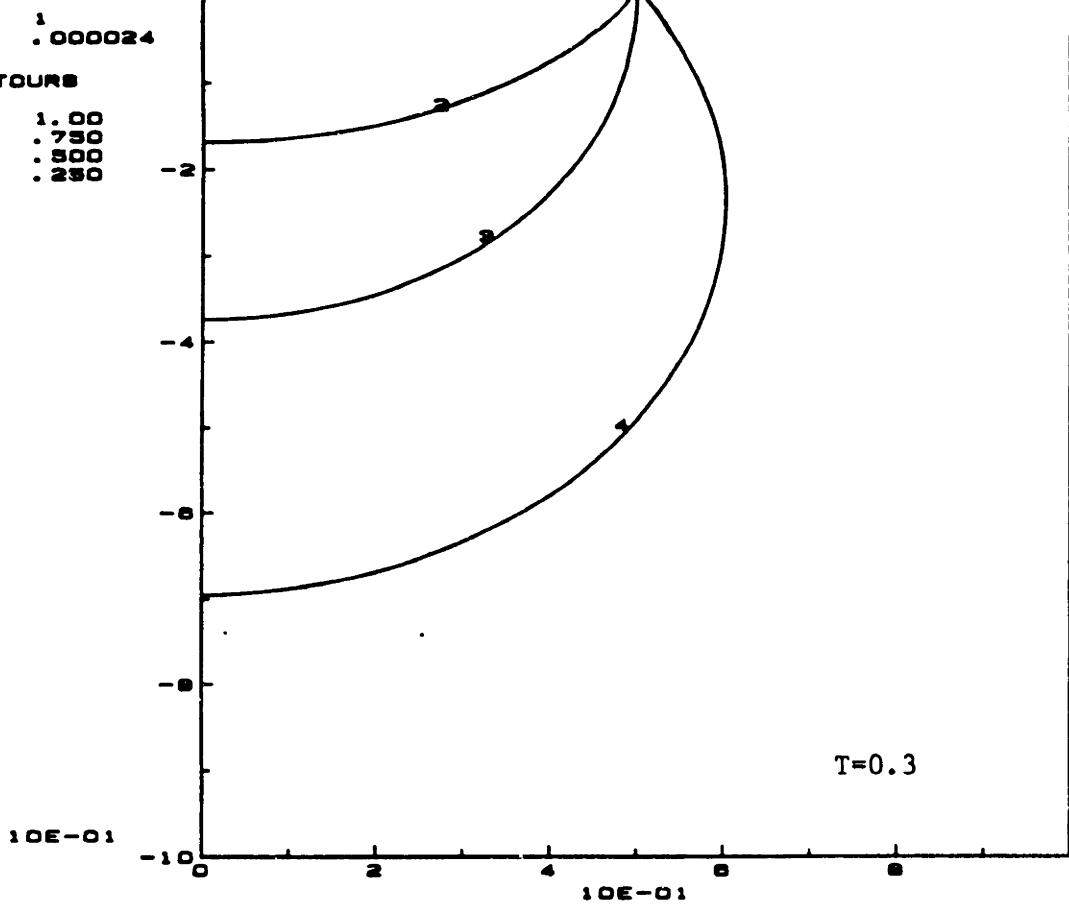


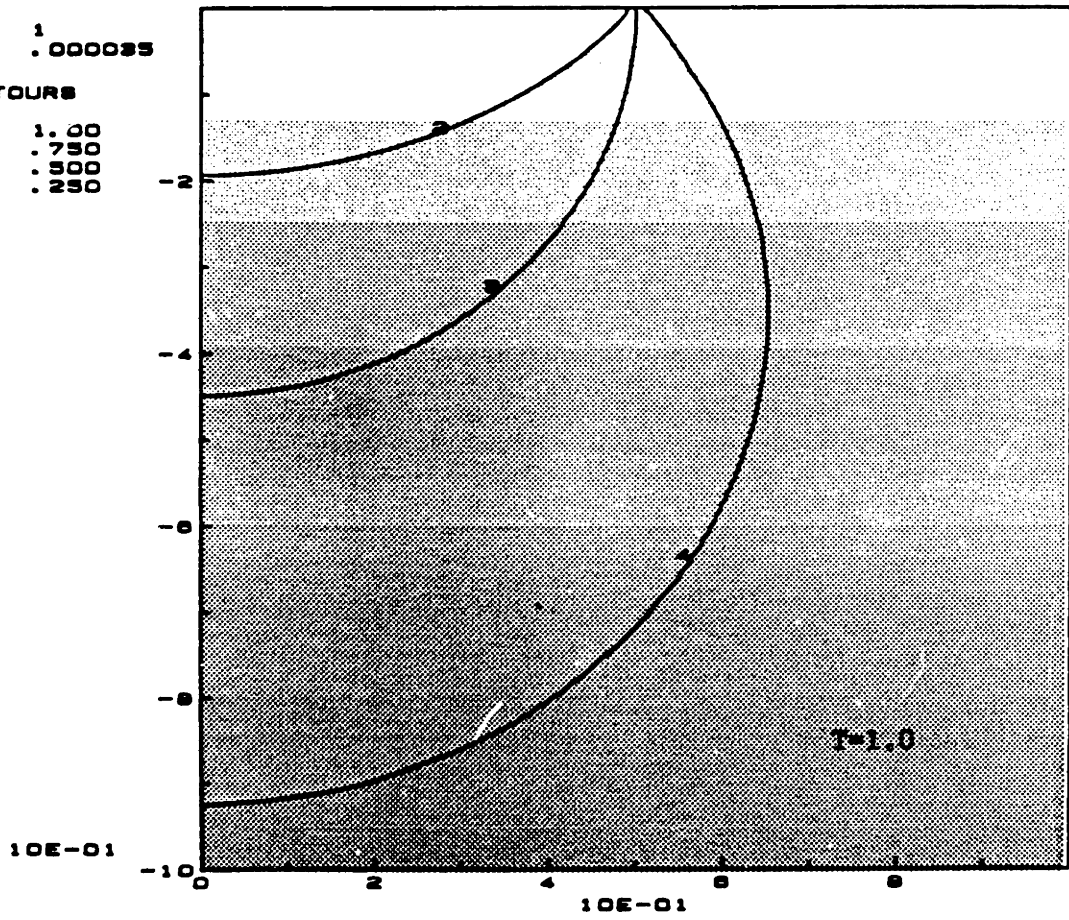
Figure 3.3b Symmetric Strip Source (Constant Matrix Potential at Saturation)
b. Heterogeneous in x Soil ($S_x=1.0$, $S_z=0.0$)

MAX 1
 MIN .000024
 CONTOURS
 1 1.00
 2 .7500
 3 .5000
 4 .2500



T=0.3

MAX 1
 MIN .000035
 CONTOURS
 1 1.00
 2 .7500
 3 .5000
 4 .2500



T=1.0

Figure 3.3c Symmetric Strip Source (Constant Matrix Potential at Saturation)
 c. Heterogeneous in z Soil ($S_x=0.0$, $S_z=1.0$)

Known Matric Potential at Saturation at the Surface

$$\Phi_p(z,T) = \frac{\theta\alpha}{K_o} = \frac{1}{2} \exp\{Z(1-S_z)\} \left[\exp\{Z(1-S_z)\} \operatorname{erfc}\left\{\frac{Z}{2\sqrt{T}} + (1-S_z)\sqrt{T}\right\} + \exp\{-Z(1-S_z)\} \operatorname{erfc}\left\{\frac{Z}{2\sqrt{T}} - (1-S_z)\sqrt{T}\right\} \right]$$

The equivalence of the above forms to the integral forms of the solutions (Equations (3.12) and (3.13)) can be proved by direct differentiation.

However, since our objective is to relate one- and two-dimensional solutions the integral forms facilitate this task, as it is shown in the next section.

We have not found in the literature two-dimensional solutions of the transport equation with equivalent boundary conditions as in the infiltration problem (except for the homogeneous soil case). Several published solutions to the problem of linearized infiltration can be easily identified as special cases of our two-dimensional results. This comparison is summarized as follows:

<u>Philip</u>	1968 ss. homog.	2-D line	Soln(3.18) with $S_x = S_z = 0, T \rightarrow \infty$
	1971 ss. heterog.	2-D line	Soln(3.18) with $S_x = 0, T \rightarrow \infty$
<u>Lomen & Warrick</u>	1974 td. homog.	2-D line	Soln(3.18) with $S_x = S_z = 0$
	1976 td. homog.	2-D strip	Soln(3.19) with $S_x = S_z = 0$
<u>Batu</u>	1977 ss. homog.	2-D strip	Soln(3.21) with $S_x = S_z = 0, T \rightarrow \infty$
	1978 ss. homog.	2-D strip	Soln(3.19) with $S_x = S_z = 0, T \rightarrow \infty$
	1982 td. homog.	2-D strip(s)	Soln(3.21) with $S_x = S_z = 0$

where ss: steady state and td: time dependent.

The derived solutions hold also for negative values of the soil heterogeneity parameters S_x and S_z , i.e., in the case where the hydraulic conductivity K_s increases exponentially with the spatial coordinates x and z . Although the hypothesized functional form of K_s , which allows for analytical treatment of the equations, is restrictive, our results are useful in providing insight on the importance of soil heterogeneity and uniformity of boundary conditions on the solutions of the infiltration problem. This topic is investigated in the next section.

3.4 THE MARGIN OF VALIDITY OF THE ONE-DIMENSIONAL APPROXIMATION

Our stated objective is to check under what conditions a set of non-interacting soil columns accurately represents the process of infiltration in a heterogeneous soil. In this section we use the derived analytical solutions of the linearized infiltration equation (for a special functional form of the saturated hydraulic conductivity in space), in order to derive a criterion for the margin of validity of the one-dimensional approximation. Since the known flux boundary condition is physically meaningful only for uniform soils in the x direction, we focus on the known matric potential case (Equations (3.13) and (3.21)).

The one-dimensional approximation uses the one-dimensional solutions in order to derive solutions for the two-dimensional flow problem. Consider a two-dimensional heterogeneous profile in the vertical and horizontal direction. Then

$$\tilde{\theta}_{2D}(X,Z,T) = \frac{K(X,\phi)}{\alpha} = \frac{K_s(X) \exp\{\alpha\phi\}}{\alpha} = \frac{K_o f(X) \exp\{\alpha\phi\}}{\alpha} \quad \text{or}$$

$$\tilde{\theta}_{2D}(X,Z,T) = \theta_{1D}(Z,T) f(X) \quad \text{and}$$

$$\tilde{\Phi}_{2D}(X,Z,T) = \Phi_{1D}(Z,T) f(X)$$

where the subscripts denote the dimensionality, \sim stands for an approximation and $f(X)$ is the dependence of K_s on the coordinate X , for example, in the studied case $f(X) = \exp\{-2S_x X\}$.

To study the validity of the one-dimensional approximation when the soil is heterogeneous in the horizontal direction, $S_x \neq 0$, we want to use Equation (3.13) to recover the behavior of Equation (3.21). If the approximation is possible, it has to hold for $X = 0.0$. Solution (3.21) for $X = 0.0$ reads

$$\Phi(0,Z,T) = \int_0^{\sqrt{T}} h_p(Z,\xi) \left[\operatorname{erf}\left\{S_x \xi + \frac{L}{2\xi}\right\} - \operatorname{erf}\{S_x \xi\} \right] d\xi$$

The term in brackets is plotted in Figure 3.4 for different values of L and S_x . The closer this term is to one the more accurate is the one-dimensional approximation. For a uniform soil ($S_x=0$) increasing the source length makes the approximation valid for a longer time. In a heterogeneous soil ($S_x \neq 0$) the same is true but the larger the heterogeneity parameter S_x , the larger the source required to maintain one-dimensional behavior for the same time period.

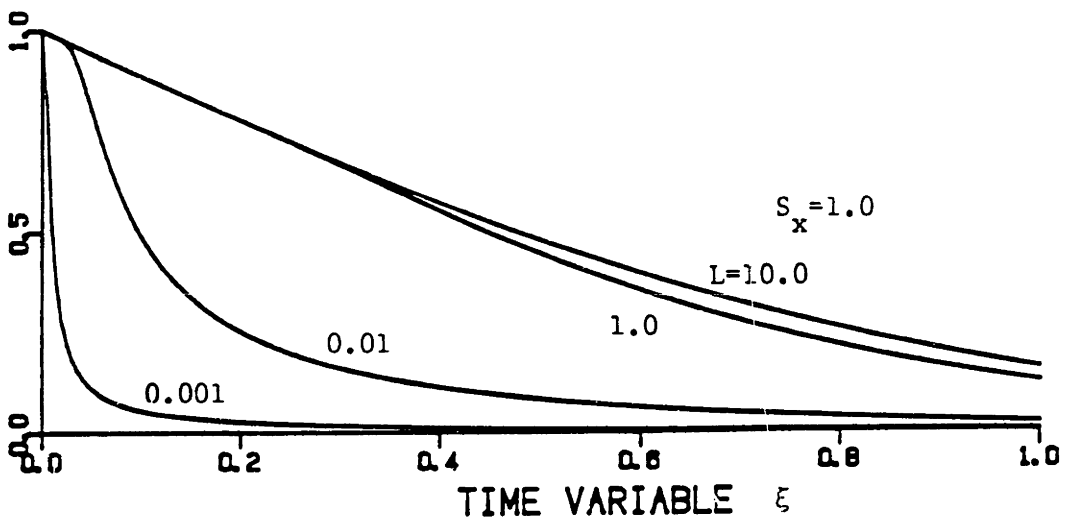
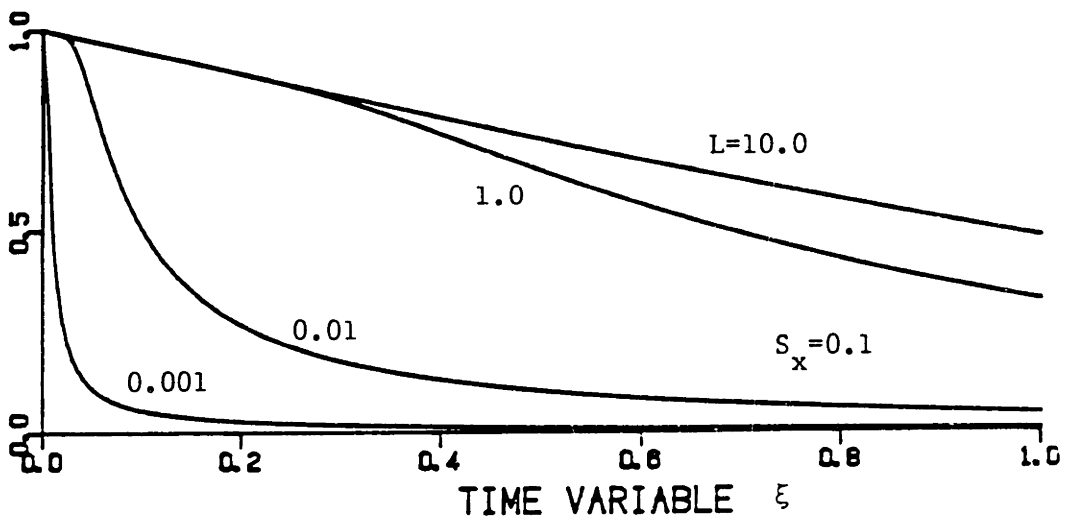
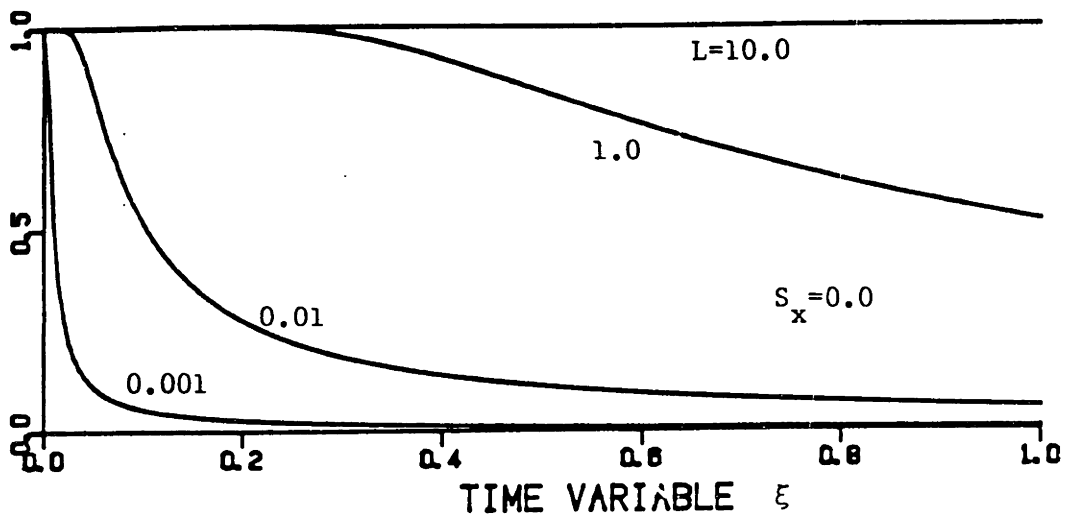


Figure 3.4 Effect of Soil Heterogeneity (S_x) and Source Length (L) Parameters on the One-Dimensional Approximation

Clearly, since $\text{erf}\{x\}$ takes values in the interval zero to one and increases monotonically with x , the term in brackets can only be positive and less than one (for $S_x \neq 0$ and finite source). Therefore, Solution (3.13) and Solution (3.21) cannot match exactly. We can only seek conditions under which they are close enough for the particular problem of interest. Let us at this point make the assumption that $S_x \xi \ll L/2\xi$, which is to be checked later with typical soil parameters. Then, for a certain level of accuracy, represented by the parameter $\varepsilon > 0$, the requirement of maximum (closer to one) value for the term in brackets is equivalent to making the difference between terms as large as possible. This translates to the following conditions (since ξ in $[0, \sqrt{T}]$)

$$\text{erf}\left\{S_x \xi + \frac{L}{2\xi}\right\} \approx \text{erf}\left\{\frac{L}{2\xi}\right\} \geq 1-\varepsilon \text{ or } \frac{L}{2\xi} \geq \chi_{1-\varepsilon} \text{ or } \frac{L}{2\chi_{1-\varepsilon}} \geq \sqrt{T}$$

$$\text{erf}\{S_x \xi\} \leq \varepsilon \text{ or } S_x \xi \leq \chi_\varepsilon \text{ or } \frac{\chi_\varepsilon}{S_x} \geq \sqrt{T}$$

where $\varepsilon > 0$ is a small number which represents the tolerance limit of the one-dimensional approximation and $\chi_\varepsilon, \chi_{1-\varepsilon}$ are the values of the argument of the error function corresponding to values of error function equal to ε and $1-\varepsilon$, respectively. Combining the above conditions

$$\min\left\{\frac{L}{2\chi_{1-\varepsilon}}, \frac{\chi_\varepsilon}{S_x}\right\} \geq \sqrt{T} \quad (3.22)$$

or in terms of physical variables

$$\min\left\{\frac{\alpha\lambda^2}{4\mu\chi_{1-\varepsilon}^2}, \frac{4\alpha\chi_\varepsilon^2}{\lambda_x^2\mu}\right\} \geq t \quad (3.23)$$

where α = capillarity or sorptive constant (in meters⁻¹)

μ = slope of the linear relation between K and θ (in m/day)

λ = length of infiltrating source (in m)

λ_x = length constant of K_s variation, i.e., at $\hat{x} = 1/\lambda_x$

the K_s has dropped to the 1/e value of the value at the origin (in m⁻¹)

$\chi_\varepsilon, \chi_{1-\varepsilon}$ = values of the argument of the error function corresponding to values of error function equal to ε and $1-\varepsilon$, respectively.

L, S_x, T = dimensionless variables defined in the previous section

The above expressions are a criterion for the validity of the one-dimensional approximation, expressed in terms of the soil parameters α and μ , the boundary condition parameter λ and the soil heterogeneity parameter λ_x .

We then expect, the one-dimensional approximation to be better

- a. As α increases, i.e., for coarse soils;
- b. as μ decreases, i.e., for less variation of conductivity with soil moisture (again coarse soils);
- c. as λ increases, i.e., for more uniform boundary condition at the soil surface;
- d. as λ_x decreases, i.e., for less variation of conductivity in the horizontal, i.e., for more homogeneous soil formations.

Therefore, the time interval for which the approximation is valid is the subject of a trade-off between the uniformity of the boundary condition at the surface and the soil heterogeneity in the horizontal direction. Increasing L or reducing S_x increases the validity of the one-dimensional approximation. Consequently, the same quality approximation results for an infinite number of combinations of l and λ_x , which are given by

$$l\lambda_x = 4\chi_\epsilon\chi_{1-\epsilon} \quad \text{or} \quad LS_x = 2\chi_\epsilon\chi_{1-\epsilon}$$

We now use typical values of the soil parameters as reported in the literature to demonstrate the implications of the above results. The capillary index α varies from 5.0 to 0.2 m^{-1} for coarse to fine soils respectively. The accuracy is fixed by $\epsilon=0.05$ ($\chi_\epsilon=0.05$; $\chi_{1-\epsilon}=1.50$). The infiltration time is fixed at $t = 10$ hr.

a. Parameters from Warrick and Lomen (1976)

Clay loam $\alpha = 2 \text{ m}^{-1}$ (per meter) $\mu = 1.3 - 0.13 \text{ m/day}$

Then $X = \frac{\alpha x}{2} \rightarrow x = X$ (lengths are equal to the dimensionless value in m)

$$T = \frac{\alpha \mu t}{4} \rightarrow t = 40T \text{ hr} \quad (\mu = 1.3 \text{ m/day})$$

$$t = 400T \text{ hr} \quad (\mu = 0.13 \text{ m/day})$$

μ [m/day]	t [hr]	T	\sqrt{T}	L	l [m]	S_x	λ_x [m^{-1}]	\hat{x} [m]
1.3	10	0.25	0.5	≥ 1.5	≥ 1.5	≤ 0.10	≤ 0.2	≥ 5.0
0.13	10	0.025	0.16	≥ 0.48	≥ 0.48	≤ 0.31	≤ 0.62	≥ 1.6

For $\mu = 1.3$ m/day, these values suggest that if the infiltrating source is not localized ($\lambda \geq 1.5$ m) and the saturated hydraulic conductivity is not varying drastically in the horizontal ($\hat{x} \geq 5.0$ m), the one-dimensional approximation is valid for the considered infiltration events. For $m = 0.13$ m/day the one-dimensional approximation is valid for sources of length greater than 0.48 m and for horizontal variability in K_s such that the hydraulic conductivity is reduced by a factor of $e = 2.72$ (from its maximum value at the origin) at a distance greater than 1.60 m.

b. Parameters from Philip (1987)

$$\alpha = 4 \text{ m}^{-1} \quad \mu = 2.7 \cdot 10^{-2} \text{ m/day}$$

$$\text{Then } X = \frac{\alpha x}{2} \rightarrow x = \frac{X}{2} \text{ (m)}$$

$$T = \frac{\alpha \mu t}{4} \rightarrow t = 37T \text{ hr}$$

μ [m/day]	t [hr]	T	\sqrt{T}	L	λ [m]	S_x	λ_x [m^{-1}]	\hat{x} [m]
2.7E-2	10	0.27	0.52	≥ 1.5	≥ 1.5	≤ 0.10	≤ 0.40	≥ 2.5

In typical field cases the length of the infiltrating source and the scale over which the soil saturated conductivity is varying slowly are much larger than is required for the validity of the 1-D approximation over the infiltration period. It is also obvious that the assumption used

$$S_x \xi \leq S_x \sqrt{T} \ll \frac{L}{2\sqrt{T}}$$

is correct.

3.5 THE GENERAL CASE: NUMERICAL SOLUTIONS

The general governing equation for infiltration in heterogeneous soils, with the saturated hydraulic conductivity K_s being a function of the space coordinates, is

$$\frac{\alpha}{\mu} \frac{\partial \theta}{\partial t} = \nabla^2 \theta - \frac{\partial \ln K_s}{\partial x} \frac{\partial \theta}{\partial x} - \frac{\partial \ln K_s}{\partial y} \frac{\partial \theta}{\partial y} - \left(\frac{\partial \ln K_s}{\partial z} + \alpha \right) \frac{\partial \theta}{\partial z} - \nabla^2 \ln K_s \theta \quad (3.24)$$

with initial condition

$$\theta(x, y, z, 0) = 0.0 \quad (3.25)$$

and boundary conditions (constant matric potential at saturation at $z = 0.0$)

$$\theta(x, y, z, t) \rightarrow 0 \quad \text{as } x^2 + y^2 + z^2 \rightarrow \infty \quad (3.26)$$

$$\theta(x, y, 0, t) = \begin{cases} \frac{K_s(x, y, 0)}{\alpha} & \text{for } x \leq l \\ 0 & \text{otherwise} \end{cases} \quad (3.27)$$

Using the dimensionless variables

$$\Phi = \frac{\theta \alpha}{K_0}, \quad T = \frac{\alpha \mu t}{4}, \quad Z = \frac{\alpha z}{2}, \quad X = \frac{\alpha x}{2},$$

as suggested by the analytical solutions of the previous section, Equation (3.24) takes the form (assuming uniformity along the y coordinate):

$$\frac{\alpha}{\mu} \frac{K_0}{\alpha} \frac{\partial \Phi}{\partial T} \frac{\alpha \mu}{4} = \frac{K_0}{\alpha} \frac{\alpha^2}{4} \nabla^2 \Phi - \frac{\partial \ln K_s}{\partial X} \frac{\alpha}{2} \frac{K_0}{\alpha} \frac{\alpha}{2} \frac{\partial \Phi}{\partial X} - \left(\frac{\partial \ln K_s}{\partial Z} \frac{\alpha}{2} + \alpha \right) \frac{\alpha}{2} \frac{K_0}{\alpha} \frac{\partial \Phi}{\partial Z} - \frac{\alpha^2}{4} \nabla^2 \ln K_s \frac{K_0}{\alpha} \Phi$$

which reduces to the dimensionless form

$$\frac{\partial \Phi}{\partial T} = \nabla^2 \Phi - \frac{\partial \ln K_s}{\partial X} \frac{\partial \Phi}{\partial X} - 2 \left(\frac{\partial \ln K_s}{\partial Z} \frac{1}{2} + 1 \right) \frac{\partial \Phi}{\partial Z} - \nabla^2 \ln K_s \Phi \quad (3.28)$$

with initial condition

$$\Phi(X, Z, T) = 0.0 \quad (3.29)$$

and boundary conditions ($X \geq 0$, $Z \geq 0$)

$$\Phi(X, Z, T) \rightarrow 0 \text{ as } X^2 + Z^2 \rightarrow \infty$$

$$\Phi(X, 0, T) = \begin{cases} \frac{K_s(X, 0)}{K_0} & \text{for } X \leq L \\ 0 & \text{otherwise} \end{cases} \quad (3.30)$$

$$\left. \frac{\partial \Phi}{\partial X} \right|_{X=0} = 0.0 \quad (3.31)$$

Further we define the functions

$$P_{1X}(X) = - \frac{\partial \ln K_s}{\partial X} \quad (3.32)$$

$$P_{1Z}(Z) = -2 \left(\frac{\partial \ln K_s}{\partial Z} \frac{1}{2} + 1 \right) \quad (3.33)$$

$$P_2(X,Z) = - \left(\frac{\partial^2 \ln K_s}{\partial X^2} + \frac{\partial^2 \ln K_s}{\partial Z^2} \right) = - \nabla^2 \ln K_s \quad (3.34)$$

So that Equation (3.28) is written

$$\frac{\partial \Phi}{\partial T} = \nabla^2 \Phi + P_{1X}(X) \frac{\partial \Phi}{\partial X} + P_{1Z}(Z) \frac{\partial \Phi}{\partial Z} + P_2(X,Z) \Phi \quad (3.35)$$

subject to the same initial and boundary conditions.

In the following sections the one- and two-dimensional versions of Equation (3.35) are discretized and solved numerically for a general functional form of K_s . Solutions are shown for periodic soil media and a generalization of the results of the analytical approach is suggested.

3.5.1 One-Dimensional Numerical Solution in the General Case

The governing equation to be solved is:

$$\frac{\partial \Phi}{\partial T} = \frac{\partial^2 \Phi}{\partial Z^2} + P_{1Z}(Z) \frac{\partial \Phi}{\partial Z} + P_2(Z) \Phi \quad (3.36)$$

Subject to

$$\Phi(Z,0) = 0.0 \quad (3.37)$$

$$\Phi(Z,T) \rightarrow 0 \text{ as } Z \rightarrow \infty \quad (3.38)$$

$$\Phi(0,T) = \frac{K_s(0)}{K_o} \quad (3.39)$$

The discretization of the partial derivatives is:

$$\left(\frac{\partial \Phi}{\partial T}\right)_j^{k+1/2} = \frac{\Phi_j^{k+1} - \Phi_j^k}{\Delta T}$$

$$\left(\frac{\partial \Phi}{\partial Z}\right)_j^{k+1/2} = \frac{\Phi_{j+1}^{k+1/2} - \Phi_j^{k+1/2}}{\Delta Z} = \frac{\Phi_{j+1}^{k+1} + \Phi_{j+1}^k - \Phi_j^{k+1} - \Phi_j^k}{2\Delta Z}$$

$$\begin{aligned} \left(\frac{\partial^2 \Phi}{\partial Z^2}\right)_j^{k+1/2} &= \frac{1}{\Delta Z} \left[\left(\frac{\partial \Phi}{\partial Z}\right)_{j+1/2}^{k+1/2} - \left(\frac{\partial \Phi}{\partial Z}\right)_{j-1/2}^{k+1/2} \right] = \\ &= \frac{\Phi_{j+1}^{k+1/2} - \Phi_j^{k+1/2} - \Phi_j^{k+1/2} + \Phi_{j-1}^{k+1/2}}{\Delta Z^2} \\ &= \frac{\Phi_{j+1}^{k+1} - 2\Phi_j^{k+1} + \Phi_{j-1}^{k+1} + \Phi_{j+1}^k - 2\Phi_j^k + \Phi_{j-1}^k}{2\Delta Z^2} \end{aligned}$$

where we have used $\Phi_j^{k+1/2} = \frac{1}{2} (\Phi_j^{k+1} + \Phi_j^k)$

So that the discretized form of Equation (3.36) is:

$$\begin{aligned} \frac{\Phi_j^{k+1} - \Phi_j^k}{\Delta T} &= \frac{\Phi_{j+1}^{k+1} - 2\Phi_j^{k+1} + \Phi_{j-1}^{k+1} + \Phi_{j+1}^k - 2\Phi_j^k + \Phi_{j-1}^k}{2\Delta Z^2} \\ &+ P_{1Z}(Z_j) \frac{\Phi_{j+1}^{k+1} + \Phi_{j+1}^k - \Phi_j^{k+1} - \Phi_j^k}{2\Delta Z} + P_2(Z_j) \frac{\Phi_j^{k+1} + \Phi_j^k}{2} \end{aligned}$$

Separating unknowns and gathering terms gives:

where

$$C_j = \frac{\Delta T}{\Delta Z^2} \quad j=2, \dots, N-1; \quad C_N = 0.0; \quad C_1 = 0.0;$$

$$A_j = \frac{\Delta T}{2\Delta Z^2} + \frac{\Delta T}{2\Delta Z} P_{1j} \quad j=2, \dots, N-1; \quad A_1 = 0.0; \quad A_N = 0.0;$$

$$B_j = 1 + A_j + C_j - \frac{\Delta T}{2} P_{2j} \quad j=2, \dots, N-1; \quad B_1 = 1.0; \quad B_N = 1.0;$$

$$E_j = \Phi_j^K + \frac{\Delta T}{2\Delta Z^2} (\Phi_{j-1}^K - 2\Phi_j^K + \Phi_{j+1}^K) + \frac{\Delta T}{2\Delta Z} P_{1Zj} (\Phi_{j+1}^K - \Phi_j^K) + \frac{\Delta T}{2} P_{2j} \Phi_j^K$$

$$j=2, \dots, N-1; \quad E_1 = \frac{K_s(Z_1)}{K_o}; \quad E_N = 0.0.$$

To solve this tridiagonal system we used the algorithm described in Protopapas and Bras (1986), Appendix B, once the functional form of K_s is specified.

3.5.2 Two-Dimensional Numerical Solution in the General Case

The governing equation to be solved is (Equation (3.35)):

$$\frac{\partial \Phi}{\partial T} = \frac{\partial^2 \Phi}{\partial X^2} + \frac{\partial^2 \Phi}{\partial Z^2} + P_{1X}(X) \frac{\partial \Phi}{\partial X} + P_{1Z}(Z) \frac{\partial \Phi}{\partial Z} + P_2(X, Z) \Phi \quad (3.41)$$

subject to the initial and boundary conditions (3.29), (3.30) and (3.31).

The discretization of the partial derivatives is:

$$\left(\frac{\partial \Phi}{\partial T}\right)_{i,j}^{k+1/2} = \frac{\Phi_{i,j}^{k+1} - \Phi_{i,j}^k}{\Delta T}$$

$$\left(\frac{\partial \Phi}{\partial X}\right)_{i,j}^{k+1/2} = \frac{\Phi_{i+1,j}^{k+1} + \Phi_{i+1,j}^k - \Phi_{i,j}^{k+1} - \Phi_{i,j}^k}{2\Delta X}$$

$$\left(\frac{\partial \Phi}{\partial Z}\right)_{i,j}^{k+1/2} = \frac{\Phi_{i,j+1}^{k+1} + \Phi_{i,j+1}^k - \Phi_{i,j}^{k+1} - \Phi_{i,j}^k}{2\Delta Z}$$

$$\left(\frac{\partial^2 \Phi}{\partial X^2}\right)_{i,j}^{k+1/2} = \frac{\Phi_{i+1,j}^{k+1} - 2\Phi_{i,j}^{k+1} + \Phi_{i-1,j}^{k+1} + \Phi_{i+1,j}^k - 2\Phi_{i,j}^k + \Phi_{i-1,j}^k}{2\Delta X^2}$$

$$\left(\frac{\partial^2 \Phi}{\partial Z^2}\right)_{i,j}^{k+1/2} = \frac{\Phi_{i,j+1}^{k+1} - 2\Phi_{i,j}^{k+1} + \Phi_{i,j-1}^{k+1} + \Phi_{i,j+1}^k - 2\Phi_{i,j}^k + \Phi_{i,j-1}^k}{2\Delta Z^2}$$

which lead to the following discretized form,

$$\begin{aligned} \frac{\Phi_{i,j}^{k+1} - \Phi_{i,j}^k}{\Delta T} &= \frac{\Phi_{i+1,j}^{k+1} - 2\Phi_{i,j}^{k+1} + \Phi_{i-1,j}^{k+1} + \Phi_{i+1,j}^k - 2\Phi_{i,j}^k + \Phi_{i-1,j}^k}{2\Delta X^2} \\ &+ \frac{\Phi_{i,j+1}^{k+1} - 2\Phi_{i,j}^{k+1} + \Phi_{i,j-1}^{k+1} + \Phi_{i,j+1}^k - 2\Phi_{i,j}^k + \Phi_{i,j-1}^k}{2\Delta Z^2} \\ &+ P_{1X}(X_i) \frac{\Phi_{i+1,j}^{k+1} + \Phi_{i+1,j}^k - \Phi_{i,j}^{k+1} - \Phi_{i,j}^k}{2\Delta X} \\ &+ P_{1Z}(Z_j) \frac{\Phi_{i,j+1}^{k+1} + \Phi_{i,j+1}^k - \Phi_{i,j}^{k+1} - \Phi_{i,j}^k}{2\Delta Z} \\ &+ P_2(X_i, Z_j) \frac{\Phi_{i,j}^{k+1} + \Phi_{i,j}^k}{2} \end{aligned}$$

Separating unknowns and gathering terms (keeping some redundant factors to make this step clearer) gives

$$\begin{aligned}
& -\left\{\frac{\Delta T}{2\Delta X^2}\right\} \Phi_{i-1,j}^{K+1} + \left\{1 + 2\frac{\Delta T}{2\Delta X^2} + \frac{\Delta T}{2\Delta X} P_{1Xi} + 2\frac{\Delta T}{2\Delta Z^2} + \frac{\Delta T}{2\Delta Z} P_{1Zj} - \frac{\Delta T}{2} P_{2ij}\right\} \Phi_{i,j}^{K+1} \\
& - \left\{\frac{\Delta T}{2\Delta X^2} + \frac{\Delta T}{2\Delta X} P_{1Xi}\right\} \Phi_{i+1,j}^{K+1} - \left\{\frac{\Delta T}{2\Delta Z^2}\right\} \Phi_{i,j-1}^{K+1} - \left\{\frac{\Delta T}{2\Delta Z^2} + \frac{\Delta T}{2\Delta Z} P_{1Zj}\right\} \Phi_{i,j+1}^{K+1} \\
& = \left\{\frac{\Delta T}{2\Delta X^2}\right\} \Phi_{i-1,j}^K + \left\{1 - 2\frac{\Delta T}{2\Delta X^2} - 2\frac{\Delta T}{2\Delta Z^2} - \frac{\Delta T}{2\Delta X} P_{1Xi} - \frac{\Delta T}{2\Delta Z} P_{1Zj} + \frac{\Delta T}{2} P_{2ij}\right\} \Phi_{i,j}^K \\
& + \left\{\frac{\Delta T}{2\Delta X^2} + \frac{\Delta T}{2\Delta X} P_{1Xi}\right\} \Phi_{i+1,j}^K + \left\{\frac{\Delta T}{2\Delta Z^2}\right\} \Phi_{i,j-1}^K + \left\{\frac{\Delta T}{2\Delta Z^2} + \frac{\Delta T}{2\Delta Z} P_{1Zj}\right\} \Phi_{i,j+1}^K
\end{aligned}$$

where

$$P_{1Xi} = P_{1X}(X_i), P_{1Zj} = P_{1Z}(Z_j), P_{2ij} = P_2(X_i, Z_j) \text{ and } j=2, \dots, N-1$$

At the soil surface ($Z = 0$), the boundary condition gives

$$\Phi_{i,1}^{K+1} = \begin{cases} \frac{K_s(X_i, 0)}{K_o} & \text{for } i=1, \dots, i_L \\ 0 & \text{for } i = i_L+1, \dots, N \end{cases}$$

At infinity the boundary conditions are approximated by specifying

$$\Phi_{N,j}^{K+1} = 0.0 \quad \text{for all } j$$

$$\Phi_{i,N}^{K+1} = 0.0 \quad \text{for all } i$$

The boundary condition at $X = 0$ accounts for the symmetry of the solution around the Z axis. To implement this condition we introduce an imaginary node 0, symmetric to node 1 with respect to the $X = 0$ boundary. Then the approximation of the zero flux boundary condition is

$$\frac{\partial \Phi}{\partial X} \Big|_{1,j}^{k+1/2} = 0 = \frac{\Phi_{1,j}^{k+1} + \Phi_{1,j}^k - \Phi_{0,j}^{k+1} - \Phi_{0,j}^k}{2\Delta X} \text{ or } \Phi_{1,j}^{k+1} + \Phi_{1,j}^k - \Phi_{0,j}^k = \Phi_{0,j}^{k+1}$$

The discretized equation still holds and therefore,

$$\begin{aligned} & - \left\{ \frac{\Delta T}{2\Delta X^2} \right\} \Phi_{0,j}^{k+1} + \left\{ 1 + \frac{2\Delta T}{2\Delta X^2} + \frac{\Delta T}{2\Delta X} P_{1X}(1) + \frac{2\Delta T}{2\Delta Z^2} + \frac{\Delta T}{2\Delta Z} P_{1Z}(j) - \frac{\Delta T}{2} P_2(1,j) \right\} \Phi_{1,j}^{k+1} \\ & - \left\{ \frac{\Delta T}{2\Delta X^2} + \frac{\Delta T}{2\Delta X} P_{1X}(1) \right\} \Phi_{2,j}^{k+1} - \left\{ \frac{\Delta T}{2\Delta Z^2} \right\} \Phi_{1,j-1}^{k+1} - \left\{ \frac{\Delta T}{2\Delta Z^2} + \frac{\Delta T}{2\Delta Z} P_{1Z}(j) \right\} \Phi_{1,j+1}^{k+1} \\ & = \left\{ \frac{\Delta T}{2\Delta X^2} \right\} \Phi_{0,j}^k + \left\{ 1 - \frac{\Delta T}{\Delta X^2} - \frac{\Delta T}{\Delta Z^2} - \frac{\Delta T}{2\Delta X} P_{1X}(1) - \frac{\Delta T}{2\Delta Z} P_{1Z}(j) + \frac{\Delta T}{2} P_2(1,j) \right\} \Phi_{1,j}^k \\ & + \left\{ \frac{\Delta T}{2\Delta X^2} + \frac{\Delta T}{2\Delta X} P_{1X}(1) \right\} \Phi_{2,j}^k + \left\{ \frac{\Delta T}{2\Delta Z^2} \right\} \Phi_{1,j-1}^k + \left\{ \frac{\Delta T}{2\Delta Z^2} + \frac{\Delta T}{2\Delta Z} P_{1Z}(j) \right\} \Phi_{1,j+1}^k \end{aligned}$$

Substituting for $\Phi_{0,j}^{k+1}$ from the previous equation and doing the algebra yields

$$\begin{aligned} & \left\{ 1 + \frac{\Delta T}{2\Delta X^2} + \frac{\Delta T}{2\Delta X} P_{1X}(1) + 2 \frac{\Delta T}{2\Delta Z^2} + \frac{\Delta T}{2\Delta Z} P_{1Z}(j) - \frac{\Delta T}{2} P_2(1,j) \right\} \Phi_{1,j}^{k+1} \\ & - \left\{ \frac{\Delta T}{2\Delta X^2} + \frac{\Delta T}{2\Delta X} P_{1X}(1) \right\} \Phi_{2,j}^{k+1} - \left\{ \frac{\Delta T}{2\Delta Z^2} \right\} \Phi_{1,j-1}^{k+1} - \left\{ \frac{\Delta T}{2\Delta Z^2} + \frac{\Delta T}{2\Delta Z} P_{1Z}(j) \right\} \Phi_{1,j+1}^{k+1} \\ & = \left\{ \frac{\Delta T}{2\Delta Z^2} \right\} \Phi_{1,j-1}^k + \left\{ 1 - \frac{\Delta T}{2\Delta X^2} - \frac{\Delta T}{2\Delta X} P_{1X}(1) - 2 \frac{\Delta T}{2\Delta Z^2} - \frac{\Delta T}{2\Delta Z} P_{1Z}(j) + \frac{\Delta T}{2} P_2(1,j) \right\} \Phi_{1,j}^k \\ & + \left\{ \frac{\Delta T}{2\Delta Z^2} + \frac{\Delta T}{2\Delta Z} P_{1Z}(j) \right\} \Phi_{1,j+1}^k + \left\{ \frac{\Delta T}{2\Delta X^2} + \frac{\Delta T}{2\Delta X} P_{1X}(1) \right\} \Phi_{2,j}^k \end{aligned}$$

valid for $j=2, \dots, N-1$ and $i=1$.

Let $\underline{\Phi}^{k+1} = [\Phi_{11}^{k+1} \ \Phi_{12}^{k+1} \ \dots \ \Phi_{1N}^{k+1} \ \Phi_{21}^{k+1} \ \dots \ \Phi_{2N}^{k+1} \ \dots \ \Phi_{N1}^{k+1} \ \dots \ \Phi_{NN}^{k+1}]^T$ be a vector($N^2, 1$) of the unknowns of the above set of equations which has the following matrix form (for $N = 3$):

$$\begin{bmatrix}
 1 & & & \vdots & & & \vdots & & & \\
 X & X & X & \vdots & & X & \vdots & & & \\
 & & & 1 & & & \vdots & & & \\
 \dots & \dots & \dots & \dots & \dots & \dots & \dots & \dots & \dots & \\
 & & & \vdots & 1 & 0 & \vdots & & & \\
 0 & X & 0 & \vdots & X & X & X & \vdots & 0 & X & 0 \\
 & & & \vdots & & & & 1 & \vdots & & \\
 \dots & \dots & \dots & \dots & \dots & \dots & \dots & \dots & \dots & \dots & \\
 & & & \vdots & & & \vdots & 1 & 0 & 0 & \\
 & & & \vdots & & & \vdots & & 1 & & \\
 & & & \vdots & & & \vdots & & & 1 & \\
 & & & \vdots & & & \vdots & & & & 1
 \end{bmatrix}
 \begin{bmatrix}
 \Phi_{11}^{k+1} \\
 \Phi_{12}^{k+1} \\
 \Phi_{13}^{k+1} \\
 \dots \\
 \Phi_{21}^{k+1} \\
 \Phi_{22}^{k+1} \\
 \Phi_{23}^{k+1} \\
 \dots \\
 \Phi_{31}^{k+1} \\
 \Phi_{32}^{k+1} \\
 \Phi_{33}^{k+1}
 \end{bmatrix}
 =
 \begin{bmatrix}
 X \\
 X \\
 0 \\
 \dots \\
 X \\
 X \\
 0 \\
 \dots \\
 X \\
 X \\
 0
 \end{bmatrix}$$

This five diagonal form is characteristic of two-dimensional problems solved by finite differences. An iterative successive-over-relaxation (SOR) method was used to solve for Φ^{k+1} . An equally spaced square grid of size 2.0 x 2.0 with $\Delta X = \Delta Z = 0.02$, $\Delta T = 5E-3$ was used. In Figure 3.5 we compare the two-dimensional numerical solution for a homogeneous soil to the analytical one (Equation (3.21) with $S_x=S_z= 0.0$). We notice an effect of the dry soil boundary condition imposed at the right side of the finite numerical grid, while the analytical solutions assume dry soil at infinity. Otherwise the solutions agree very well.

5.3 Application for Periodic Soil Formations

We solved the two-dimensional problem with the same grid and time step for the following three forms of variation of K_s :

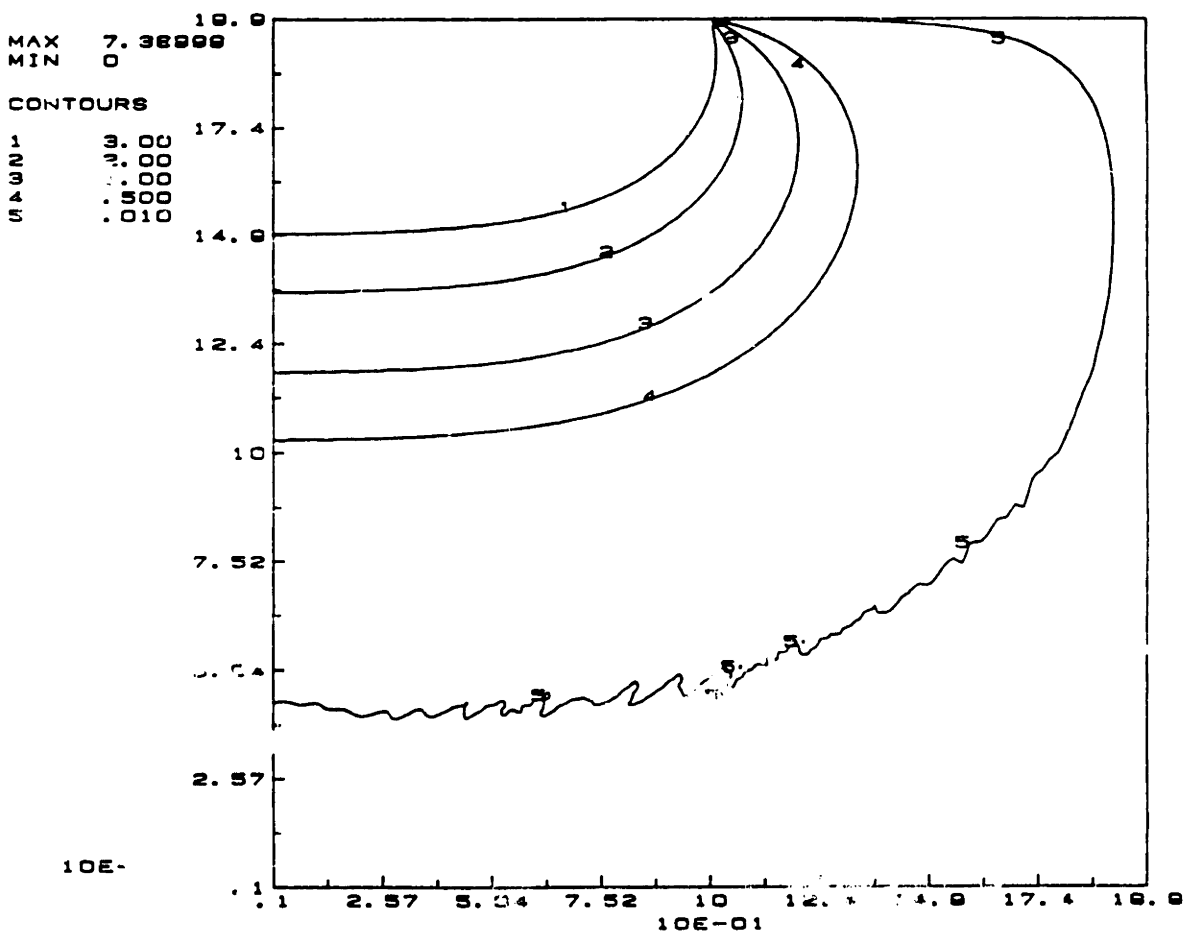
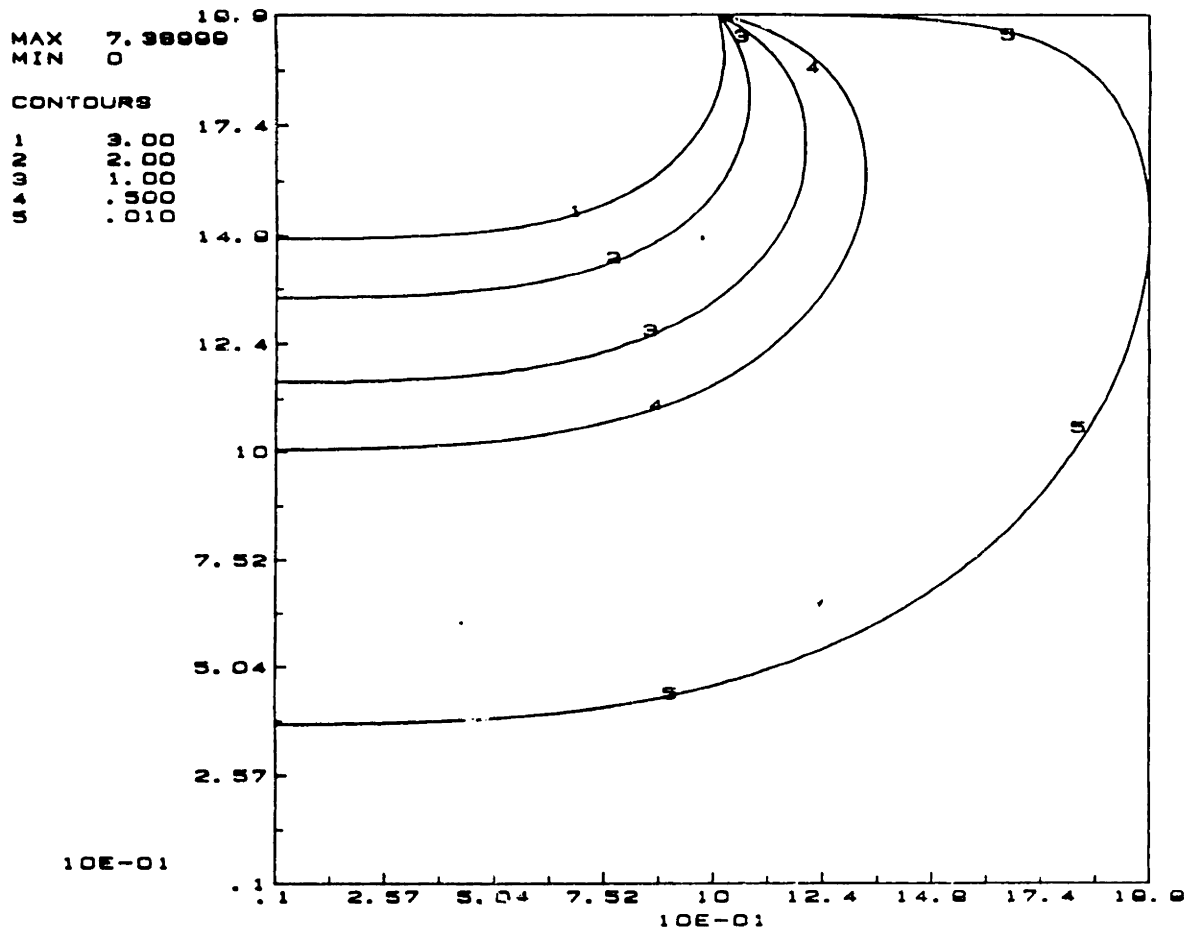


Figure 3.5 Comparison of Two-Dimensional Analytical and Numerical Solution for Homogeneous Soil ($T=0.1$)

Case A:

$$K_s(X, Z) = K_o \exp\{\cos(2\omega_x X) + \cos(2\omega_z Z)\}$$

$$\ln K_s(X, Z) = \ln K_o + \cos(2\omega_x X) + \cos(2\omega_z Z)$$

$$\frac{\partial \ln K_s}{\partial X} = -\sin(2\omega_x X) 2\omega_x$$

$$P_{1X}(X) = 2\omega_x \sin(2\omega_x X)$$

$$\frac{\partial \ln K_s}{\partial Z} = -\sin(2\omega_z Z) 2\omega_z$$

$$P_{1Z}(Z) = 2\omega_z \sin(2\omega_z Z) - 2$$

$$\frac{\partial^2 \ln K_s}{\partial X^2} = -\cos(2\omega_x X) 4\omega_x^2$$

$$\frac{\partial^2 \ln K_s}{\partial Z^2} = -\cos(2\omega_z Z) 4\omega_z^2$$

$$P_2(X, Z) = 4\omega_x^2 \cos(2\omega_x X) + 4\omega_z^2 \cos(2\omega_z Z)$$

Case B:

$$K_s(X, Z) = K_o \exp\{\cos(2\omega_x X) - 2S_x X + \cos(2\omega_z Z)\}$$

$$\ln K_s(X, Z) = \ln K_o + \cos(2\omega_x X) - 2S_x X + \cos(2\omega_z Z)$$

$$\frac{\partial \ln K_s}{\partial X} = -\sin(2\omega_x X) 2\omega_x - 2S_x$$

$$P_{1X}(X) = 2\omega_x \sin(2\omega_x X) + 2S_x$$

$$\frac{\partial \ln K_s}{\partial Z} = -\sin(2\omega_z Z) 2\omega_z$$

$$P_{1Z}(Z) = 2\omega_z \sin(2\omega_z Z) - 2$$

$$\frac{\partial^2 \ln K_s}{\partial X^2} = -\cos(2\omega_x X) 4\omega_x^2$$

$$\frac{\partial^2 \ln K_s}{\partial Z^2} = -\cos(2\omega_z Z) 4\omega_z^2$$

$$P_2(X, Z) = 4\omega_x^2 \cos(2\omega_x X) + 4\omega_z^2 \cos(2\omega_z Z)$$

Case C:

$$K_s(X, Z) = K_o \exp\{\cos(2\omega_x X) + \cos(\omega_x X) + \cos(2\omega_z Z) - 1\}$$

$$\ln K_s(X, Z) = \ln K_o - 1 + \cos(2\omega_x X) + \cos(\omega_x X) + \cos(2\omega_z Z)$$

$$\frac{\partial \ln K_s}{\partial X} = -\sin(2\omega_x X) 2\omega_x - \sin(\omega_x X) \omega_x$$

$$P_{1x}(X) = 2\omega_x \sin(2\omega_x X) + \omega_x \sin(\omega_x X)$$

$$\frac{\partial \ln K_s}{\partial Z} = -\sin(2\omega_z Z) 2\omega_z$$

$$P_{1z}(Z) = 2\omega_z \sin(2\omega_z Z) - 2$$

$$\frac{\partial^2 \ln K_s}{\partial X^2} = -\cos(2\omega_x X) 4\omega_x^2 - \cos(\omega_x X) \omega_x^2$$

$$\frac{\partial^2 \ln K_s}{\partial Z^2} = -\cos(2\omega_z Z) 4\omega_z^2$$

$$P_2(X, Z) = 4\omega_x^2 \cos(2\omega_x X) + \cos(\omega_x X) \omega_x^2 + 4\omega_z^2 \cos(2\omega_z Z)$$

In Figure 3.6 a periodic soil (Case A) with $\omega_x = 0.0$ and $\omega_z = 2\pi$ is irrigated with a strip source of length $L = 1.0$, symmetric with respect to the origin. This situation corresponds to stratified soil formations. The solution contours, which can be interpreted as soil moisture contours (up to

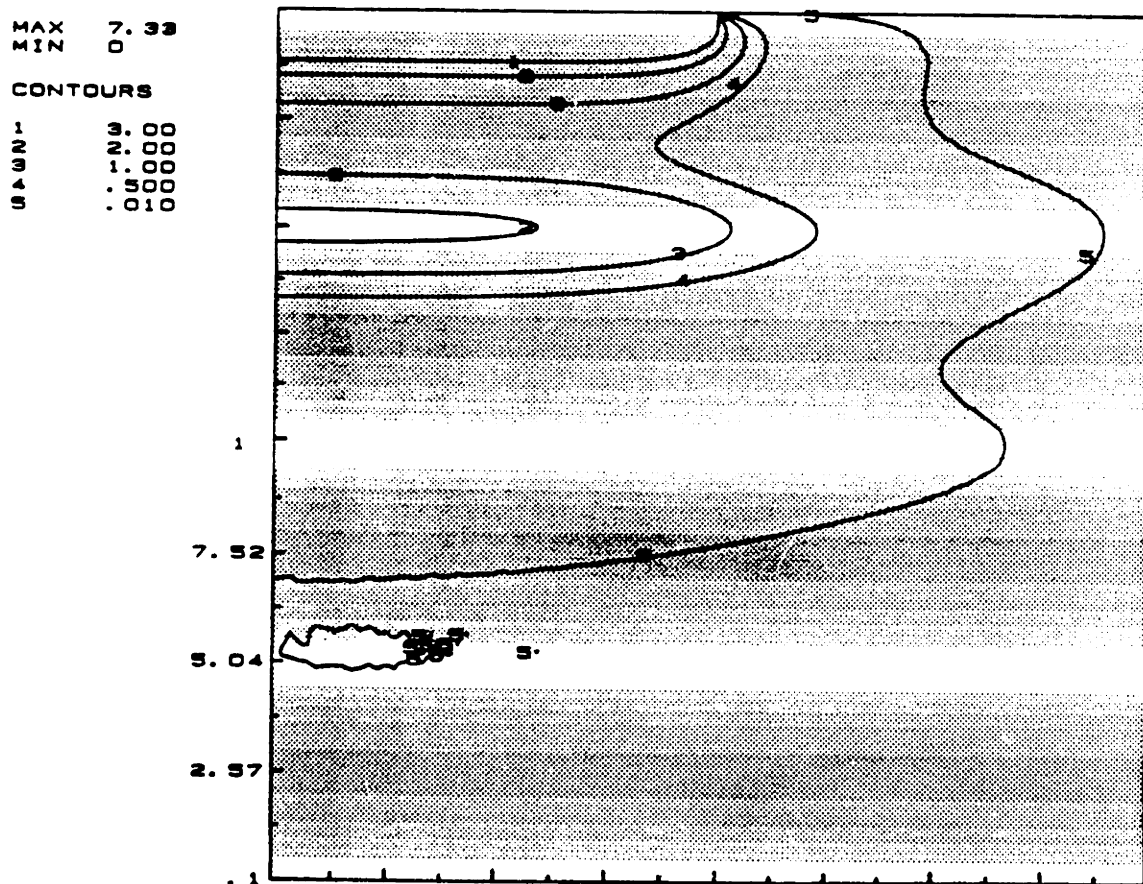
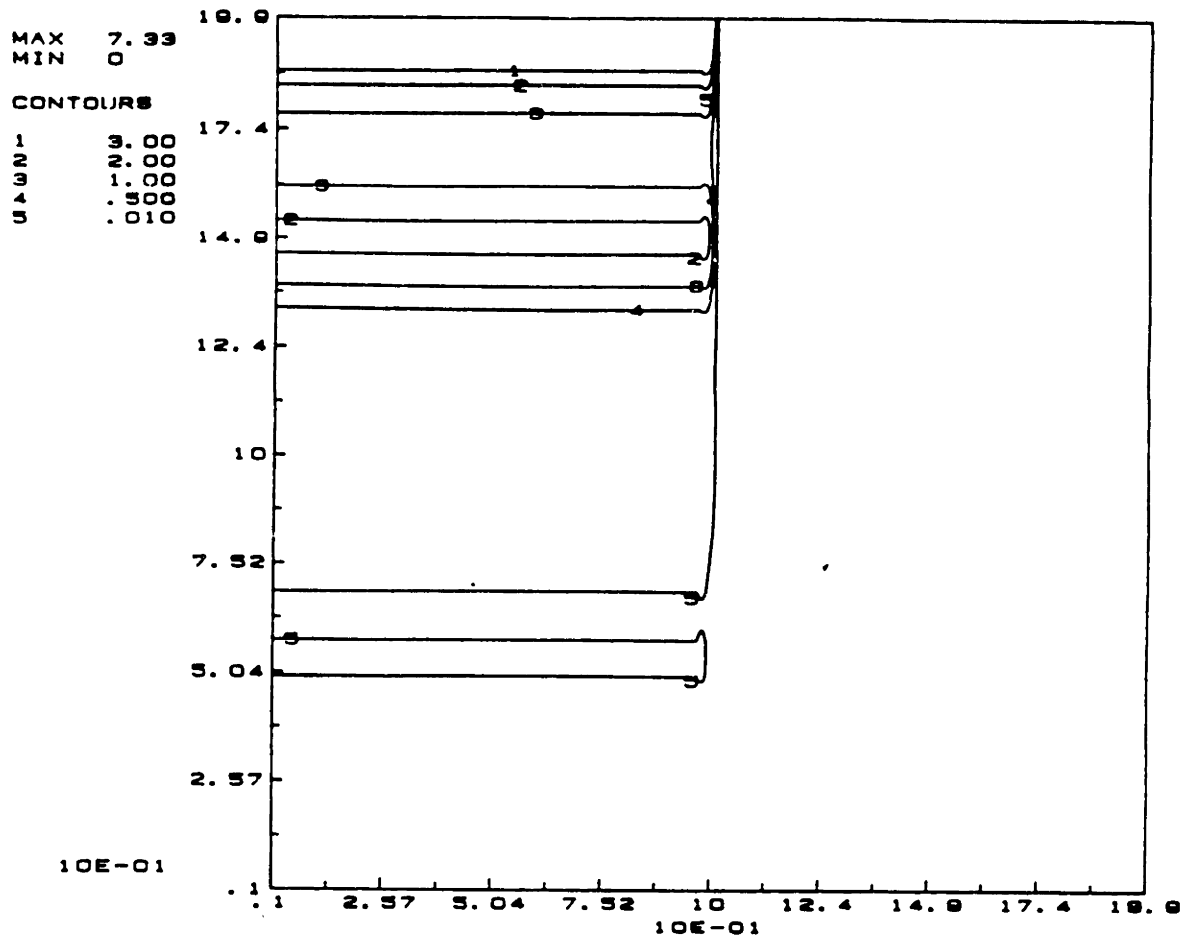


Figure 3.6 Strip Source; One-Dimensional Approximation vs. Two-Dimensional Solution (Case A; $\omega_x=0.0$, $\omega_z=2\pi$; $T=0.1$)

a proportionality constant) show the preferential wetting of the more conductive layers. Underneath the source the one-dimensional approximation (upper part) gives exactly the same location of the contours, while at the edges of the source the two-dimensional characteristics of the flow cannot be captured. These features are found to hold for any variational form of K_S in Z , for any time period, as long as the soil is homogeneous in X . It is also implied that in such soils questions of practical interest, such as how far a tracer has been propagated towards the water table by advection, can be answered correctly by just solving the much easier one-dimensional problem. It is also not surprising that in the case of stratified soils the vertical movement of water is much slower than in homogeneous soils (Figure 3.5). The less conductive layers obstruct the penetration of the moisture front and tend to spread water laterally. The extent of the lateral flow is greatly related to the imposed boundary condition. Underneath the source, the flow is essentially one-dimensional.

We now want to address the issue of heterogeneity in the X direction. From the analytical solutions we find that the soil heterogeneity parameter S_x plays an important role in limiting the validity of the one-dimensional approximation only during early times, if the hydraulic conductivity varies rapidly in X . Consider the case of K_S varying arbitrarily in X . If we define local coordinate systems at the local maximum values of K_S and place an infiltrating source at each origin, at early times the flow problem in each system will be approximately the same with those already studied analytically. Therefore in each of the local problems for a certain time period the one-dimensional approximation is valid (at a given level of accuracy) and

depends on the length of the source and the scale of variation of the saturated hydraulic conductivity. Increasing the source length (since we are interested in problems where the boundary condition at the soil surface is uniform), the critical value of time is determined entirely by the soil heterogeneity parameters. It is desirable to find a sufficient parameter describing the heterogeneity in the X coordinate (equivalent to the S_x parameter in the exponential case) and use this parameter in order to decide on the validity of the one-dimensional approximation.

In Figure 3.7 a soil with $\omega_x = \omega_z = 2\pi$ (Case A) is studied under the same conditions of Figure 3.6. Again the one-dimensional approximation (upper part) recovers the two-dimensional solution (lower part) very accurately underneath the source. The same is not observed in Figure 3.8 for a soil with $S_x = 1.0$, $\omega_x = \omega_z = 2\pi$ (Case B), where even at early time ($T=0.1$) the 0.5 contour penetrates deeper in the upper figure. Figure 3.9 where $\omega_x = 2\pi$, $\omega_z = 0.0$ (Case C) shows similar behavior of the 0.5 contour. In Figure 3.10a,b, where $\omega_x = \omega_z = 2\pi$ (Case C), the discrepancy is observed for the 0.01 contour at early time ($T=0.1$) and for all contours at later time ($T=0.5$).

These numerical investigations indicate that the characteristic length scale is related not to the variation of K_s itself, but to the variation of its extreme values in space. As long as the K_s values are bounded within a uniform envelope of maximum and minimum values, as in the case of Figure 3.7, the one-dimensional approximation remains valid. In the opposite case the length constant of the spatial variation of this envelope should define S_x , which then should be used as a sufficient parameter in the derived criterion (Equation (3.22)) to obtain the critical time for the one-dimensional

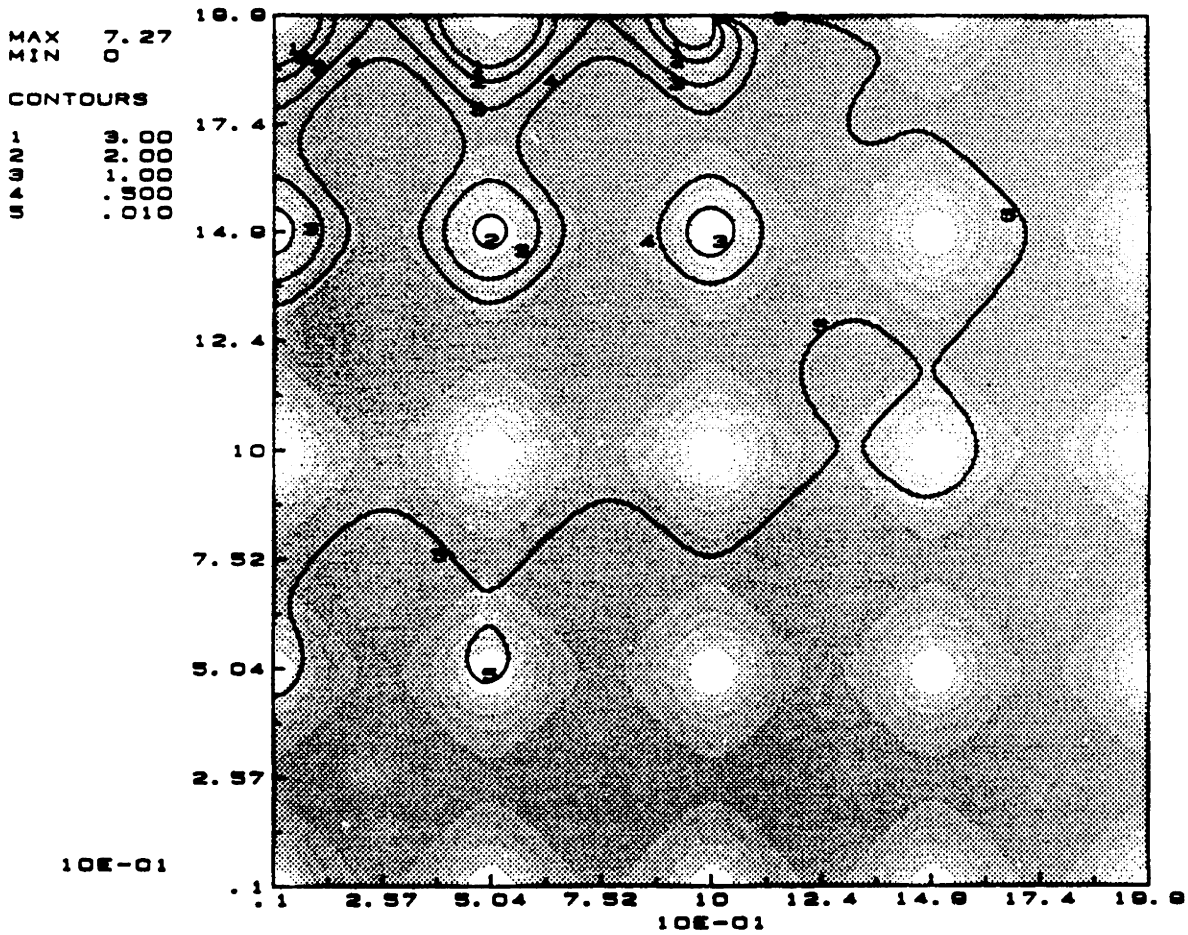
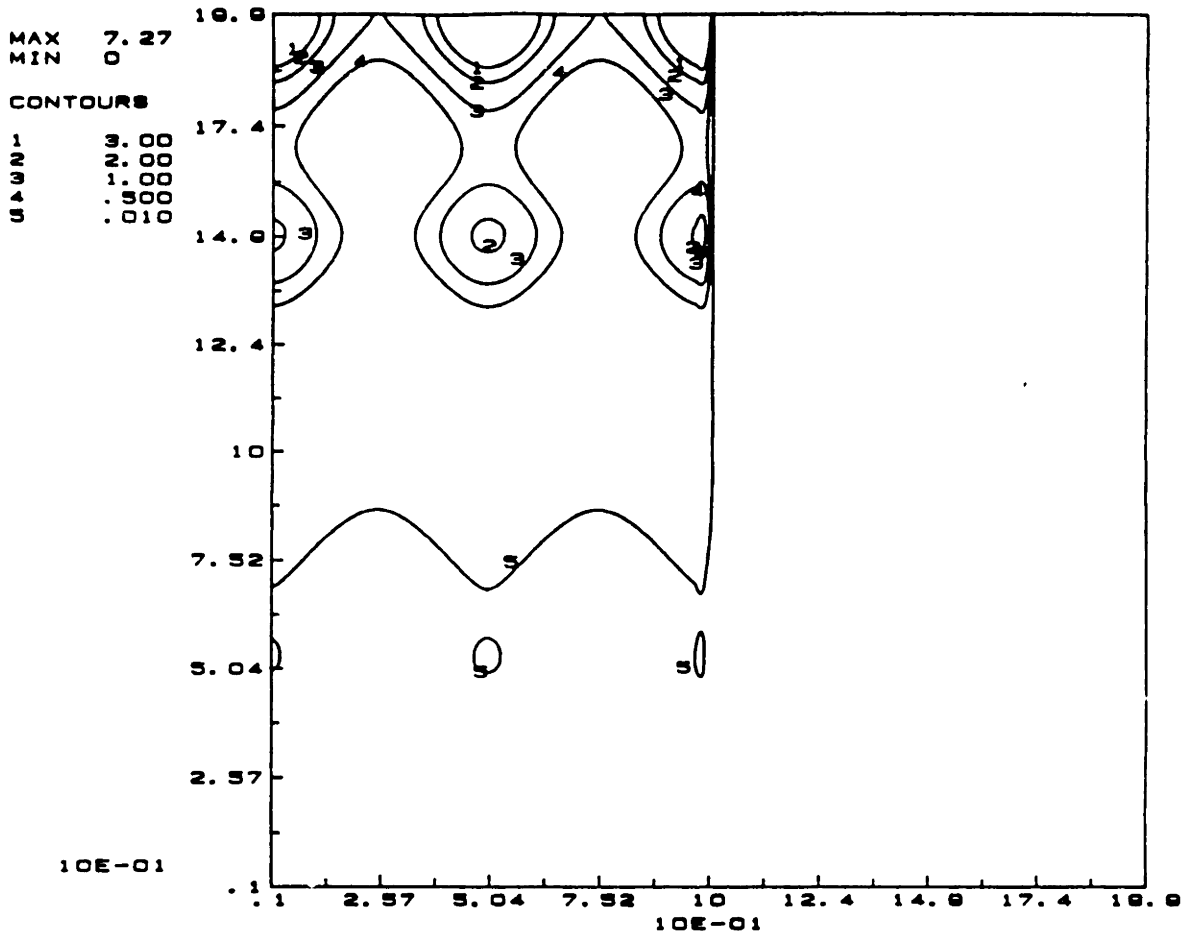


Figure 3.7 Strip Source; One-Dimensional Approximation vs. Two-Dimensional Solution (Case A; $\omega_x=2\pi$, $\omega_y=2\pi$; $T=0.1$)